Development of a bioactive coating for the specific gene silencing of pathogenetic processes after intravascular stent implantation

Entwicklung einer bioaktiven Beschichtung zum spezifischen Gen-Silencing pathogenetischer Prozesse nach intravaskulärer Stentimplantation

Dissertation

der Mathematisch-Naturwissenschaftlichen Fakultät

der Eberhard Karls Universität Tübingen

zur Erlangung des Grades eines

Doktors der Naturwissenschaften

(Dr. rer. nat.)

vorgelegt von

Olivia Maria König

aus Böblingen

Tübingen

2019

Gedruckt mit Genehmigung der Mathematisch-Naturwissenschaftlichen Fakultät der Eberhard Karls Universität Tübingen.

Tag der mündlichen Qualifikation:	15.06.2020
Dekan:	Prof. Dr. Wolfgang Rosenstiel
1. Berichterstatter:	PD. Dr. Andrea Nolte-Karayel
2. Berichterstatter:	Prof. Dr. Stefan Stevanović

„Man muß das Unmögliche versuchen, um das Mögliche zu erreichen."

Hermann Hesse

Table of contents

Zusammenfassung

Kardiovaskuläre Erkrankungen weisen die höchste Sterblichkeitsrate in der westlichen Welt auf. Zu ihnen gehören viele verschiedene Krankheiten, wie z.B. die koronare Herzkrankheit (KHK). Der Hauptauslöser für die Entwicklung dieser Erkrankungen ist die Atherosklerose. Sie ist ein fortschreitender, entzündlicher Prozess, bei dem eine Verengung der Arterien durch die Bildung von atherosklerotischen Plaques auftritt. Dadurch kann weniger Blut zum Herzen transportiert werden, was zu einer generellen Unterversorgung des Herzmuskels oder im schlimmsten Fall zu einem Myokardinfarkt führen kann. Um den natürlichen Blutfluss in dem verengten Abschnitt der Arterie wiederherzustellen, sind zwei interventionelle Therapieoptionen üblich: 1) die Koronararterien-Bypass-Operation (CABG) oder 2) die perkutane transluminale Koronarangioplastie (PTCA). Während bei der CABG überwiegend autologe Venentransplantate verwendet werden, wird bei der PTCA ein Ballon für die Erweiterung der Arterie verwendet, mit der Option, einen Stent über den Katheter zu platzieren. Beim Einbringen der bisher üblichen Stents, wie Bare Metal Stents (BMS) oder Drug Eluting Stents (DES), kann das Endothel durch das Expandieren des Stents und durch dessen Drahtgeflecht geschädigt werden und es kann zu einer nachfolgenden Entzündungsreaktion und einem Wiederverschluss (Restenose) kommen. Mit den DES wird dieses Risiko minimiert, da sie antiproliferative oder immunsuppressive Wirkstoffe freisetzen. Jedoch birgt dieser Vorteil auch einen Nachteil, da die Wirkstoffe gleichzeitig das Wachstum von Endothelzellen hemmen und Patienten länger auf antithrombotische Medikamente angewiesen sind. Gegenwärtig gibt es viele verschiedene Ansätze zur Entwicklung von Stents der nächsten Generation, um unerwünschte Reaktionen wie die In-Stent-Restenose (ISR) und eine späte Stentthrombose zu verringern.

Ein initialer Prozess während der Entwicklung der Atherosklerose und nach Verletzung des arteriellen Gewebes durch die Stent-Implantation ist die Rekrutierung von Leukozyten. Diese wird durch verschiedene zelluläre Adhäsionsmoleküle (CAMs) wie z. B. dem interzellulären Adhäsionsmolekül 1 (ICAM–1), welches im Bereich der Verletzung von Endothelzellen vermehrt gebildet wird, vermittelt. ICAM–1 gehört zur sogenannten Leukozytenadhäsionsmolekülkaskade.

Wenn es möglich wäre die Bildung des ICAM–1 sowie die Bildung weiterer relevanter Proteine spezifisch durch siRNA zu hemmen, so könnte die initiale Leukozytenadhäsionsmolekülkaskade durchbrochen und die Restenosegefahr vermindert werden.

Drei verschiedene Stent-Beschichtungssysteme zur substratvermittelten small interfering RNA (siRNA)-Freisetzung gegen ICAM–1 wurden in dieser Arbeit entwickelt. Als Basis für die Schichtsysteme dienten Lipoplexe aus Lipofectamine®2000 und spezifische sowie fluoreszenzmarkierte siRNA oder Polyplexe aus Poly(ethylenimin) (PEI) und siRNA. Als Biomaterialien für die Einbettung der Lipo- oder Polyplexe wurden Atelokollagen, verschiedene Poly(lactid-*co*-glycolid) (PLGA) Resomere oder Polyelektrolyt-Mehrschicht (PEM)-Schichtsysteme aus PEI und Hyaluronsäure (HA) verwendet. Die Aufnahme bzw. Transfektion von siRNA in

Zellen der Zelllinie EA.hy926 konnte mit allen drei Stent-Beschichtungssystemen nachgewiesen werden. Darüber hinaus wurde untersucht, ob die Schichtsysteme über eine Langzeitfreisetzung verfügen oder die siRNA über einen kurzen Zeitraum abgeben. Die langfristige Freisetzung von siRNA ist besonders interessant für die Stent-Therapie, da der Stent in der Arterie verbleibt, um ihn offen zu halten, und die Heilung eines verletzten Endothels bis zu drei Monate dauern kann.

Die erwünschte Langzeitfreisetzung von Lipoplexen, die in die PLGA-Beschichtungen eingebettet waren, konnte vom ersten bis zum zwanzigsten Tag gezeigt werden. Die etablierte Atelokollagen-Beschichtung mit siICAM–1-Lipoplexen bewirkte eine signifikante Reduktion der ICAM–1-Expression bis zum achten Tag. In beiden Ansätzen wurde die spezifische Spaltung der ICAM–1 messenger RNA (mRNA) gezeigt und eine gute Zellviabilität und Hämokompatibilität der Beschichtungen nachgewiesen.

Der PLGA-Mehrschichtaufbau eignet sich außerdem zur simultanen Kotransfektion der grün fluoreszierenden (eGFP)mRNA und siRNA. Die beiden substratvermittelten siRNA-Freisetzungssysteme mit Langzeitwirkung ebnen den Weg für neue therapeutische Stentbeschichtungen, um das ISR-Risiko nach der Stentimplantation zu reduzieren.

Das PEM-System mit HA und Polyplexen zeigte eine schnelle Freisetzung von siRNA-Partikeln innerhalb der ersten Stunde. Eine signifikante Verringerung des ICAM–1 Proteins wurde nachgewiesen und die Zellviabilität war nicht signifikant reduziert. Somit liefert diese Entwicklung ein weiteres lokales Anwendungssystem, das in die PTCA integriert werden kann.

Summary

Cardiovascular diseases have the highest mortality rate in the western world. They include many different diseases, such as the coronary heart disease (CHD). The main trigger for the development of these diseases is atherosclerosis. It is a progressive, inflammatory process in which arterial narrowing occurs through the formation of atherosclerotic plaques. As a result, less blood can be transported to the heart, which can lead to a general undersupply of the heart muscle or in worst case to a myocardial infarction. To restore natural blood flow in the narrowed section of the artery, two interventional therapy options are common: 1) coronary artery bypass graft (CABG) or 2) percutaneous transluminal coronary angioplasty (PTCA). While CABG uses predominantly autologous vein grafts, the PTCA uses a balloon to dilate the artery, with the option of placing a stent by catheter. When introducing conventional stents, such as bare metal stents (BMSs) or drug-eluting stents (DESs), the endothelium can be damaged by the expansion of the stent and its wire mesh, and a subsequent inflammatory reaction and re-occlusion (restenosis) can occur. DES minimizes this risk by releasing antiproliferative or immunosuppressant drugs. However, this advantage also has a disadvantage, since the active ingredients simultaneously inhibit the growth of endothelial cells and patients are more dependent on antithrombotic drugs. There are currently many different approaches to developing next-generation stents to minimize adverse reactions such as in-stent restenosis (ISR) and late stent thrombosis.

An initial process is the recruitment of leukocytes during the development of atherosclerosis and after injury of the arterial tissue by the stent implantation. This is mediated by various cellular adhesion molecules (CAMs), such as the intercellular adhesion molecule 1 (ICAM–1), which is increasingly formed around injury to endothelial cells. ICAM–1 belongs to the so-called leukocyte adhesion molecule cascade.

If it were possible to specifically inhibit the formation of ICAM–1 and the formation of other relevant proteins by siRNA, the initial leukocyte adhesion molecule cascade could be disrupted, and the risk of restenosis reduced.

Three different stent coating systems for substrate-mediated siRNA release against ICAM–1 were developed in this work. Lipoplexes of Lipofectamine®2000 and specific and fluorescently labeled siRNA or polyplexes of poly (ethyleneimine) (PEI) and siRNA served as basis for the coating systems. As biomaterials for embedding the lipo- or polyplexes, atelocollagen (ATCOL), various poly (lactide-co-glycolide) (PLGA) resomers or polyelectrolyte multilayer (PEM) systems of PEI and hyaluronic acid (HA) have been used. The uptake or transfection of siRNA into cells of the cell line EA.hy926 was detected with all three stent coating systems. In addition, it was investigated whether the layer systems have a sustained release or release the siRNA over a short period of time. The long-term release of siRNA is particularly interesting for stent therapy because the stent remains in the artery to keep it open, and the healing of an injured endothelium can take up to three months.

The desired sustained release of lipoplexes embedded in the PLGA coatings could be demonstrated from the first to the twentieth day. The established ATCOL coating with siICAM–1 lipoplexes resulted in a significant reduction in ICAM–1 expression until the eighth day. Both approaches demonstrated specific cleavage of the ICAM–1 messenger RNA (mRNA) and demonstrated good cell viability and hemocompatibility of the coatings.

The PLGA multilayer construction is also suitable for simultaneous co-transfection of green fluorescent (eGFP)mRNA and siRNA. The two long-acting substrate-mediated siRNA release systems pave the way for new therapeutic stent coatings to reduce ISR risk after stent placement.

The HA and polyplex PEM system showed rapid release of siRNA particles within the first hour. Significant reduction of the ICAM–1 protein was demonstrated, and cell viability was not significantly reduced. Thus, this development provides another local application system that could be integrated into the PTCA.

1 Introduction

1.1 Cardiovascular disease and the coronary heart disease

Cardiovascular diseases (CVDs) claimed more than 17.7 million deaths in 2015 and are responsible for a death rate of 31% worldwide, leading the mortality statistics on global scale [1-3]. Within this group, there are different classifications of this disease, such as the coronary heart disease (CHD) where arterial vessels are affected that generally apply oxygen-rich blood to the myocardium. The occurrence of arteriosclerosis in the CHD causes a narrowing of the artery due to atherosclerotic plaques and a lower blood flow to the heart. As a result, the heart muscle is no longer sufficiently supplied with oxygen and nutrients and parts of it can die off resulting in the worst case in myocardial infarction [4]. The main risk factors for the development of an atherosclerosis are: hypertension, diabetes mellitus, hyperlipidemia, obesity, smoking, genetic abnormalities and lack of physical activity and should therefore be treated with preventive care [5, 6].

1.1.1 Atherosclerosis and its genesis

Atherosclerosis represents the most common cause for CVD like CHD, coronary artery disease (CAD) and peripheral artery disease that are special types of arteriosclerosis. While arteriosclerosis describes the loss of elasticity of the large arteries, atherosclerosis is a progressive disease where an atherosclerotic plaque is formed by lipids and fibrous elements causing the hardening of the artery. Although not all factors of atherogenesis have been revealed, it is known that the morphology of the endothelial cells (ECs) and low-density lipoproteins (LDLs) play a major role in the initial step of vascular lesions. ECs in tubular regions with laminar blood flow have an ellipsoid shape and are aligned to the bloodstream. However, ECs in branching or curvature regions show polygonal undirected shape with a thin glycocalyx layer and are predominated for endothelial lesion [7, 8]. The spontaneous damage of the arterial endothelium due to turbulence blood flow, low fluid shear stress or other endothelial injuries leads to increased permeability for macromolecules [7, 9]. In this process, the two proteins endothelial nitric oxide synthase (eNOS) and superoxide dismutase (SOD) show reduced expression. Consequently, their reduction causes the retention of LDL via apolipoprotein B (apoB) leading to accumulation of LDL in the subendothelial layer, the tunica intima [10]. Generally, a normal nitric oxide (NO) level acts as a protector against

the development of atherosclerosis and inhibits platelet and leukocyte aggregation, prevents platelet, leukocyte and monocyte adhesion on the endothelium, and reduces vascular smooth muscle cell (VSMC) proliferation [11, 12]. Additionally, SOD is necessary for the cells to protect them against the superoxide anion radical [13]. One major cause for atherogenesis is the activation of endothelial cells via increased transcription factor NF-κB due to the oxidation of LDL by reactive oxygen or enzymes and the subsequent inflammatory processes [14, 15]. Oxidized LDL (oxLDL) accumulates in the subendothelial layer and stimulates the ECs to produce macrophage colony-stimulating factor (M-CSF), monocyte chemoattractant protein–1 (MCP–1), and the increased expression of cellular adhesion molecules (CAMs) which attract leukocytes and platelets to the endothelium (exactly described in chapter 1.1.2) [16, 17]. After monocyte infiltration into subendothelial layer, M-CSF causes the phenotypically change into macrophages. The scavenger receptors, CD36, lectin-like receptor–1 (LOX–1) or CXCL16 on the macrophages are responsible for the internalization of the oxLDL leading to its accumulation and foam cell building of macrophages [18]. The ongoing formation of foam cells lead to fatty streaks in the tunica intima. Fatty streaks can appear in arteries in early life and can regress again, if foam cells do not recruit VSMCs ending up in advanced lesion. Different types of atherogenic cytokines or chemoattractants form foam cells. ECs and T-cells induce the migration and proliferation of the VSMCs from the tunica media to the intima and are responsible for intimal thickening (Figure 1) [19]. Here, phenotypic change of VSMCs causes expression of different receptors like scavenger receptors, CD36, and LOX–1 for the uptake of oxLDL [20]. Additionally, VSMCs are responsible for vascular remodeling due to the production of extracellular matrix (ECM) proteins like collagen, proteoglycans, fibronectin and elastin and the formation of a fibrous cap protecting the underlying core of foam cells and necrotic tissue [18, 21]. Different cytokines of the ongoing inflammatory process destabilize the atherosclerotic plaque. The apoptosis of macrophages and foam cells causes an enlargement of the lipid core and the fibrous cap gets thinner due to VSMC death as well as the lack of stabilizing ECM proteins [19]. This thin layer of the fibrous cap can break up very easily in the arterial lumen and the thrombogenic lipid core, and its high amount of tissue factor are released [22]. The coagulation cascade starts and platelets react with adhesion and aggregation leading to thrombosis and consequently to clinical incidences like myocardial infarction or stroke [23, 24].
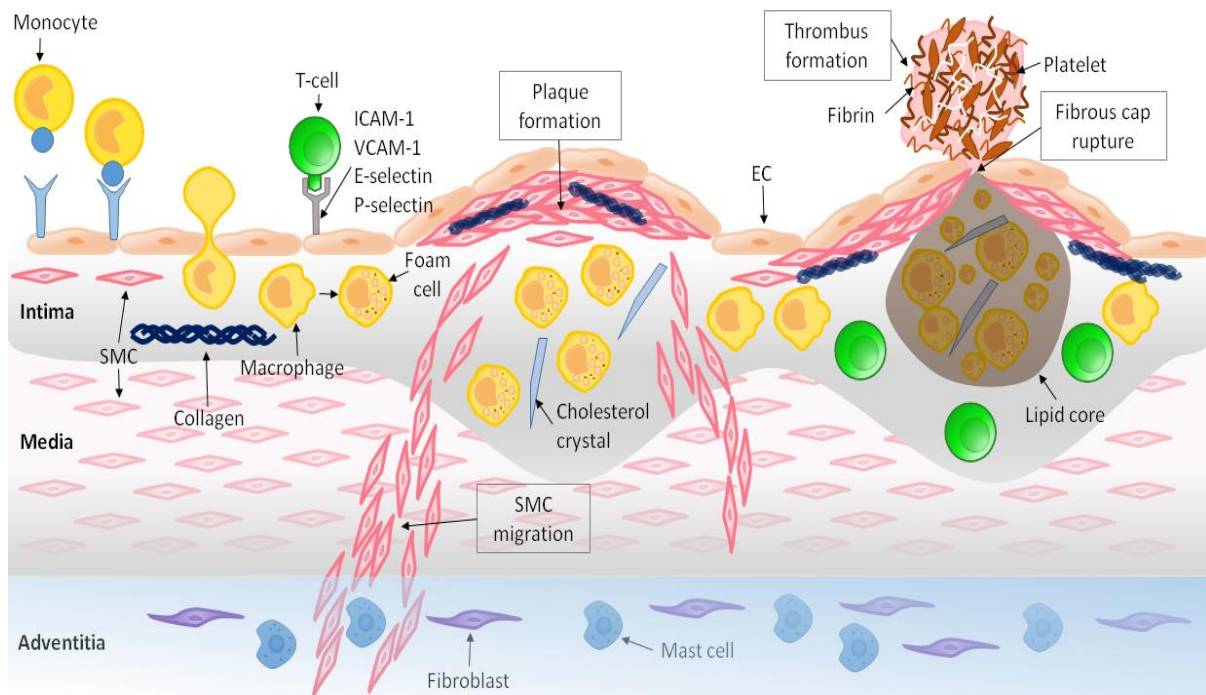
Figure 1: The development of atherosclerosis. It begins with monocyte infiltration and leukocyte adhesion with diapedesis, followed by plaque formation, plaque rupture and ends with the formation of a thrombus. Redesigned an inspired by the image of Libby *et al.*, 2011 [25].

1.1.2 Cellular adhesion molecules and leukocyte adhesion cascade

Tissue injury or inflammation is the trigger for the recruitment of leukocytes from the blood to the site of injury or inflammation where the immune response is needed for tissue repair. The leukocyte migration and the following diapedesis is targeted and controlled by proinflammatory cytokines that lead the leukocytes to the site of inflammation, so the surrounding healthy tissue is not attacked. The cytokines Interleukin–1 (IL–1), Interleukin–6 (IL–6), tumor necrosis factor-α (TNF-α) and chemokines are distributed and activate endothelial cells which react with increasingly expression of the CAMs like intercellular adhesion molecule–1 (ICAM–1), vascular cell adhesion molecule–1 (VCAM–1), P-selectin, and E-selectin [26, 27]. An important factor for the adhesion of leukocytes and platelets is the slowing down of the blood stream due to the inflammation, which simplifies their binding to the adhesion molecules. The leukocyte adhesion cascade is divided into three sections according to the original model: 1) selectin-mediated leukocyte rolling, 2) chemokine-mediated leukocyte activation, and 3) integrin-mediated leukocyte arrest [28] (Figure 2).
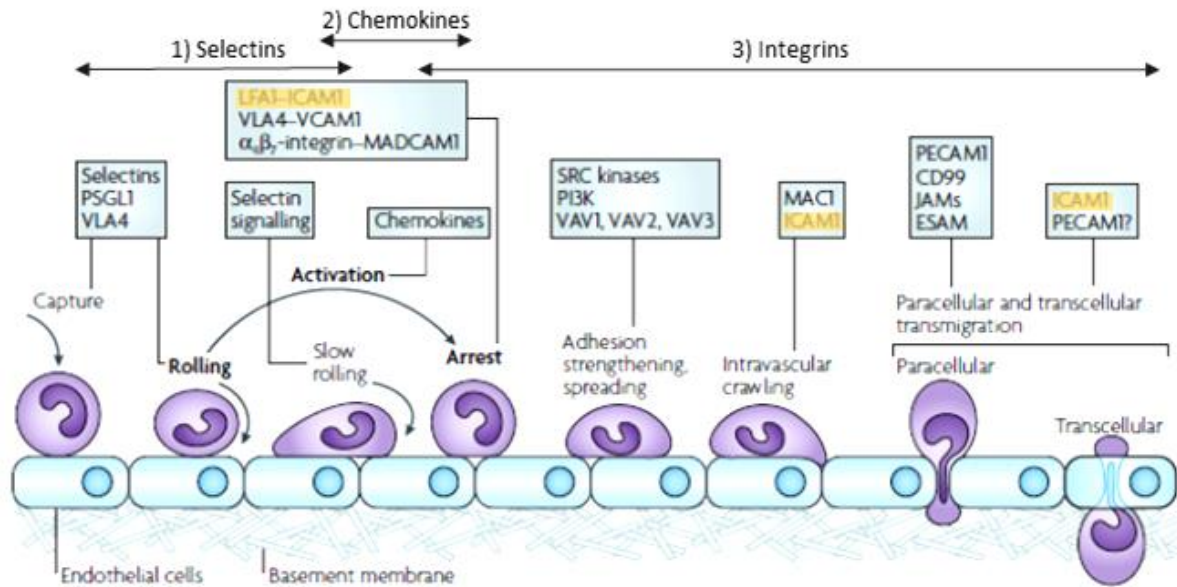
Figure 2: The leukocyte adhesion cascade during inflammation with leukocyte rolling, activation, arrest, and transmigration. ICAM–1 is marked in yellow because it is important for this thesis. Different selectins, chemokines, and integrins are involved in this process: PSGL–1: P-selectin glycoprotein ligand–1; VLA4: very late antigen 4; LFA1: lymphocyte function-associated antigen 1; MADCAM1: mucosal vascular addressin cell adhesion molecule 1; PI3K: phosphoinositide 3–kinase; MAC1: macrophage–1 antigen; VCAM–1: vascular cell adhesion molecule–1; ICAM–1: intercellular adhesion molecule–1; VCAM–1: vascular cell adhesion molecule–1; PECAM–1: platelet/endothelial-cell adhesion molecule–1; JAM: junctional adhesion molecule; ESAM: endothelial cell specific adhesion molecule. Adapted and modified from Ley *et al.*, 2007 [29].

First, rolling of leukocytes is mediated by E-selectin and P-selectin of activated ECs. It is a low-affinity and reversible interaction with fast on and off rates between the selectins and their ligands of leukocytes where the aminoterminal lectin domain of the selectins binds carbohydrate groups attaching to the proteins of leukocytes [26]. The rolling of the leukocytes allows further activation of the cells by chemokines. The chemokine receptors of the leukocytes interact with the chemokines and the integrins of leukocyte are activated. The integrin lymphocyte function-associated antigen 1 (LFA1) of the β_2 family binds firmly to ICAM–1 of the immunglobulin superfamily as well as the integrin very late antigen 4 (VLA4) of the β_1 family to VCAM–1 [30]. The adhered leukocyte reaches by crawling, also called locomotion, the site for transmigration with the interaction of integrins and ICAM–1 [31]. Adhesion molecules like platelet/endothelial-cell adhesion molecule–1 (PECAM–1) or vascular endothelial cadherin (VE-cadherin) lead to transmigration of leukocytes and move to the tunica intima [30].

1.1.3 Therapy of atherosclerosis and its pitfalls

Patients suffering from atherosclerosis can significantly improve the prognosis for CVD by changing their lifestyle. These include, for instance, weight loss, termination of smoking or physical activity [32, 33]. The second prevention step is the drug therapy with β-blockers, statins, angiotensin-converting enzyme (ACE) inhibitors, antiplatelet therapy or the new drug proprotein convertase subtilisin/kexin type–9 inhibitor (PCSK–9) which is intended for patients who are symptom-free or clinically stable [33, 34]. Surgery intervention is unavoidable for patients with persistent or exacerbating symptoms after the first and second prevention step could not improve the ordeal [35]. The discovery of the coronary angiography paved the way for the development of the following two surgical techniques: 1) coronary artery bypass surgery (CABG), 2) percutaneous transluminal coronary angioplasty (PTCA), recently called percutaneous coronary intervention (PCI) due to a broader spectrum. CABG was developed and performed in the 1960s by several physicians and Vasilii Kolesov succeeded in a sutured anastomosis of a coronary artery to an artery [36]. Afterwards, the performance of a saphenous vein-coronary bypass was introduced by Michael DeBakey's team [37]. This surgical revascularization method gained center stage in the treatment of CAD and is still of enormous importance, especially for patients with complex lesions [38]. In 1977, Andreas Grüntzig achieved another milestone in CAD therapy by laying the foundation for PTCA as an alternative treatment [39]. During an angioplasty treatment, the stenotic vessel can be expanded via a balloon or stent insertion using a minimally invasive catheter inserted (Figure 3). For the implementation of balloon angioplasty, various parameters have to be clarified individually for each patient, like the diameter of the balloon, the pressure for inflation, and the duration of inflation. Uncoated balloons, as well as coated ones are recommended for therapy by the ESC/EACTS Guidelines on myocardial revascularization in 2014 [40]. Scheller *et al.* clearly could prove using a paclitaxel-coated balloon which was able to minimize restenosis after use of a BMS [41]. Paclitaxel is known as a chemotherapeutic for cancer and is also used as an antiproliferative agent in balloons or stents with an antirestenotic effect. Drug-coated balloons are different from stent therapy because they do not require prolonged dual antiplatelet therapy, leave no foreign body inside the vessel, which can lead to restenosis, and release the active substance within seconds.
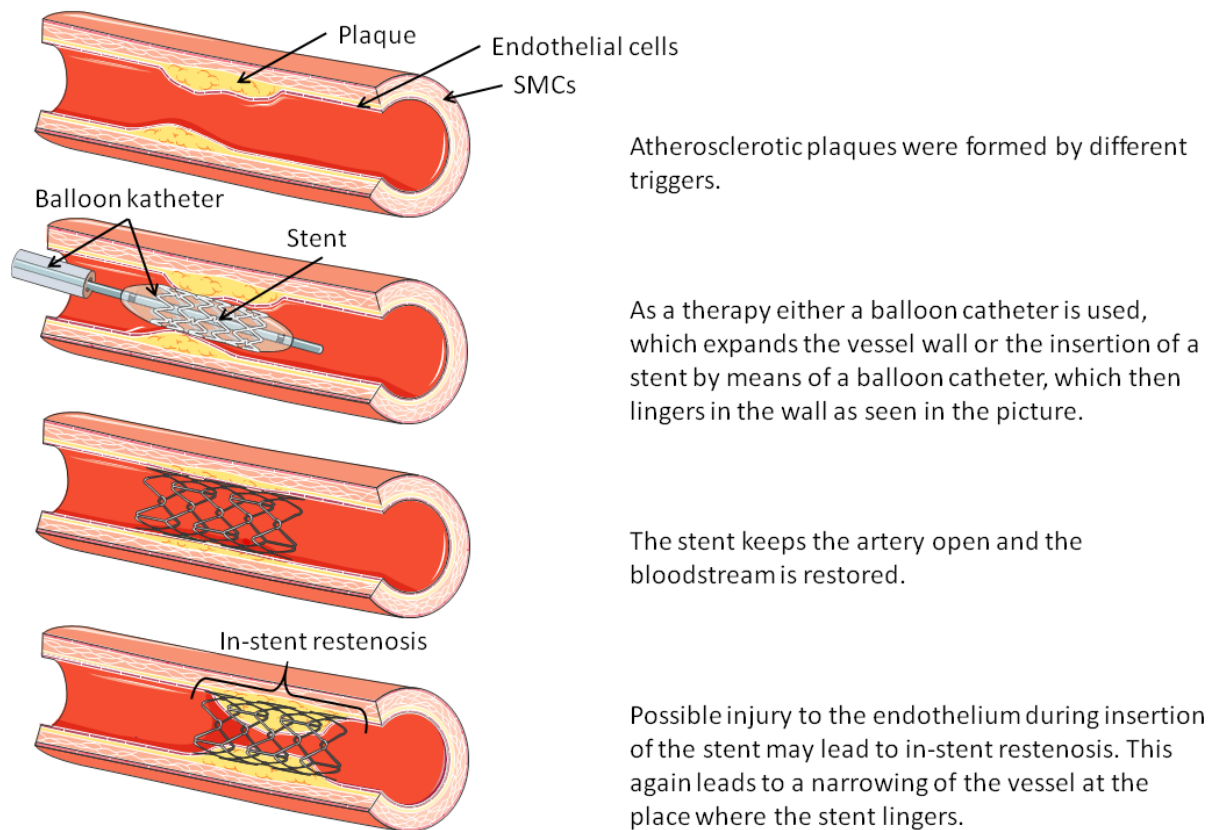
Figure 3: Therapy of atherosclerosis with PTCA and the insertion of a stent. In worst case, it may come again after insertion of a stent to narrowing of the vessel lumen, the so-called in-stent restenosis (shown in the last vessel). Designed with smart, Servier Medical Art.

Nevertheless, in 2004, a meta-analysis revealed that in non-acute coronary disease the insertion of stents reduced mortality rather than balloon angioplasty at 6 months [42]. Moreover, the ESC/EACTS Guidelines on myocardial revascularization recommend stenting over balloon angioplasty in a first PTCA application [40]. The insertion of a stent works via balloon catheter over which the stent is inverted in an unexpanded and 'crimped' state. Inflation of the balloon causes the stent to expand against the arterial wall and remains in that formation as the deflated balloon catheter is removed. The first generation of stents belongs to the bare metal stent (BMS). However, the risk of an early stent thrombosis and an ISR after stent implantation is comparably high [43, 44]. This is due to the occurring trauma to the intimal structure as well as an atherosclerotic plaque rupture during stent implantation causing a cascade of wound-healing mechanisms, known as neointimal hyperplasia [45, 46]. This adverse effect is known as rapid progression of atherosclerosis starting with the infiltration of inflammatory cells besides a cascade of various events like smooth muscle cell proliferation and migration, platelet aggregation, release of growth factors, and extracellular matrix remodeling [45] (described in detail in chapter 1.1.2). The risk

of stent thrombosis can be minimized with drugs such as aspirin and platelet aggregation inhibitors such as clopidrogel [47], but not the ISR. This unwanted occurrence led to the development of the second generation of stents inhibiting neointimal hyperplasia: the drug-eluting stent (DES). The DES has as a basic skeleton a BMS, which is coated with polymer and drug, and which is delivered to the arterial wall after stent implantation. The first two Food and Drug Administration (FDA) approved DESs were the sirolimus-eluting Cypher™ stent in 2003 and the paclitaxel-eluting Taxus™ stent in 2004 [47]. Sirolimus is an immunosuppressive agent and paclitaxel an antiproliferative one. These first generation DES agents prevent smooth muscle cell proliferation and accumulation of macrophages on the stent, thereby reducing the incidence of ISR. Unfortunately, the proliferation of endothelial cells is negatively affected as well as the migration, proliferation and differentiation of endothelial progenitor cells from blood for the mandatory re-endothelialization of the stented region [48]. Further, after discontinuing the dual antiplatelet therapy with aspirin and clopidrogel, the risk of late stent thrombosis increases [49]. The development of the second-generation DES with thinner struts provoked indeed a faster re-endothelialization [50]. However, new approaches for re-endothelialization are being sought. One approach for next-generation stents is the coating with anti-CD34 antibodies to bind the endothelial progenitor cells from the blood to the stent [51]. Similarly, the development of bioabsorbable stents is being researched with mainly two different materials like polymers, which are degraded by hydrolysis, for example poly(lactic acid), and alloys with magnesium [52]. These stents may also be provided with an antiproliferative agent to minimize restenosis. Recent results show however, that the polymer-based bioabsorbable stents cause more heart attacks than the metal stents a few years after insertion. The background probably lies in the irregular degradation of the polymers and the deformation of the inserted stent. The degradation products of magnesium also appear to have a negative effect [53]. Another promising approach is the coating of stents with nucleic acids like siRNA for gene silencing, which is described in the following chapters.

1.1.4 Chances for DES with siRNA against CAMs

As stated above, the onset of ISR is an inflammatory process that results from injury to the intima upon insertion of the stent. A crucial mechanism is the enhanced expression of the CAMs like ICAM–1, E-selectin, P-selectin, and VCAM–1 on the endothelial cells, which leads to increased binding of leukocytes and platelets with

following leukocyte diapedesis into the intima. Additionally, the activation of VSMCs induces their proliferation and migration from the media into the neointima producing extracellular matrix proteins and a chronic inflammatory process is evoked [28, 54]. The focus of research is now on siRNAs directed against these CAMs. Petersen *et al.* proved the effectiveness of an siRNA against VCAM–1 in isloated smooth muscle cells (SMCs) from aorta of C57BL/6 mice. The transfected cells reacted in a scratched area of an SMC monolayer with reduced migration in comparison to non-transfected cells [55]. The inhibition of VCAM–1 by siRNA even reduced restenosis in a surgical mechanical de-endothelialized rat carotid [56]. Recently, Sager *et al.* demonstrated the effect of an siRNA mixture of ICAM–1/–2, VCAM–1, E-selectin, and P-selectin on the fibrotic cap and necrotic core. The matrix metalloproteinases (MMPs) from inflammatory cells are responsible for the degradation of fibrous caps, vessel remodeling, and weakening of the atherosclerotic plaques and hence, a further pivotal point in the development of DES with siRNA. The mixture of siRNAs provoked 85% reduction of mRNA level of several MMPs in mice, protease activity was significantly reduced, and plaque collagen was increased leading to smaller necrotic cores and thicker fibrous caps [57]. ICAM–1 is of particular interest as it plays a key role in leukocyte endothelial adhesion. Walker *et al.* succeeded in reducing ICAM–1 after mimicking an inflammation by TNF-α treatment with siRNA against ICAM–1 [58]. Furthermore, Chung *et al.* demonstrated in a mouse model with flow-induced atherosclerosis that polyplexes with siICAM–1 bound to the flow-disturbed endothelium and reduced ICAM–1 expression [59]. The idea behind the application of ICAM–1 siRNA is that early intervention in the inflammatory cascade may inhibit leukocyte-endothelial adhesion and subsequent processes as SMC mobilization. The other participating CAMs, such as VCAM–1 or E-selectin, should also be considered for a holistic approach [60]. The advantage of siRNAs used as therapeutic is their specific function, which will be explained in the following sections.

1.2   The RNA interference using small interfering RNA

RNA interference (RNAi) is a conserved self-defense mechanism in eukaryotic cells that prevents the integration of foreign DNA or double-stranded RNA (dsRNA) by viruses, transposons or transgenes and regulates gene expression of protein-coding genes [61]. In 1990, this mechanism was first revealed in petunia, when it was attempted to alter the flower color via the introduction of a gene responsible for flower pigmentation [62]. The RNAi mechanism was also described by Fire and Mello, who

received the Nobel Prize in Medicine in 2006 for their discovery. They detected the mechanism in the nematode *Caenorhabditis elegans* by introducing dsRNA into the organism and the resulting degradation of messenger RNA (mRNA), which is essential for the translation of proteins [63]. Understanding the RNAi pathway, it has been discovered that the dsRNA was shortened into an RNA piece of approximately 21 nucleotides (nt), which is called small interfering RNA (siRNA) or micro RNA (miRNA). Both small RNAs arise via the RNAi pathway, differing in biogenesis by other proteins and complexes. However, the function of repression of mRNA translation is the same [64]. In 2001, Elbashir et al. artificially produced 21 nt siRNA for post-transcriptional gene silencing in mammalian cell lines, which has paved the way for further promising RNAi applications with siRNA [65].

1.2.1 The RNAi pathway of siRNA

The pathway of mRNA degradation by RNAi is divided into two different phases: 1) the initiation phase and 2) the effector phase. The pathway is described in Figure 4. In the first step, precursor dsRNA from exogenous or endogenous sources enters the cytoplasm. There, the long dsRNA is cleaved in a 21–23 nt RNA unit by the endonuclease RNase III, called Dicer [66, 67]. The resulting siRNA has a 5'–phosphate and a 3'–hydroxyl group with 2–3 nt overhanging 3'–ends on each strand, which are necessary for the correct cleavage targeting [68]. With the beginning of the second phase, the siRNA is incorporated into the RNA induced silencing complex (RISC) containing a sequence-specific nuclease [69]. Here, the ATP-dependent unwinding of the siRNA duplex takes place and activates the RISC [70]. Central importance in the RNAi pathway is attributed to the Argonaute protein 2 (Ago2) which is located in the RISC [71]. Ago2 binds the guide (antisense) strand and extrudes the passenger strand [72]. The guide strand of the now single-stranded siRNA guides the endonuclease Ago2 to the complementary or nearly complementary target mRNA via base-pairing followed by its cleavage [68, 73]. Generally, the mRNA is cleaved in the middle of the complementary region, where the siRNA/RISC complex binds [74, 75]. This results in an RNA 5'–fragment with a 3'–hydroxyl group and a 3'–fragment with a 5'–phosphate group. Due to the unprotected RNA ends, different exonucleases degrade the mRNA fragments [76]. The degradation of the mRNA causes the decrease of the mRNA amount for translation and consequently, less protein is synthesized and present. The RISC can be recovered and can perform multiple cleavage cycles [77, 78].
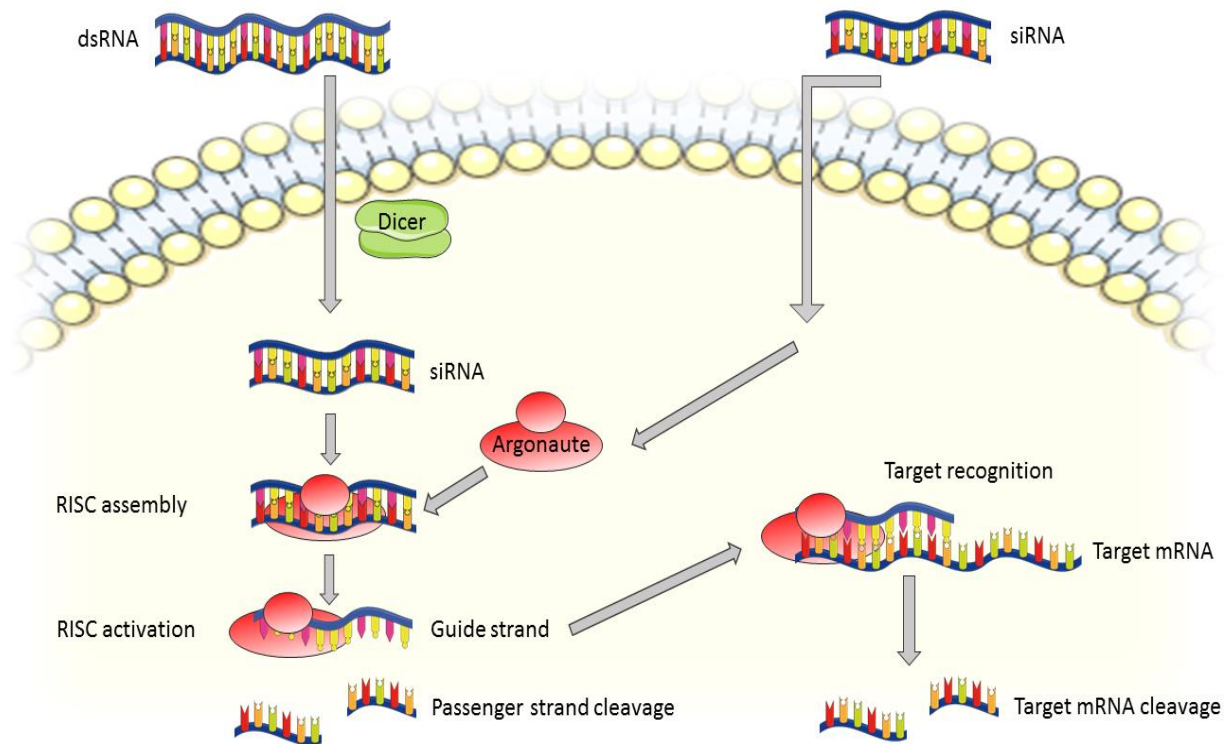
Figure 4: The mechanism of the RNAi pathway. Designed with smart, Servier Medical Art. The illustration is based on basics of the publications [66-75].

1.3   Small interfering RNA and its stabilization

The use of siRNA as a molecular therapeutic agent in acquired and inherited diseases is becoming increasingly important. The exogenous, chemically synthesized siRNA arises from created algorithms which allows the siRNA to bind to the complementary target mRNA. Important parameters for this purpose are for instance: suitable length of siRNA, low GC content, and asymmetry between guide and passenger strand with a less stable 5'–end of the guide strand [79, 80]. Despite promising therapeutic approaches, the main challenging aspects are the stabilization of siRNA, the cellular uptake, and its target delivery. Free and naked siRNA runs the risk of being digested by endo- and exonucleases that are found in blood, serum, and living cells by minimizing its half-live *in vivo* [81, 82]. Chemical modifications are known to protect siRNA from degradation with nucleases by its stabilization. Different modifications at the 2' position of the backbone ribose like 2'-*O*-methyl, 2'-deoxyribose or 2'-fluoro help to stabilize the siRNA at the 3'–end of the guide strand [82-84]. Soutschek et al. was able to produce a functional siRNA by chemical modifications of the apoB siRNA, which led to a reduction of the mRNA level. The 3'–end of both strands were stabilized using phosphorothioate and two 2'-O-methyl nucleotides were added at the 3' end of the

guide strand, while the passenger strand was modified with cholesterol [82]. Nevertheless, chemical modifications are often not sufficient for high transfection or efficient gene silencing which is partly due to the large molecular weight of about 13 kDa and the polyanionic character of about 40 negative phosphate charges [85]. The way to enable a high transfection rate and the target delivery of siRNA is discussed in the following chapters 1.3.1-1.3.3.

1.3.1 Transfection methods

For the successful transfection of cells with exogenous RNA, several important requirements have to be considered. After the appropriate siRNA has been designed and synthesized, the molecular characteristics (as described in 1.1.2) hinder the entrance of naked siRNA through the negatively charged and hydrophobic cell membrane by passive diffusion. Various methods of transfection are available, such as the biological method with viruses as a vector, the physical method by electroporation or laser irradiation, and the chemical method with lipids, polymers or calcium phosphate [86]. Transfection with genetic material differentiates between a stable and a transient one. While in a virus-mediated stable transfection, also called transduction, DNA is integrated into the host genome, a transient transfection leads to a short-term change in gene expression without integration. Incidentally, in transient transfection *in vitro* and *in vivo*, the introduced genetic material can be minimized by cell division. Due to these facts, the choice of the transfection method depends on which purpose would be achieved, for instance up- or downregulation of gene expression or the production of recombinant proteins [86]. The chemical transfection agents like cationic lipids or cationic polymers are suitable for transient transfection of cells and are used in the present thesis for the purpose of substrate-mediated gene silencing.

The chemical transfection agents should fulfill the following aspects for successful and efficient siRNA delivery into cells: protection of siRNA against degradation, high biocompatibility and low toxicity, uptake into cells, escape from endosomes and lysosomes, prevention of errant siRNA compartmentalization (correct localization: cytoplasm), siRNA availability at the site of action, and maintaining siRNA gene silencing activity [87].

1.3.2 Lipids and liposomes as transfection agent

Lipids or liposomes are often used for siRNA transfection due to their advantages as a reliable delivery vector. Lipids consist of a positively charged, hydrophilic head with nitrogen atoms which interacts with the negatively charged sugar-phosphate backbone of the nucleic acid. The spacer of the lipid is followed by the hydrophobic tail with hydrocarbon chains [88]. The amphiphilic character of lipid molecules enables the self-assembly of lipid bilayers followed by the formation of liposomes due to energetic advantages [88]. Within the liposomes, polar drugs, such as the nucleic acid, can be encapsulated in the aqueous core for gene delivery. The lipid structure has the great advantage that the head group can be modified and the neutral lipid can be changed into a negatively or positively charged lipid. Cationic lipids are produced by modifying the head group with positively charged amine groups and are eminently suitable for the transfection of the polyanionic nucleic acids including siRNA. The negatively charged phosphate backbone of the siRNA interacts via electrostatic binding with the positively charged head group and the so called lipoplex is formed by self-assembly [89]. The mixing ratio of nucleic acid and lipid is crucial for the subsequent liposomal net charge [90]. A slight positive net charge of the lipoplex enables the interaction with the negatively charged cell membrane and the following uptake mainly by endocytosis [89]. Although the mechanism of lipoplex release from the endosome cannot yet be fully explained, Elouahabi and Ruysschaert suggest that a detergent-like destabilization of the endosomal membrane releases the lipoplexes into the cytosol [90]. After the interaction of the lipoplex with different cell organelles like the endoplasmic reticulum, Golgi, mitochondria, and nuclear membrane, the complex dissociates and releases the nucleic acid into the cytosol [90].

A well-known cationic lipid for siRNA transfection is the commercially available Lipofectamine consisting of two different lipid types: 2,3-dioleyloxy-N-[2(sperminecarboxamido)ethyl]-N,N-dimethyl-1-propanaminium trifluoroacetate (DOSPA) and 1,2-dioleoyl-*sn*-glycero-3-phosphoetanolamine (DOPE). The cationic lipid DOSPA and the neutral lipid DOPE occur in the ratio 3:1 [88]. DOPE is considered as a helper lipid because it destabilizes the endosomatic membrane and thus the lipoplex ends up in the cytosol [91]. The formation of the lipoplexes with siRNA is very simple, since only the two products are mixed together. However, care should be taken that the mixing ratio of nucleic acid and lipofectamine matches because uncomplexed cationic liposomes may compete with the lipoplexes during transfection process [90].

1.3.3 Polycationic transfection agent

Cationic polymers can bind nucleic acids via electrostatic interactions and, like cationic lipids, are an excellent carrier for transfections. The complexation of cationic polymers and nucleic acids is called polyplex. Several polycationic molecules are known as potent candidates like the natural polymers chitosan, atelocollagen or the synthetic polymers like poly-L-lysine or poly(ethylenimine) (PEI). Among them, PEI is one of the most popular synthetic polymers for nucleic acid delivery, as it was discovered as the first transfection agent in 1995 [92]. An important chemical property is the high cationic charge density. PEI possesses an amino nitrogen on every third atom that can be protonated in an endosome [92]. Therefore, PEI is capable to act as a buffer at virtually any pH, protects the nucleic acids against lysosomal degradation and provokes the influx of chloride anions. Water is thereby drawn into the endosome and osmotic swelling is the result. This 'proton sponge effect' is responsible for the bursting of the endosome and the following release of PEI-nucleic acid complexes into the cytoplasm [93]. Successful transfection efficiency is influenced by several characteristics of the polymer like the choice of branched or linear polymer structure, the molecular weight with the possible occurrence of toxicity as well as the nitrogen/phosphate (N/P) ratio. For each transfection, these parameters and the type of cells to be transfected should be taken into account. Branched PEIs are known to have greater ability to complex nucleic acids compared to the linear ones, since the structure here is more flexible (Figure 5). Unfortunately, branched PEIs provoke stronger complexation and smaller transfection complexes which leads to lesser transfection efficiency [94].

Likewise, the molecular weight is of great importance for transfection efficacy, as the molecular weight of PEI increases, the toxicity also increases [95]. The cytotoxic effects are probably caused by the permeabilization of the cell membrane [96]. Here, Zintchenko *et al.* described the modification of branched 25 kDa PEI with organic substances like ethyl acrylate, succinic or acetic anhydride, and 3–propionic acid which caused an improvement in compatibility and a reduction of the toxicity [97]. Another possibility is to combine PEI polyplex applications with the natural polymer hyaluronic acid (HA), as HA is able to reduce the cytotoxic effects of PEI [98, 99]. The N/P ratio has also a crucial meaning for an efficient gene delivery. The ratio is defined as quotient of the moles of the positive charged amine groups of the cationic polymer to the negative charged phosphate groups of the nucleic acid. The ratio determines the size of the particles and as N/P ratio increases, the complex sizes decreases [100-

102]. A complex size of about 200 nm should not be exceeded [100]. Nevertheless, it is imperative to test polyplexes from PEI for the respective cell type, since this can react differently to the transfection complexes.
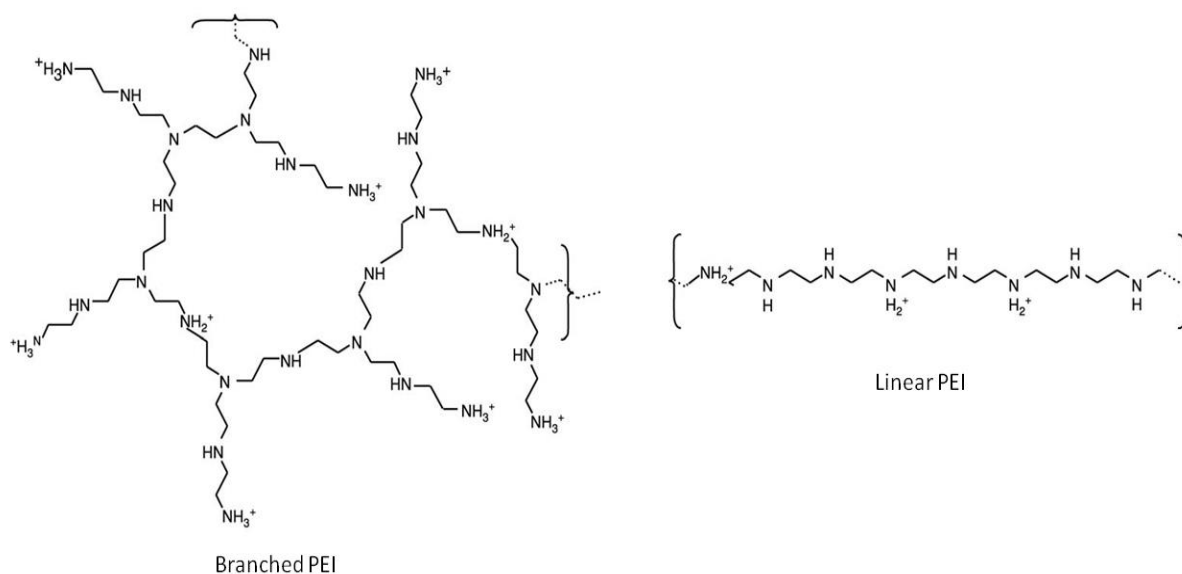

Figure 5: Branched and linear PEI. The branched molecule is known to complex nucleic acids more easily than the linear one due to its greater flexibility. The figure is adopted from Demeneix and Behr, 2005 [103].

1.3.4 Therapeutic potential of RNAi with siRNA

The possibilities for using siRNA therapy for gene silencing are very diverse and currently of particular interest for the development of new therapeutic approaches. Due to the RNA interference mechanism, targeted siRNA therapy can be used to switch off genes coding for proteins and are associated with a disease. Although RNAi therapy is referred to as gene therapy by the regulatory authorities, siRNA is not integrated into the genome. The siRNA only intervenes in the process of gene expression for a certain time. This has the advantage that the therapy can take place as long as it is necessary and desired for the cure of a disease. Great hopes are placed in the siRNA therapy, especially in diseases that are not yet to cure or show only moderate success according to the state of current therapies. These include the fight against viral infections such as HIV or HBV, the treatment of neurological diseases like Parkinson's disease or amyotrophic lateral sclerosis (ALS), the therapy of different cancers, the elimination of inflammatory processes [104], such as atherosclerosis and in-stent restenosis (ISR). In fact, the world's first siRNA therapeutic was developed by Alnylam and approved by the FDA in August 2018. ONPATTRO™ is a lipid siRNA complex

injection and used for the therapy of the polyneuropathy of hereditary transthyretin-mediated amyloidosis [105].

1.4   Delivery systems for siRNA gene silencing

The way of clinical administration of therapeutic siRNA is important for therapeutic success besides the above-mentioned stabilization of the siRNA. Three different delivery systems for siRNA are approved in clinical therapy: systemic, targeted, and local delivery. Each application has its advantages and disadvantages and should be considered when developing an siRNA application system. A systemic delivery system is easy to realize in clinical application and is often used in therapeutic cases, where the target of interest is quite difficult to reach or is widely found in the body, as in cancer or metastases. The administration of the therapeutic agent can occur via intravenous or intraperitoneal injections and oral administration, respectively [106-108]. However, in this mode of administration, a systemic infiltration of the drug takes place, care being taken to ensure that no uninvolved cells or tissues are affected in their function by siRNA transfection. Release systems can be developed that bind targeted by specific binding to the place where gene silencing is desired to prevent adverse side effects. Targeted release of an siRNA silencing therapeutic can ensure the accumulation of the therapeutic at the target site, as is often desired in clinical applications. Consequently, the amount of drug can be reduced for therapy. An excellent approach for targeted siRNA delivery in cancer therapy is the folate-mediated uptake, as cancer cells overexpress the folate receptor [109]. Folate can be covalently linked to siRNA for instance with poly(ethylene glycol) (PEG) for successful gene silencing [110]. Further modification approaches are the linkage of antibodies or antibody fragments and the arginine-glycine-aspartate (RGD) sequence [111-113]. Another approach for a site-specific siRNA release is the local delivery via local application systems or medical devices to different kinds of organs. In this case, unwanted systemic off target effects can be avoided and the amount of drugs can be reduced due to the location-limited release. Several methods have already been successfully tested like the intraocular injection of siRNA Bevasiranib (Acuity Pharmaceuticals) as well as Ranibizumab (Merck-Sirna therapeutics) for inhibiting neovascularization as a therapy in wet-age macular degeneration [114]. Likewise in respiratory diseases caused by viral infections, a local intranasal administration with siRNA may be a treatment option. Alnylam Pharmaceuticals developed successfully an antiviral siRNA for the treatment of the respiratory syncytial virus provoking no side effects [115]. Some experimental

approaches also show great promising results such as an siRNA collagen-chitosan/silicone membrane for reducing scars in wound healing or an siRNA poly(caprolactone)-PEG nanofibrous mesh for the treatment of diabetic ulcers [116]. Local delivery of siRNA shows great potential in the field of atherosclerosis or associated (in-stent) restenosis. The long-time delivery by stents or short delivery by balloons might be methods of choice to prevent the progression of inflammatory processes. In the next chapter, different approaches to local nucleotide acid release in combating atherosclerosis will be discussed.

1.4.1 Local delivery in atherosclerotic therapy

Although BMS and DES are well accepted in atherosclerotic therapy, the above mentioned pitfalls require new therapeutic strategies in stent or balloon angioplasty therapy. Various efforts have already led to promising results in recent years. San Juan *et al.* developed a gene silencing stent coating of cationized pullulan hydrogel which is loaded with siRNA targeting MMP2 in VSMCs. The siMMP2 loaded stent was implanted in balloon-injured hypercholesterolemic carotid arteries of white rabbits leading to a significant reduction of pro-MMP2 and a decrease in MMP2 activity without influencing pro-MMP9 [117]. In another study of Li *et al.*, the NOX2 protein (*Cybb*) was down-regulated after balloon angioplasty of carotid artery in an atherosclerotic rat model with an amino-acid-based nanoparticle HB-OLD7 and siCybb complex. The investigations showed significant reduction of *Cybb*, NOX2, reactive oxygen species production, and neointima formation. Since the NOX2 seems to be the major oxidase affecting intimal SMCs, it is a meaningful participant in the development of restenosis and atherosclerosis [118]. Focusing on the release system, the polymer PLGA is promising for cardiovascular stent coating as a drug carrier as thin coatings or PLGA NPs. Currently commercially available DES like Nevo™(Johnson & Johnson) and Supralimus™(Sahajanand Medical) with PLGA coating are already being used to prevent ISR [119]. A study of Brito et al. demonstrated the effectiveness and long-term effect of a PLGA and gelatin coating with eNOS expressing plasmid DNA lipoplexes that coated stainless steel stents. The use of stents in a rabbit iliac artery restenosis model resulted in eNOS production which provoked suppressed SMC proliferation and a re-endothelialization of the artery followed by a significant reduction in restenosis [120]. Additionally, Klugherz et al. transfected successfully in pig stent-angioplasty studies the arterial wall with plasmid DNA-loaded PLGA NPs that were coated on expandable stents [121]. Another promising local delivery system approach is the use

of polyelectrolyte multilayers (PEMs) that can be produced using the versatile layer-by-layer (LbL) technique. The use of positive and negative charged materials creates electrostatic interactions that stabilize the structure on the substrate. Several biomaterials are popular in PEM research work due to their positive charge like poly(L-lysine), chitosan, and PEI and their negative charge like alginate, HA, and polyacrylic acid [122-127]. PEI is much favored for siRNA PEM build-up, as it forms a non-covalent bond with its strong cationic charge density. Because drugs can be incorporated into PEMs, this system is predestined for incorporation and a substrate-mediated release of siRNA particles for gene silencing [128-134]. Hossfeld *et al.* established a PEM depot system with HA and incorporated fluorescence labeled siRNA/chitosan NPs. Cell culture tests with ECs demonstrated the occurrence of siRNA NPs until day six in the cells. The coated stent with HA and siRNA/chitosan NPs provoked an uptake of the siRNA NPs in the cells of the arterial wall in an *ex vivo* model with carotid porcine arteries [133].

1.5   Characteristics of biomaterials for medical applications

Biomaterials are of natural or synthetic origin and are used for medical devices or implants where they come into contact with the biological system. Generally, biomaterials are used to support or replace a damaged organ or tissue. It is therefore essential that the implanted biomaterial does not induce short-term or long-term defense reactions in the body or cause life-shortening damage. Biomaterials can be divided into three fields: bio-inert materials that do not interact with the tissue and do not trigger an immune response, bioactive materials that can mimic natural tissue, and biodegradable materials that are absorbed by the body and replaced by tissue regeneration [135]. Bioactive biomaterials are of particular interest for research in biomaterial-based devices as the biomaterial can be modified by introducing biological agents, drugs, peptides, and nucleic acids or by transforming it via temperature change or light and is therefore comparable with a drug.

When developing a biomaterial for the biotechnology field or medical application, the following aspects are of importance: the interaction between the biomaterial surface and the cells, the stability or instability of the material with respect to degradation, the micro- and macro-mechanical properties compared to the tissue and the ability to sterilize the biomaterial [136]. In addition, the proof that the material or the medical device is biocompatible is a prerequisite for market approval and is defined in EN ISO 10993. The product, which may later come into contact with tissue, blood or other body

fluids, is hereby investigated for possible side effects. For this, different tests can be carried out in cell culture experiments already during the selection of the biomaterial and during various development steps of the medical device. These include for instance the determination of the cell adhesion and morphological evaluation, the examination of an immune response and cytotoxicity as well as the hemocompatibility.

1.5.1 Biomaterials for bioactive applications and gene delivery systems

One of the most popular and FDA-approved biomaterial in drug delivery systems is poly(lactic-*co*-glycolic acid) (PLGA) that is a copolymer of poly lactic acid (PLA) and poly glycolic acid (PGA) [137, 138]. A significant advantage of PLGA in medical applications is the low systemic toxicity it exerts. The majority suggests that PLGA degrades by hydrolysis. However, it cannot be completely ruled out that enzymes are involved in the degradation process. During hydrolysis, the ester bond is broken and the monomers PLA and PGA are formed. Lactic acid naturally occurs in the tricarboxylic acid cycle and therefore PLA can be included in this cycle, metabolized and excreted as water and carbon dioxide [138]. Presumably, the same thing happens with PGA or it is excreted via the kidneys [138]. For the development of a bioactive coating for implants, the duration of the degradation is mostly important, so that the duration of effect can be maintained for the respective application. The physico-chemical properties of PLGA like the molecular weight, the end groups that can be capped or uncapped, and PLA:PGA ratio determine the degradation time from months up to years [139-141]. A higher content of PGA leads to a faster degradation of PLGA with the exception of PLGA 50:50 with the fastest degradation time of one to two months [142, 143].

A naturally occurring polymer which is often used as a biomaterial in different applications is HA. It is a negatively charged glycosaminoglycan consisting of D-glucuronic acid and N-acetyl-D-glucosamine linked by ß–1,4– and ß–1,3–glycosidic bonds [144]. HA is a major component of the extracellular matrix and occurs in biological fluids like synovial fluid, umbilical cord and blood with a molecular range from 10^3–10^7 Da [144-147]. Due to its biocompatibility, biodegradability, and no signs of immunogenicity, HA is excellent for wound healing, treatment of osteoarthritis, and for scaffolds in tissue engineering [148-151]. Although HA is not a classic transfection agent because of its negative charge, it is often used in combination with biomaterials like chitosan, poly-L-arginine, collagen or PEI for nucleic acid delivery and is able to reduce cytotoxic effects of PEI as mentioned before [98, 152-155]. Likewise, HA seems

to enhance transfection. An experiment by Han *et al.* showed that the complex of PEI-siRNA/HA provoked higher gene knockdown in different tumor cells than the complex without HA [98]. HA is also able to interact with cell surface receptors like HA-mediated motility receptor, CD44 or ICAM–1 that are responsible for cellular processes like migration, proliferation, differentiation and angiogenesis [156-160]. Since CD44 and ICAM–1 are over-expressed in atherosclerotic processes, it seems likely that good or better transfection results can be achieved in combination with HA.

Atelocollagen (ATCOL) is an enzymatically modified collagen type I without telopeptides, the N- and C-terminal ends [161]. The modification leads to the absence of immune stimulatory effects and the biocompatibility of collagen creates a well-tolerated material for medical application like cartilage repair or wound-healing [162, 163]. ATCOL can exist in different states of aggregation depending on the temperature and concentration. ATCOL is liquid when temperature is below 10° C and a gel at 37° C with a concentration above 0.5%. Higher concentrations cause liquefaction of the polymer with a viscosity similar to blood. Several studies dealing with the delivery of siRNA confirmed ATCOL as a potent carrier as well as an amplifier for gene silencing and protector against nucleases [162, 164-167]. Takei *et al.* demonstrated the gene delivery efficiency of ATCOL with siRNA against VEGF [168]. The polyplex remained for at least 8 days in the tumor tissue, whereas naked siRNA showed low persistence at day 1, and no occurrence at day 8. Furthermore, the tumor growth and the microvessel density were lower than in the control showing the efficiency of siRNA/ATCOL transfection.

1.6 Aim of the thesis

Cardiovascular atherosclerosis is often treated by PTCA, in which a stent can be inserted at the affected narrowed site. Unfortunately, inserting a BMS or a DES may damage the endothelium, causing a wound-healing mechanism, followed by an ISR or stent thrombosis. The mechanism causes an up-regulation of the CAMs like ICAM–1, VCAM–1, E-selectin and P-selectin. Thus, the leukocytes have more receptors available, to which they can bind and migrate into the tunica intima – a chronic, inflammatory process arises. The pivotal point of the thesis was the establishment of bioactive surface coatings consisting of a biomaterial and an embedded, complexed siRNA against the endothelial surface receptor ICAM–1 for local gene silencing. This approach is intended to further develop eluting stents with the aim of specifically minimizing the expression of ICAM–1 to prevent ISR. For this purpose, different biomaterials, such as natural or synthetic polymers should be applied to model substrates. Monolayer and multilayer systems, as well as polyelectrolyte layers should be investigated for the release of complexed siRNA particles. The biocompatibility of the polymers could be determined either with fluorescence microscopy, cell viability or cell number. Different siRNA complexes should be evaluated with a liposomal transfection reagent and a cationic synthetic polymer as transfection reagent. One intention was the substrate-mediated transfection of an endothelial cell line with the embedded and complexed siRNA particles. Therefore, the transfection efficiency of these siRNA particles should be determined by flow cytometry. Also, a major aim of this thesis was the substrate-mediated gene knockdown of ICAM–1. The ICAM–1 expression of the receptors should be examined by flow cytometry after TNF-α activation and antibody staining. Additionally, the site specific ICAM–1 knockdown by siICAM–1 can be proven by 5'-RLM-RACE-PCR. Of particular interest in terms of stent or balloon coatings are the duration of the siRNA release from the coatings, the duration of transfection and gene knockdown. The supernatants and the coated substrates of the incubated biomaterials with fluorescence labeled siRNA should be examined for their fluorescence intensity with a fluorescence reader. Since the long-term goal of this work is clinical application, the hemocompatibility of the coatings should be confirmed as well as a possible immune response against the biomaterial and siRNA lipoplexes.

2 Results

2.1 Publication I

Koenig O., Nothdurft D., Perle N., Neumann B., Behring A., Degenkolbe I., Walker T., Schlensak C., Wendel HP., and Nolte A.

An atelocollagen coating for efficient local gene silencing by using small interfering RNA

Molecular Therapy Nucleic Acids, 2017 March; 6:290-301

CVDs lead the mortality statistic on a global scale with 17.3 million deaths per year and caused especially with CHD 20% dead in the European population. The development of a CHD is mainly triggered by atherosclerotic processes. Different treatment strategies like medication with ACE inhibitors, antiplatelets, and ß-blockers or surgical interventions by CABG or PTCA with or without stent insertion are helpful and widely used. Nonetheless, tissue trauma in the tunica intima often occurs after deployment of stents, resulting in ISR. The trauma creates an inflammatory process that causes the endothelial cells to increasingly express adhesion molecules such as E-selectin, VCAM–1 and ICAM–1. Leukocytes migrate via leukocyte diapedesis into the tunica intima and cause proliferation of smooth muscle cells and further inflammatory processes. Re-narrowing and an occlusion of stented atherosclerotic vessel is the result. DESs release anti-proliferative agents to counteract neointimal hyperplasia. However, these agents are suspected to cause unwanted late restenosis as they prevent re-endothelialization of the vessel. The aim of this study was to develop a local siRNA delivery system as a stent coating for the endothelial adhesion molecule ICAM–1 which is able for long-term release and ICAM–1 knockdown. ATCOL, known for its low immunogenicity, was selected as a suitable biomaterial with transfection and depot effect. First, the most biocompatible ATCOL coating was determined by testing four different ATCOL concentrations on cell viability with EA.hy926 cells. ATCOL coatings of 0.008%, 0.016%, 0.032%, and 0.064% solution were prepared by diluting the stock solution with 5 mM sodium acetate buffer (pH 5.5) and 100 µL were air-dried on glass slides (10 x 10 x 1 mm). The cell viability was tested after 48 h cultivation of EA.hy926 seeded onto the coated glass slides by determination of the cell number by CASY cell counter and by microscopy images. The coatings of 0.008%, 0.016%, and 0.032% showed instead of 0.064% no significant decrease in cell number and morphology and

were comparable to the cells cultured on the uncoated glass control. Therefore, in the following experiments, the 0.008% and 0.032% ATCOL coatings were tested as possible siRNA transfection coatings. Both ATCOL solutions were mixed with different siRNA-Lipofectamine®2000 solutions of 1 µg siRNA + 1 µL Lipofectamine, 2.5 µg siRNA + 2 µL Lipofectamine, and 5 µg siRNA + 3 µL Lipofectamine and incubated for 20 min for complexation before 100 µL were air-dried on glass slides. ATCOL/siRNA coatings were observed for the release kinetic of siRNA AF 488 particles and the transfection efficiency with and without Lipofectamine by flow cytometry. The ICAM–1 expression was tested with ATCOL/siICAM–1 coatings after 48 h cultivation of EA.hy926 on coated glass slides and activation with TNF-α for 14 h. Long-term knockdown of ICAM–1 was determined over eight days with cells either cultivated on ATCOL/siICAM–1 coated glass slides or cells seeded one day prior experiment before incubation with ATCOL/siICAM–1 complexes in liquid form for 4 h and replaced by cell culture medium. The siICAM–1 mediated cleavage site of *ICAM–1* mRNA after transfection was analyzed with the 5'-RLM-RACE-PCR technique. Hemocompatibility of the coatings was determined with human blood incubation and ELISAs. The transfection potential of ATCOL was tested using the transfection efficiency and ICAM–1 knockdown experiments. No significant transfection efficiency could be detected with 0.008% or 0.032% ATCOL/siRNA AF 488 coatings without the use of Lipofectamine. The addition of Lipofectamine resulted in a significant increase in efficiency with a maximum value of 68.9% positive cells with 5 µg siRNA and 0.008% ATCOL coating, and 75.2% with the same amount of siRNA and 0.032% ATCOL. The ICAM–1 expression of cells cultivated on 0.008% ATCOL and siICAM–1 without Lipofectamine also showed no reduction of the ICAM–1 expression. However, coatings with Lipofectamine caused a concentration dependent decrease in expression. An ICAM–1 knockdown of 47.9% was observed with 0.008% ATCOL and 5 µg siRNA showing significant decrease compared to the control with siSCR (scrambled siRNA). The same results were achieved with the 0.032% coating, whereby a higher ICAM–1 knockdown of 60.4% was seen here. The long-term knockdown experiment revealed the effectiveness of the ATCOL-mediated local transfection in comparison to the conventional transfection, where transfection particles linger in suspension. The 0.008% ATCOL and 5 µg siICAM–1 coating achieved significant knockdowns after cultivation day 2, 4, and 6 and a knockdown until day 8 with 11.6%. Highest knockdown was seen on day 2 with 68.9%, followed by day 4 and 6 with 63.3% and 48.7%,

respectively. In contrast, transfection particles in suspension could not provoke a significant ICAM–1 knockdown during the whole experiment and furthermore, showed significant higher ICAM–1 values until day 6 in comparison to the ATCOL/siICAM–1 coatings. The 0.032% coating caused a lower knockdown than the 0.008% ATCOL coating, and therefore, only a significant reduction of ICAM–1 expression was seen until day 4. Additionally, there were no significant ICAM–1 differences between the ATCOL coating- and the suspension-mediated transfection process. Knockdown with 41.1% and 41.0% was observed on day 2 and 4. The results of the release study were comparable and in line with the knockdown experiments. After 9 days release of siRNA AF 488, 0.032% ATCOL with 5 µg siRNA contained the highest residual amount of siRNA followed by 0.008% ATCOL with the same amount siRNA. A significant difference between 1 µg and 5 µg siRNA AF 488 with 0.032% ATCOL coating was observed at this time. The highest amount of siRNA release from all coatings happened within the first 4 h. After 24 h, the release rate of 0.008% ATCOL coating was higher than the one of the 0.032% coating. The specific mRNA degradation by knockdown experiments with ATCOL/siICAM–1 coatings was proven with the 5'-RLM-RACE-PCR technique. The specific cleavage site at bp 1,818 was detected only with this coating and not in control layers without siICAM–1. The hemocompatibility of the highest concentration 0.032% ATCOL/siICAM–1 coating was analyzed after 1 h incubation with human blood. The cell numbers of leukocytes, erythrocytes, platelets, lymphocytes, monocytes and granulocytes showed no significant changes in comparison to the 1 h control. Additionally, SC5b9 and C3a of the complement system and PMN elastase also revealed no change in values. Furthermore, a significant increase in hemolysis values was detected, wherein the limit for hemolysis of 40 mg/100 mL was not exceeded.

2.2   Publication II

Koenig O., Zengerle D., Perle N., Hossfeld S., Neumann B., Behring A., Avci-Adali M., Walker T., Schlensak C., Wendel HP., and Nolte A.

RNA-eluting surfaces for the modulation of gene expression as a novel stent concept

The coronary artery disease is caused by atherosclerosis in heart coronary vessels triggering stroke and heart attack. A common treatment used in vasoconstriction is the established PTCA method. In this minimally invasive procedure a balloon catheter can be introduced, with which at the same time a coronary stent can be placed at the affected atherosclerotic site. Nevertheless, the insertion of stents, such as BMS or DES involves the risk of ISR or stent thrombosis. Placing of the metal mesh at the affected artery damages the endothelial cells in the tunica intima and provoke atherosclerotic plaque rupture. Consequently, the wound-healing mechanism, called neointimal hyperplasia, starts with the first step: inflammatory cell infiltration. Inflammatory mediators and chemoattractant factors recruit leukocytes from the blood system for their diapedesis at the damaged tissue. ECs react with an enhanced expression of their binding sites, the CAMs like ICAM–1, VCAM–1, E-selectin, and P-selectin. The leukocytes adhere on the endothelial binding sites and migrate into the tunica intima. Additionally, the vascular smooth muscle cells proliferate and migrate from the intima to the neointima due to the chronic inflammatory process. A promising approach to circumvent these adverse effects by bare metal stents was the development of DES with chemotherapy medication or immunosuppressants. Although ISR could be reduced up to 60%–80%, DESs provoke slow re-endothelialization causing a late in-stent thrombosis and demand a prolonged antiplatelet therapy. All these adverse effects have to be eliminated with new approaches in the design of drug eluting stents. The purpose of this study was to establish a long-term drug-eluting coating system with three different derivatives of the approved biomaterial PLGA which were: PLGA Resomer® RG 752 H, 75:25, acid terminated, 4,000–15,000 Da (= PLGA 1); PLGA 85:15, ester terminated, 50,000–75,000 DA (= PLGA 2); PLGA Resomer® RG 756 S, 75:25, ester terminated, 76,000–115,000 Da (= PLGA 3). The degradation of PLGAs by hydrolysis depends on their molecular weight, end groups (capped or uncapped) and the PLA:PGA ratio, whereby the increase of PGA accelerates the degradation. The eluting drug was siRNA against ICAM–1 alone or with eGFPmRNA together. They

were Lipofectamine® 2000–encapsulated and locally transfected. The PLGA was freshly dissolved in ethyl acetate before each use with a concentration of 1 µg/µL. Coverslips (15 mm diameter) were used for pH value analysis, cell viability assay and hemocompatibility test with air-dried coating of 50 µg of each PLGA (1 to 3). For co-transfection with siRNA and mRNA 13 mm diameter coverslips were air-dried with PLGA 1 (50 µg/ µL) containing a transfection mix of 10 µg eGFPmRNA, 3 µg siRNA, and 2 µL Lipofectamine. Glass slides (10 x 10 x 1 mm) were coated for all other transfection experiments to evaluate transfection efficiency, knockdown and 5'-RLM-RACE-PCR. For this, Lipofectamine and siRNA were complexed in Dulbecco's Modified Eagle Medium (DMEM) for 30 min with different amounts: 1 µg siRNA and 1 µL Lipofectamine, 3 µg and 2 µL, and 6 µg and 4 µL. Subsequently, PLGA and Lipofectamine/ siRNA complexes were mixed 1:1 and 100 µL of this solution were pipetted onto one glass slide. First of all, the degradation of PLGA 1–3 alone was tested over four weeks in cell culture medium under standard culture conditions regarding the pH value stability. Furthermore, the cell viability of EA.hy926 was tested with the supernatants after one, two, three, and four weeks of cultivation of the pH value test with the CASY® cell counter and the MTT-assay after 48 h cultivation. Hemocompatibility of PLGA 1–3 was tested with fresh human blood after 1 h gently shaking at 37° C. Different inflammatory markers were determined after the incubation of human vascular endothelial cells (hVECs) with PLGA 1–3 coatings and in combinations with Lipofectamine alone or with siICAM–1 or scrRNA by quantitative Real-Time PCR (qRT-PCR). The uptake of PLGA-eluting siRNA AF 488 was analyzed by flow cytometry after 24 h incubation of coated slides laying on EA.hy926 cells. The ICAM–1 knockdown and the ICAM–1 expression was determined after 48 h of transfection with coatings consisting of PLGA1–3 and 3 µg siICAM–1/Lipofectamine complex by flow cytometry and qRT-PCR with EA.hy926 and hVECs. The ICAM–1 specific cleavage site was determined with the 5'-RLM-RACE-PCR. PLGA mediated long-term release was tested with siRNA AF 488 and a multilayered coating system consisting of eight alternately dried layers of 500 µg PLGA and 3 µg siRNA complexed with Lipofectamine and a capping layer of 1 mg PLGA. The co-transfection of eGFPmRNA and siRNA AF 555 in PLGA 1 was examined by flow cytometry. The first result of pH stability examination showed the same variations in pH value in all three PLGA samples and the uncoated coverslip control. Lower pH values were observed for PLGA 1 after two, three and four weeks and for PLGA 2 after two and four weeks

in comparison to PLGA 3. The cultivation of EA.hy926 and the supernatants of PLGA 1–3 caused no significant changes in cell viability. The highest but not significant decrease in cell viability was seen with the three-week-old supernatant, with viability decreasing to 85% with the PLGA 2 and 3 supernatant and to 90% with PLGA 1. The hemocompatibility of PLGA 1–3 could be proven by the tests with fresh human blood after 1 h incubation. The blood cells like erythrocytes, platelets, leukocytes, lymphocytes, monocytes, and granulocytes showed no significant changes after 1 h incubation with PLGA 1–3 coated slides in comparison to the control slides. Also, no significant changes in the values of the parameters of the complement system C3a and SC5b9 were found between 1 h control and samples. Significant increases in complement system samples and blood parameters were only seen between 0 h controls and the 1 h control. The PLGA 1–3 coatings did not provoke a significant change within these parameters. The results of ß-Thromboglobulin, polymorphonuclear granulocyte (PMN)-elastase, and thrombin-antithrombin III-complex (TAT) examination with PLGA 1–3 coatings did not differ significantly from the 1 h control. The analysis of the immune response regarding inflammatory markers CXCL–7, CXCL–10, signal transducer and activator of transcription 1 (STAT1), and OAS detected no augmentation in mRNA level when only PLGA 1–3 was used. The addition of Lipofectamine caused an increase in mRNA expression, which was intensified by siICAM–1 and scrRNA. However, dsRNA augmented the mRNA expression of CXCL–10, STAT1, and 2'-5'-oligoadenylate synthetase (OAS) to a much greater extent. When analyzing the data of the short-term uptake of siRNA AF 488, the appropriate amount of siRNA could be determined for further experiments. The amount of 3 µg siRNA with Lipofectamine and PLGA 1–3 effected significant higher transfection efficiencies than with 1 µg. Although, the increase to 6 µg resulted in the highest level with 96% and 95% for PLGA 2 and PLGA 1, this increase was not significant. Consequently, 3 µg siRNA was used in the following experiments, whereby PLGA 1 revealed the highest efficiency. Also in the knockdown experiment, the 3 µg siRNA amount resulted in the highest significant ICAM–1 knockdown of 36% with EA.hy926 and the highest knockdown of 22% with hVECs. While significant ICAM–1 knockdown could be observed with EA.hy926 in comparison to the controls with TNF-α, PLGA 1 and TNF-α, and PLGA 1 with scrRNA and TNF-α, hVECs did not show such clear results. Subsequently, it was demonstrated that the siICAM–1 transfection and the following mediated knockdown correctly cleaved the mRNA transcript at the base

pair 1818. The long-term uptake experiment of siRNA AF 488 revealed high transfection efficiency values until day six and long-lasting efficiency until day twenty. Very high values were reached with at least 80% after the first incubation day and 85% after the second. PLGA 1 noted the highest efficiency with 96%. Within the third to sixth day, efficiency dropped to a baseline of 1–2%. The co-transfection experiment of siRNA AF 555 and eGFPmRNA proved that PLGA 1 is suitable as a coating system for this purpose. The co-transfection yielded 11% positive cells for siRNA AF 555 and eGFPmRNA. Separate transfection of PLGA 1 with siRNA AF 555 complexes showed 26% positive cells and PLGA 1 with eGFPmRNA 11%.

2.3   Publication III

Koenig O., Neumann B., Schlensak C., Wendel HP., and Nolte A.

Hyaluronic acid/poly(ethylenimine) polyelectrolyte multilayer coatings for siRNA-mediated local gene silencing

The RNAi mechanism is a promising approach for various therapeutic applications, like infectious diseases, cancer or CVDs with the aim of transient specific gene silencing. Local gene silencing is of particular importance for therapeutic approaches where a local and specific knockdown via siRNA is desired. PEMs offer the possibility to build a construction via the versatile LbL technique into which active agents can be integrated and afterwards released. The build-up of PEMs is generally carried out with familiar biomaterials of opposite charges such as with the synthetic cationic polymer PEI. It is known as a transfection agent for gene delivery with its condensing ability and is often used with siRNA. The negatively charged polymer is the naturally occurring HA. Its high molecular weight variant is attributed a cytotoxic-reducing effect of PEI. During an inflammatory process such as in atherogenesis, different CAMs like E-selectin, VCAM–1, and ICAM–1 are increasingly synthesized by overexpressed genes on activated endothelial cells. The consequence of this is that leukocytes interact with the receptors of the CAMs and the diapedesis with previous rolling and tethering occurs. In case of stent insertion, the endothelium may be injured at the site of placement, which also causes an inflammatory process with leukocyte diapedesis. As a result, this can lead to reocclusion of the artery as well as to stent occlusion. Hence, in this study an LbL build-up of HA and PEI-siRNA were established and tested as a novel local gene silencing construction for the cell adhesion molecule ICAM–1. Herein, 20 µM siRNA and 25 kDa branched PEI were both diluted in 0.15 M NaCl for 10 min and afterwards mixed with a ratio of 18,75 mN/P. After 20 min of incubation, the PEI-siRNA complexes were ready for LbL build-up on 10 x 10 x 1 mm glass slides. Sodium hyaluronate 95% was dissolved with 1 mg/mL in 5 mM sodium acetate buffer (pH 5.5). First, precursor layers, consisting of a monolayer with 750 kDa PEI and two following bilayers of HA and 25 kDa PEI, were deposited on the slides by a 10 min dipping and in between 3 x 2 min washing steps. Bioactive bilayers of HA/PEI-siRNA were applied afterwards in the same way.

Preseeded EA.hy926 cells were incubated in a "reverse assay" for 24 h with the LbL coated glass slides. Afterwards, the ICAM–1 receptor expression was examined by flow cytometry. Here, control cells incubated with uncoated slides, cells with PEI-siICAM–1 coated slides, and cells with PEI-siSCR coated slides were stimulated with TNF-α for 14 h to induce ICAM–1 expression. However, neither the 3 nor the 10 bilayers of PEI(HA/PEI)$_2$(HA/PEI-siICAM–1) provoked a significant reduction of the ICAM–1 expression. Consequently, the LbL technique was modified by exchange the dipping steps of HA and PEI-siRNA to drying steps. An advantage of this technique was that the amount of incorporated siRNA could be provided. With every drying step of PEI-siRNA, 0.5 µg siRNA was deposited in one bilayer. In this case, the ICAM–1 expression of EA.hy926 was significantly decreased with PEI(HA/PEI)$_2$(HA/PEI-siICAM–1)$_{3,5,7,10,12}$ in comparison to the TNF-α control and to their PEI(HA/PEI)$_2$(HA/PEI-siSCR)$_{3,5,7,10,12}$ controls. The highest ICAM–1 reduction was determined with 10 bilayers and 44% remaining ICAM–1 expression.

Afterwards, this successful established transfection system was tested for transfection efficiency with fluorescence labeled siRNA (siRNA$_f$), for duration of siRNA$_f$ release and ICAM–1 knockdown, and for cell number determination. The transfection efficiency test of 3 and 10 bilayers confirmed the effectiveness of the bilayer system with a result of 50% transfection efficiency using coated slides with PEI(HA/PEI)$_2$(HA/PEI-siRNA$_f$)$_{10}$. Since it was noted in the ICAM–1 knockdown experiment that 12 bilayers could not provoke a higher knockdown than 10 bilayers, it was of interest whether a significant increase in bilayers can further reduce the ICAM–1 expression. However, the augmentation of bilayers up to 24 did not reduce the ICAM–1 expression more than the 10 bilayers. To determine the duration of the release, the PEM coated slides already cultured for 24 h were cultured again on preseeded cells for further 24 hours. A non-significant reduction of ICAM–1 expression was found in both PEMs PEI(HA/PEI)$_2$(HA/PEI-siICAM–1)$_{12,24}$. The release study confirmed this result showing an initial burst release within the first hour of all PEM bilayers followed by a minor release until 48 h at 37 °C in PBS. Additionally, the fluorescence intensity of the completely scanned coated PEMs showed highest values at time point zero before incubation and a significant decrease of intensity after 1 h incubation under same conditions. The living cell number of PEM PEI(HA/PEI)$_2$(HA/PEI-siICAM–1 or -siSCR)$_{10}$ dried coatings was compared to a monolayer with the same amount of siRNA.

The results showed a significant reduction of living cell number in the monolayer consisting of 5 µg siICAM–1 or siSCR.

3   Discussion

3.1   Efficient local gene silencing mediated by ATCOL coatings with embedded siRNA lipoplexes

Cardiovascular stent therapy needs new ways to improve the outcome of long-term therapy. During angioplasty therapy, inserting the stent is seen as a trauma to the intimal structure of the arterial wall, resulting in an immune reaction and ultimately a re-narrowing of the vessel due to wound-healing mechanisms [169]. The commonly-used DESs were introduced to inhibit neointimal hyperplasia and consequently, reduce the risk of ISR. However, first and possibly also second generation of DESs fail to prevent late stent thrombosis after discontinuing the dual anti-platelet therapy [48]. The development of gene-eluting stents is a promising new approach for the alteration in gene expression involved in vascular wall regeneration. For this purpose, a surface coating with ATCOL was developed in this project, which can release a complexed siRNA over a longer period of time. Different ATCOL concentrations were tested in a cell culture assay with the immortalized EC line EA.hy926 to determine the cell viability on the surfaces. ATCOL has the property that its physical state changes depending on the temperature and concentration. At a temperature less than 10° C ATCOL is liquid and with increasing temperature the protein becomes a gel between room temperature and 37° C depending on the concentration [166]. Cultivation of cells on the coatings with 0.008%, 0.016%, and 0.032% ATCOL showed cell counts comparable with cells growing on the uncoated glass slide. The 0.064% ATCOL coating provoked a significant reduction of the cell number in comparison to all samples. In addition, the light microscopic images showed an atypical morphology with a rounded cell body and hardly any pseudopodia. The stiffness of the substrate plays a crucial role in cell adhesion, migration, proliferation, and differentiation [170-175]. Each cell type is adapted to its environment and therefore prefers either a hard or a soft substrate for cell growth. Also, Nolte et al. achieved lower cell viability and/or adhesion in a softer substrate with PEMs from natural polymers compared to a stiffer material with synthetic polymers [176]. Likewise, the softer substrate caused the rounding of the cells. Consequently, an increasing ATCOL concentration is responsible for softer coatings. During the development of a gene-releasing coating, release and transfection are the pivotal point. Despite literature statements from studies with ATCOL [161, 162, 165, 166], the embedded siRNA particles did not allow efficient uptake into the cells with

0.008% and 0.032% ATCOL concentrations in combination with 1, 2.5, and 5 µg siRNA AF 488 after 48 h. Likewise, no reduction of the ICAM–1 protein could be achieved with these coatings when using siRNA against ICAM–1. Other studies, however, showed successful transfection with an efficiency of 40–60% with 0.008% ATCOL layers and gene silencing with siRNA [161, 177]. The difference with our static method is that the coating was made by rotating the ATCOL solution with siRNA. This could be the reason for the different efficiencies and outcome as well as the use of other cell lines. By complexing the siRNA with Lipofectamine®2000, the transfection efficiency could be significantly increased. Highest transfection efficiency was reached with 5 µg fluorescent-labelled siRNA and 0.008% ATCOL with 68.9% fluorescence positive cells and 0.032% ATCOL with 75.2%. Overall, the 0.032% ATCOL coatings provoked higher transfection efficiency values than the 0.008% ATCOL.

The gene silencing of ICAM–1 was tested in a short-term experiment with 0.008% and 0.032% ATCOL coatings with embedded 1, 2.5 or 5 µg siICAM–1 lipoplexes. A significant reduction in ICAM–1 was achieved with 5 µg siICAM–1 and the 0.008% and 0.032% coatings, respectively. Thus, the ICAM–1 gene silencing approach for preventing the leukocyte adhesion cascade could be a promising therapeutic option to prevent an inflammatory process after stent placement. This involves intervening in an early state of wound healing before the inflammatory process provokes for instance the SMCs recruitment [28, 54]. The functionality of the local ATCOL delivery system with embedded siICAM–1 lipoplexes showed the proof of the correct cleavage site for the ICAM–1 mRNA by 5`-RLM RACE PCR by 5-RLM RACE. This demonstrates that the gene silencing of ICAM–1 was due to the specific siRNA for ICAM–1 and no side effects have influenced the process.

Since sustained release of the lipoplexes is desired for substrate-mediated gene silencing, release with complexed siRNA AF 488 to day 9 was tested. The combination of 0.032% ATCOL and 5 µg siRNA showed the highest release over time until day 9 followed by 0.008% ATCOL and 5 µg siRNA. An initial burst release within the first 4 h was observed followed by a sustained release until the end of the experiment. In the first days of transfection, burst release seems to be an important prerequisite for high and long lasting gene silencing [178, 179]. The difference between the releases of the siRNA AF 488 with the two differently concentrated ATCOL coatings is due to the collagen matrix density. A lower collagen concentration leads to a reduced matrix density, which leads to a faster escape out of the matrix [167]. The results of the

release study and of the long-term transfection experiment support this finding of Sano et al.

During the long-term gene-silencing experiment, the superiority of substrate-mediated transfection and gene silencing compared to the suspension-mediated variant was clearly demonstrated with 0.008% ATCOL coating and 5 µg siICAM–1. The gene silencing of ICAM–1 was significantly higher until day 6 using substrate-mediated transfection and the gene silencing still showed a knockdown of 11.6% on day 8, whereas no effect was seen in the suspension-mediated transfection. In general, the 0.032% ATCOL coating could not provoke such considerable ICAM–1 knockdown values and significant gene silencing was observed until day 4 by substrate-mediated transfection. The higher transfection efficiencies and higher release values of 0.032% ATCOL with 5 µg siRNA could be explained by chemical processes. If the amount of ATCOL for the complexation of the siRNA is increased next to Lipofectamine, the two positively charged substances compete for the negative siRNA. Therefore, there could be more naked siRNA, which increases levels in the release and transfection efficiency study. Consequently, naked siRNA could be degraded by nucleases and led to lower gene silencing with 0.032% ATCOL coating.

With regard to application of the coating on coronary stents, the hemocompatibility of ATCOL/lipoplex coating was proved. No significant reduction of blood parameters was observed and the parameters of the complement system SC5b9 and C3a as well as the PMN elastase were not increased. Additionally, the coatings provoked no hemolysis.

3.2 PLGA layers for the modulation of ICAM–1 gene expression as a stent concept for atherosclerosis

As already mentioned, new approaches to PTCA treatment with the insertion of stents are being sought in order to improve the outcome. The combination of gene therapy and eluting stents may be important for the suppression of the inflammatory reaction after stent insertion. Gene therapy is a promising approach because it can be used to target and control the expression of proteins [180]. The aim of this study was to develop and evaluate a long-term release coating for siRNA delivery with the FDA- and EMA-approved biomaterial PLGA for the healing of the artery which can take up to three months [181]. The three PLGA 1–3 resomers with different lactide:glycolide ratios, different molecular weights, and end-capped or non-end-capped polymers proved their biocompatibility by one aspect, which was checking the pH value of the cell culture medium with PLGA coated slides and the cell viability after cultivation with EA.hy926. During the hydrolysis of PLGA, acids are formed which are considered to be a disadvantage for the use of the biomaterial in drug release [182]. However, the pH value showed no shift in the acidic region, but remained in the neutral to basic range. Presumably, the cell culture medium with its buffering properties is responsible for the stability of the pH and the slight basic shift is due to the storage in the refrigerator. PLGA 1 coatings showed a lower pH value from the second to the fourth week compared to the other PLGAs. This confirms the fact that PLGA 1 degrades faster with its smaller molecular weight and free carboxyl end groups than PLGA 2 and 3 with capped end groups [140, 141]. All three PLGA coatings were considered non-toxic as cell viability remained constant during the first and second week and decreased less than 30% in the third and fourth week (according to EN ISO 10993–5). In addition to non-cytotoxic effects, hemocompatibility as another aspect for biocompatibility also plays an important role in the development of a bioactive coating. This includes, for example, that the coating does not affect blood parameters, the complement system is not activated, and the platelets are not activated and aggregated. The hemocompatibility of the three PLGA coatings has been proven by not detecting any decrease in the number of platelets, leukocytes, lymphocytes, monocytes, and granulocytes. This suggests that there is no unwanted adhesion of blood cells to the polymer coating. Furthermore, activation of the complement system and the platelets can be ruled out since the associated parameters such as ß-Thromboglobulin, TAT,

PMN-elastase, C3a, and SC5b9 showed no change after blood incubation. Consequently, there is no risk of thrombus formation due to the PLGA coating.

Since in one of our previous study, the activation of inflammatory markers was detected by Lipofectamine, this effect was also observed here [183]. While the PLGA did not increase the expression of the inflammatory and interferon response markers, the addition of the Lipofectamine resulted in an increase in the markers. In addition to the specific binding of the siRNA, a binding to the Toll-like receptor 3 may also occur, as in the case of the dsRNA, where a very high reaction takes place.

The main focus of the study was on the determination of transfection efficiency and gene silencing of ICAM–1 via PLGA-mediated delivery. The preliminary short-term study showed that even with 3 µg siRNA AF 488 and PLGA 1 the highest transfection efficiency (95%) with fluorescent labelled siRNA was achieved. PLGA 2 and 3 showed significantly lower efficiency values. Although an increased siRNA amount of 6 µg increased the efficiency in the coating with PLGA 2 and 3, the values were not significantly different from 3 µg siRNA. This means that the cells are already saturated with an amount of 3 µg siRNA and increasing the amount would not bring any significant added value. As noted in the pH determination, PLGA 1 degrades the fastest. This can now again be proven with the highest transfection efficiency. The faster the polymer degrades, the more siRNA lipoplexes are released for transfection, as proven in other studies [133, 184]. The long-term experiment to determine the transfection efficiency showed that up to the end of the test on day 20 where an uptake of the siRNA AF 488 had taken place. Within the first two days, the efficiency was very high and reached the highest level with the PLGA 1 coating at 96%. Such a burst release is seen as a positive effect in the transfection of cells, as this affects the effectiveness for a long-term gene silencing. A phase with decreasing uptake of siRNA NPs from day 3 to 6 followed and from day 7 to 20 a phase with progressively low uptake of siRNA NPs. The results suggest that the developed PLGA multilayer coating is a promising approach for a stent coating to release an active agent over a period of time.

In addition, co-transfection with an eGFPmRNA and siRNA AF 555 was achieved with the multilayer PLGA construction. To our knowledge, this is the first time that cells have been transfected with both siRNA and mRNA. This proves that it is possible to include active ingredients in different layers of the multilayer system and to deliver them simultaneously. Furthermore, this shows that EA.hy926 and possibly cells in general

are able to control two opposing mechanisms in protein expression by external intervention.

The PLGA coatings were tested for the release of lipoplexes with siICAM–1 and thus for the potential of gene silencing. Once again PLGA 1 coating was the most effective as it reduced ICAM–1 expression of EA.hy926 with 64% the most. Although PLGA 2 and 3 significantly reduced ICAM–1 expression, they did not reduce it as much as PLGA 1. The results of the primary hVECs showed reduced but not significant reduced ICAM–1 expression levels after transfection with the siICAM–1 integrated lipoplexes in the PLGA layers compared to EA.hy926. This result is consistent with the literature, as it is also described here that primary cells are generally more difficult to transfect [185, 186]. The correct cleavage site of ICAM–1 was confirmed by 5`-RLM RACE PCR after siICAM–1 transfection. In summary, the PLGA 1 coating with integrated lipoplexes is a promising approach for stent therapy of arteriosclerosis.

3.3 Local gene silencing of ICAM–1 by polyelectrolyte multilayer coating of hyaluronic acid and poly(ethylenimine)

Due to their complex structure, PEMs are excellently suited for embedding active ingredients and releasing them in the system. The structure with oppositely charged polymers is stable due to the electrostatic interactions. The transfection agent PEI is very well suited for a PEM construction, because it can complex the siRNA and mediates transfection. Moreover, with its positive charge it can bind with a negatively charged polymer, such as HA. The aim of the study was to develop a PEM system with integrated siRNA polyplexes for substrate-mediated gene silencing of ICAM–1. The multilayer build-up of HA and PEI with complexed siRNA took place with two different coating methods (dipping and drying) and showed that the modified system (drying) yields the desired success in gene silencing. The dipping method for PEM build-up did not cause significant reduction of the adhesion molecule ICAM–1 with PEI(HA/PEI)$_2$(HA/PEI-siRNA)$_{3,10}$ and 1.5 µg siICAM–1 and 5 µg siICAM–1, respectively. The modified LbL technique, in which the HA layers and the polyplex layers were alternately dried by air drying, resulted in a significant reduction of ICAM–1. The highest reduction of 44.4% remaining ICAM–1 adhesion molecule was achieved with 10 bilayers and the lowest reduction of 74.0% with 3 bilayers. The transfection efficiency test underlined the effectiveness of the air drying method, where 50.3% cells were transfected by 10 bilayers in comparison to 3 bilayers with 21.1% transfected cells. These results suggest that the dipping time of 10 minutes may not be sufficient for the required amount of polyplexes to bind to the HA layer. In another study, the dip and wash method used a dip time of 2 h for DNA lipoplexes with glycol-chitosan and HA layers. Both cell types, NIH3T3 and HEK293, were successfully transfected [129]. The drying method allowed effective application of the HA and polyplex layers. It is advantageous that the amount of siRNA dried up can be determined precisely, since liquid is not left over like during dipping. The results of transfection efficiency and gene silencing also demonstrate that the amount of 5 µg siRNA makes a significant difference, as was the case in our previous studies [179, 187]. The gene silencing experiment was performed with 3, 5, 7, 10, and 12 bilayers and all bilayers showed a significant reduction of ICAM–1 as a function of the number of layers. With increasing number of layers and thus also the amount of siRNA, the reduction of ICAM–1 up to the tenth double layer became higher. The 12 bilayers showed no further reduction of ICAM–1 and the value was slightly higher than that of 10 bilayers. Even a significant

increase in the bilayers to 24 did not yield any higher reduction of ICAM–1. This leads to the assumption that EA.hy926 from a siICAM–1 amount of 5 µg are already saturated and do not take up any further siRNA in the cell or that the PEM structure has reached its maximum after 10 bilayers. The successful bilayer construction of HA and the polyplexes was confirmed in the gene silencing experiment and further underpinned by scanning the different bilayer platelets for fluorescence intensity. As the bilayers increased, so did the intensity. The drying method thus shows the controlled assembly and incorporation of the bilayers and the siRNA$_f$.

The release experiment showed a rapid release of the siRNA$_f$ particles from all bilayers (3, 5, 7, and 10). Within the first hour almost all of the siRNA$_f$ was released from all bilayers and the subsequent measurement times after 4, 24 and 48 h showed comparable values to the controls. Thus, the fast release of siRNA$_f$ during the first hour is responsible for the high transfection efficiency and gene silencing of ICAM–1. As shown in previous studies, such a burst release is responsible for a very high efficiency of gene transfection and especially gene silencing [178, 179, 187]. Evidence of rapid release of polyplexes also revealed that the re-cultivation of the 10 and 24 double-layered PEMs could not achieve gene silencing of ICAM–1 after renewed 24 h cultivation. The release time of polyplexes from the PEMs is of particular importance for use in the field of atherosclerosis therapy. Depending on how fast the particles are released and the cells transfected, coatings can be used differently. For example, a rapid-release coating system may employ the use of a balloon catheter, which briefly expands the atherosclerotic narrowed artery and transfects cells at the same time. An advantage of this therapy is that no foreign body remains in the vessel, which could cause a defense reaction of the body. Furthermore, drug eluting balloons are promising in the therapy of coronary interventions including ISR as shown in many studies with paclitaxel or sirolimus [188-190].

Although in our experiments the reverse assay was used for the transfection experiments, viability of the cells is important for successful transfection. The multilayer structure of HA and the polyplexes is better tolerated in terms of viability for the EA.hy926 cells than a monolayer of the polyplexes. The cell numbers of the multilayer coatings with 10 bilayer siICAM–1 or siSCR were both significantly higher than the comparable samples with the monolayer. The HA had a positive effect on the cell number and seems to have a protective effect on the cells. Similarly, one study showed that the combination of HA and PEI has less toxic effects on the cells than PEI alone

[98]. High molecular weight HA which was used in our and Han's study is credited with an anti-inflammatory effect [191].

4   Future perspectives

The current interventional therapy in the treatment of arteriosclerosis is seeking new approaches to reduce the rate of restenosis following stent implantation. Many new approaches are being investigated which have the potential to release drug-eluting substances from substrates to effect endothelial healing or re-endothelialization.

With this thesis, three different bioactive coatings with siICAM–1 have been developed that can improve the outcome of atherosclerotic interventional therapy with a stent or balloon catheter. Since not only ICAM–1 as one adhesion molecule is responsible for the leukocyte-adhesion molecule cascade; several other adhesion molecules like E-selectin, P-selectin, VCAM–1 and PECAM–1 should be tested. In addition, it could investigate how simultaneous transfection with a cocktail of the siRNAs of the above-mentioned adhesion molecules affects the respective gene expressions. Furthermore, the promising co-transfection of ICAM–1 and eGFPmRNA should be further investigated with a functional mRNA. The insertion of the natural anti-platelet protein CD39 as mRNA could increase gene expression and thus counteract thrombosis which was already described in our group. This is a promising approach in stent therapy, as on the one hand oral antiplatelet therapy can act locally and on the other hand the risk of ISR is reduced. For the desired re-endothelialization of the stent area, the anti-CD34 antibody could also be integrated into the long-term coatings. This can bind the endothelial progenitor cells from the blood, which then differentiate into ECs and prevent thrombosis from developing. The emergence of the rapid progression of atherosclerosis is a multifactorial process, which is why many more types of intervention are possible, such as the suppression of smooth muscle cell proliferation or growth factors.

Further, *in vivo* experiments are needed to test the effect of long-term release with PLGA and ATCOL coatings. Likewise, this should also be checked with the fast-release HA/PEI coating. The *in vivo* experiments with atherosclerotic vessels might also provide information on how long a release and transfection with the applied ICAM–1 siRNA is needed to prevent the unwanted leucocyte adhesion. If a longer release for stent therapy is evident, further intermediate layers of slowly degradable PLGA could be incorporated in the PLGA multilayer structure. Similarly, in the case of the ATCOL coating, a capping layer of a polymer could be applied so that the release of the siRNA takes place with a delay. This multifactorial approach of different siRNAs and mRNAs

to improve the healing and reduction of restenosis of stents or balloons leads to a personalized and especially by the specific processes, low-side-effect therapy which could be of great benefit especially in view of aging society.

5 Reference list

1. Laslett, L.J., et al., *The Worldwide Environment of Cardiovascular Disease: Prevalence, Diagnosis, Therapy, and Policy Issues: A Report From the American College of Cardiology.* Journal of the American College of Cardiology, 2012. **60**(25, Supplement): p. S1-S49.

2. A. Alwan, T.A., D. Bettcher, T. Boerma, F. Branca, J. C.Y. Ho, C. Mathers,, et al., *Global Atlas on cardiovascular disease prevention and control.* World Health Organization 2011, 2011.

3. WHO *Cardiovascular diseases (CVDs).* 2016.

4. Henderson, A., *Coronary heart disease: Overview.* The Lancet, 1996. **348**: p. S1-S4.

5. Winniford, M.D., et al., *Cigarette smoking-induced coronary vasoconstriction in atherosclerotic coronary artery disease and prevention by calcium antagonists and nitroglycerin.* Am J Cardiol, 1987. **59**(4): p. 203-7.

6. Wilson, P.W., *Established risk factors and coronary artery disease: the Framingham Study.* Am J Hypertens, 1994. **7**(7 Pt 2): p. 7s-12s.

7. Lusis, A.J., *Atherosclerosis.* Nature, 2000. **407**: p. 233.

8. Gouverneur, M., et al., *Vasculoprotective properties of the endothelial glycocalyx: effects of fluid shear stress.* J Intern Med, 2006. **259**(4): p. 393-400.

9. Shah, P., et al., *Rapid Progression of Coronary Atherosclerosis: A Review.* Thrombosis, 2015. **2015**: p. 6.

10. Boren, J., et al., *Identification of the principal proteoglycan-binding site in LDL. A single-point mutation in apo-B100 severely affects proteoglycan interaction without affecting LDL receptor binding.* J Clin Invest, 1998. **101**(12): p. 2658-64.

11. Bian, K., M.F. Doursout, and F. Murad, *Vascular system: role of nitric oxide in cardiovascular diseases.* J Clin Hypertens (Greenwich), 2008. **10**(4): p. 304-10.

12. Lei, J., et al., *Nitric oxide, a protective molecule in the cardiovascular system.* Nitric Oxide, 2013. **35**: p. 175-185.

13. Fukai, T., et al., *Extracellular superoxide dismutase and cardiovascular disease.* Cardiovascular Research, 2002. **55**(2): p. 239-249.

14. Pamukcu, B., G.Y. Lip, and E. Shantsila, *The nuclear factor--kappa B pathway in atherosclerosis: a potential therapeutic target for atherothrombotic vascular disease.* Thromb Res, 2011. **128**(2): p. 117-23.

15. de Winther, M.P.J., et al., *Nuclear Factor κB Signaling in Atherogenesis.* Arteriosclerosis, Thrombosis, and Vascular Biology, 2005. **25**(5): p. 904-914.

16. Legein, B., et al., *Inflammation and immune system interactions in atherosclerosis.* Cell Mol Life Sci, 2013. **70**(20): p. 3847-69.

17. Lin, J., V. Kakkar, and X. Lu, *Impact of MCP-1 in atherosclerosis.* Curr Pharm Des, 2014. **20**(28): p. 4580-8.

18. Badimon, L., T. Padró, and G. Vilahur, *Atherosclerosis, platelets and thrombosis in acute ischaemic heart disease.* European Heart Journal. Acute Cardiovascular Care, 2012. **1**(1): p. 60-74.

19. Ramji, D.P. and T.S. Davies, *Cytokines in atherosclerosis: Key players in all stages of disease and promising therapeutic targets.* Cytokine Growth Factor Rev, 2015. **26**(6): p. 673-85.

20. Chaabane, C., M. Coen, and M.-L. Bochaton-Piallat, *Smooth muscle cell phenotypic switch: implications for foam cell formation.* Current Opinion in Lipidology, 2014. **25**(5): p. 374-379.

21. Newby, A.C. and A.B. Zaltsman, *Fibrous cap formation or destruction — the critical importance of vascular smooth muscle cell proliferation, migration and matrix formation.* Cardiovascular Research, 1999. **41**(2): p. 345-360.

22. Fernández-Ortiz, A., et al., *Characterization of the relative thrombogenicity of atherosclerotic plaque components: Implications for consequences of plaque rupture.* Journal of the American College of Cardiology, 1994. **23**(7): p. 1562-1569.

23. Barrabés, J.A. and L. Galian, *Endogenous Thrombolysis.* A Hidden Player in Acute Coronary Syndromes?, 2010. **55**(19): p. 2116-2117.

24. Zaman, A.G., et al., *The role of plaque rupture and thrombosis in coronary artery disease.* Atherosclerosis, 2000. **149**(2): p. 251-266.

25. Libby, P., P.M. Ridker, and G.K. Hansson, *Progress and challenges in translating the biology of atherosclerosis.* Nature, 2011. **473**: p. 317.

26. Imhof, B.A. and D. Dunon, *Basic mechanism of leukocyte migration.* Horm Metab Res, 1997. **29**(12): p. 614-21.

27. Hartman, J. and W.H. Frishman, *Inflammation and Atherosclerosis: A Review of the Role of Interleukin-6 in the Development of Atherosclerosis and the Potential for Targeted Drug Therapy.* Cardiology in Review, 2014. **22**(3): p. 147-151.

28. Ley, K., et al., *Getting to the site of inflammation: the leukocyte adhesion cascade updated.* Nat Rev Immunol, 2007. **7**(9): p. 678-89.

29. Ley, K., et al., *Getting to the site of inflammation: the leukocyte adhesion cascade updated.* Nature Reviews Immunology, 2007. **7**: p. 678.

30. Ley, K., et al., *Getting to the site of inflammation: the leukocyte adhesion cascade updated.* Nat Rev Immunol, 2007. **7**(9): p. 678-689.

31. Schenkel, A.R., Z. Mamdouh, and W.A. Muller, *Locomotion of monocytes on endothelium is a critical step during extravasation.* Nat Immunol, 2004. **5**(4): p. 393-400.

32. Eckel, R.H., et al., *2013 AHA/ACC guideline on lifestyle management to reduce cardiovascular risk: a report of the American College of Cardiology/American Heart Association Task Force on Practice Guidelines.* Circulation, 2014. **129**(25 Suppl 2): p. S76-99.

33. Smith, S.C., Jr., et al., *AHA/ACCF secondary prevention and risk reduction therapy for patients with coronary and other atherosclerotic vascular disease: 2011 update: a guideline from the American Heart Association and American College of Cardiology Foundation endorsed by the World Heart Federation and the Preventive Cardiovascular Nurses Association.* J Am Coll Cardiol, 2011. **58**(23): p. 2432-46.

34. Bergheanu, S.C., M.C. Bodde, and J.W. Jukema, *Pathophysiology and treatment of atherosclerosis.* Netherlands Heart Journal, 2017. **25**(4): p. 231-242.

35. Montalescot, G., et al., *2013 ESC guidelines on the management of stable coronary artery disease: the Task Force on the management of stable coronary artery disease of the European Society of Cardiology.* Eur Heart J, 2013. **34**(38): p. 2949-3003.

36. Olearchyk, A.S., *Vasilii I. Kolesov. A pioneer of coronary revascularization by internal mammary-coronary artery grafting.* J Thorac Cardiovasc Surg, 1988. **96**(1): p. 13-8.

37. Garrett, H.E., E.W. Dennis, and M.E. DeBakey, *Aortocoronary bypass with saphenous vein graft. Seven-year follow-up.* Jama, 1973. **223**(7): p. 792-4.

38. Head, S.J., et al., *Coronary artery bypass grafting: Part 1--the evolution over the first 50 years.* Eur Heart J, 2013. **34**(37): p. 2862-72.

39. Gruntzig, A., *Transluminal dilatation of coronary-artery stenosis.* Lancet, 1978. **1**(8058): p. 263.

40.   Windecker, S., et al., *2014 ESC/EACTS Guidelines on myocardial revascularization: The Task Force on Myocardial Revascularization of the European Society of Cardiology (ESC) and the European Association for Cardio-Thoracic Surgery (EACTS)Developed with the special contribution of the European Association of Percutaneous Cardiovascular Interventions (EAPCI).* Eur Heart J, 2014. **35**(37): p. 2541-619.

41.   Scheller, B., et al., *Paclitaxel balloon coating, a novel method for prevention and therapy of restenosis.* Circulation, 2004. **110**(7): p. 810-4.

42.   Nordmann, A.J., et al., *Clinical outcomes of stents versus balloon angioplasty in non-acute coronary artery diseaseA meta-analysis of randomized controlled trials.* European Heart Journal, 2004. **25**(1): p. 69-80.

43.   Daemen, J., et al., *Long-term safety and efficacy of percutaneous coronary intervention with stenting and coronary artery bypass surgery for multivessel coronary artery disease: a meta-analysis with 5-year patient-level data from the ARTS, ERACI-II, MASS-II, and SoS trials.* Circulation, 2008. **118**(11): p. 1146-54.

44.   Cutlip, D.E., et al., *Clinical restenosis after coronary stenting: perspectives from multicenter clinical trials.* J Am Coll Cardiol, 2002. **40**(12): p. 2082-9.

45.   Tahir, H., C. Bona-Casas, and A.G. Hoekstra, *Modelling the Effect of a Functional Endothelium on the Development of In-Stent Restenosis.* PLoS ONE, 2013. **8**(6): p. e66138.

46.   Otsuka, F., et al., *The importance of the endothelium in atherothrombosis and coronary stenting.* Nat Rev Cardiol, 2012. **9**(8): p. 439-453.

47.   Serruys, P.W., M.J. Kutryk, and A.T. Ong, *Coronary-artery stents.* N Engl J Med, 2006. **354**(5): p. 483-95.

48.   Luscher, T.F., et al., *Drug-eluting stent and coronary thrombosis: biological mechanisms and clinical implications.* Circulation, 2007. **115**(8): p. 1051-8.

49.   Biondi-Zoccai, G.G., et al., *A systematic review and meta-analysis on the hazards of discontinuing or not adhering to aspirin among 50,279 patients at risk for coronary artery disease.* Eur Heart J, 2006. **27**(22): p. 2667-74.

50.   Bangalore, S., et al., *Newer Generation Ultra-Thin Strut Drug-Eluting Stents versus Older Second-Generation Thicker Strut Drug-Eluting Stents for Coronary Artery Disease: A Meta-Analysis of Randomized Trials.* Circulation, 2018.

51.   Aoki, J., et al., *Endothelial Progenitor Cell Capture by Stents Coated With Antibody Against CD34: The HEALING-FIM (Healthy Endothelial Accelerated Lining Inhibits Neointimal Growth-First In Man) Registry.* Journal of the American College of Cardiology, 2005. **45**(10): p. 1574-1579.

52.   Gonzalo, N. and C. Macaya, *Absorbable stent: focus on clinical applications and benefits.* Vasc Health Risk Manag, 2012. **8**: p. 125-32.

53.   Mishra, S., *A fresh look at bioresorbable scaffold technology: Intuition pumps.* Indian Heart J, 2017. **69**(1): p. 107-111.

54.   Welt, F.G. and C. Rogers, *Inflammation and restenosis in the stent era.* Arterioscler Thromb Vasc Biol, 2002. **22**(11): p. 1769-76.

55.   Petersen, E.J., et al., *siRNA silencing reveals role of vascular cell adhesion molecule-1 in vascular smooth muscle cell migration.* Atherosclerosis, 2008. **198**(2): p. 301-6.

56.   Qu, Y., et al., *VCAM-1 siRNA reduces neointimal formation after surgical mechanical injury of the rat carotid artery.* J Vasc Surg, 2009. **50**(6): p. 1452-8.

57.   Sager, H.B., et al., *RNAi targeting multiple cell adhesion molecules reduces immune cell recruitment and vascular inflammation after myocardial infarction.* Sci Transl Med, 2016. **8**(342): p. 342ra80.

58.   Walker, T., et al., *Suppression of ICAM-1 in human venous endothelial cells by small interfering RNAs.* Eur J Cardiothorac Surg, 2005. **28**(6): p. 816-20.

59.   Chung, J., et al., *Discovery of novel peptides targeting pro-atherogenic endothelium in disturbed flow regions -Targeted siRNA delivery to pro-atherogenic endothelium in vivo.* Sci Rep, 2016. **6**: p. 25636.

60.   Walker, T., et al., *Inhibition of adhesion molecule expression on human venous endothelial cells by non-viral siRNA transfection.* Journal of Cellular and Molecular Medicine, 2007. **11**(1): p. 139-147.

61.   Meister, G. and T. Tuschl, *Mechanisms of gene silencing by double-stranded RNA.* Nature, 2004. **431**: p. 343.

62.   Napoli, C., C. Lemieux, and R. Jorgensen, *Introduction of a Chimeric Chalcone Synthase Gene into Petunia Results in Reversible Co-Suppression of Homologous Genes in trans.* Plant Cell, 1990. **2**(4): p. 279-289.

63.   Fire, A., et al., *Potent and specific genetic interference by double-stranded RNA in Caenorhabditis elegans.* Nature, 1998. **391**(6669): p. 806-11.

64.   Tomari, Y. and P.D. Zamore, *Perspective: machines for RNAi.* Genes Dev, 2005. **19**(5): p. 517-29.

65.   Elbashir, S.M., et al., *Duplexes of 21-nucleotide RNAs mediate RNA interference in cultured mammalian cells.* Nature, 2001. **411**(6836): p. 494-8.

66.   Bernstein, E., et al., *Role for a bidentate ribonuclease in the initiation step of RNA interference.* Nature, 2001. **409**(6818): p. 363-6.

67.   Zamore, P.D., et al., *RNAi: double-stranded RNA directs the ATP-dependent cleavage of mRNA at 21 to 23 nucleotide intervals.* Cell, 2000. **101**(1): p. 25-33.

68.   Elbashir, S.M., W. Lendeckel, and T. Tuschl, *RNA interference is mediated by 21- and 22-nucleotide RNAs.* Genes & Development, 2001. **15**(2): p. 188-200.

69.   Hammond, S.M., et al., *Argonaute2, a link between genetic and biochemical analyses of RNAi.* Science, 2001. **293**(5532): p. 1146-50.

70.   Nykänen, A., B. Haley, and P.D. Zamore, *ATP Requirements and Small Interfering RNA Structure in the RNA Interference Pathway.* Cell, 2001. **107**(3): p. 309-321.

71.   Hutvagner, G. and M.J. Simard, *Argonaute proteins: key players in RNA silencing.* Nature Reviews Molecular Cell Biology, 2008. **9**: p. 22.

72.   Jinek, M. and J.A. Doudna, *A three-dimensional view of the molecular machinery of RNA interference.* Nature, 2009. **457**(7228): p. 405-12.

73.   Liu, J., et al., *Argonaute2 is the catalytic engine of mammalian RNAi.* Science, 2004. **305**(5689): p. 1437-41.

74.   Martinez, J., et al., *Single-Stranded Antisense siRNAs Guide Target RNA Cleavage in RNAi.* Cell, 2002. **110**(5): p. 563-574.

75.   Dorsett, Y. and T. Tuschl, *siRNAs: applications in functional genomics and potential as therapeutics.* Nat Rev Drug Discov, 2004. **3**(4): p. 318-329.

76.   van Hoof, A. and R. Parker, *Messenger RNA Degradation: Beginning at the End.* Current Biology, 2002. **12**(8): p. R285-R287.

77.   Haley, B. and P.D. Zamore, *Kinetic analysis of the RNAi enzyme complex.* Nature Structural &Amp; Molecular Biology, 2004. **11**: p. 599.

78.   Rivas, F.V., et al., *Purified Argonaute2 and an siRNA form recombinant human RISC.* Nature Structural &Amp; Molecular Biology, 2005. **12**: p. 340.

79.   Chan, C.Y., et al., *A structural interpretation of the effect of GC-content on efficiency of RNA interference.* BMC Bioinformatics, 2009. **10**(Suppl 1): p. S33-S33.

80.   Petri S., M.G., *siRNA Design Principles and Off-Target Effects*, in *Target Identification and Validation in Drug Discovery*, C. R., Editor. 2013, Humana Press: Totowa, NJ. p. 59-71.

81.   Dowler, T., et al., *Improvements in siRNA properties mediated by 2'-deoxy-2'-fluoro-beta-D-arabinonucleic acid (FANA).* Nucleic Acids Res, 2006. **34**(6): p. 1669-75.

82.   Soutschek, J., et al., *Therapeutic silencing of an endogenous gene by systemic administration of modified siRNAs.* Nature, 2004. **432**(7014): p. 173-178.

83.   Layzer, J.M., et al., *In vivo activity of nuclease-resistant siRNAs.* Rna, 2004. **10**(5): p. 766-71.

84.   Braasch, D.A., et al., *RNA Interference in Mammalian Cells by Chemically-Modified RNA.* Biochemistry, 2003. **42**(26): p. 7967-7975.

85.   Akhtar, S. and I.F. Benter, *Nonviral delivery of synthetic siRNAs in vivo.* The Journal of Clinical Investigation, 2007. **117**(12): p. 3623-3632.

86.   Kim, T.K. and J.H. Eberwine, *Mammalian cell transfection: the present and the future.* Analytical and Bioanalytical Chemistry, 2010. **397**(8): p. 3173-3178.

87.   Akhtar S, B.I., *Nonviral delivery of synthetic siRNAs in vivo.* The Journal of Clinical Investigation, 2007. **117**(12): p. 3623-3632.

88.   Godbey, D.A.B.a.W., *Liposomes for Use in Gene Delivery.* Journal of Drug Delivery, 2011. **vol. 2011**: p. 12 pages.

89.   Arruda, D.C., et al., *Chapter 26 - Innovative nonviral vectors for small-interfering RNA delivery and therapy*, in *Nanostructures for Novel Therapy*, D. Ficai and A.M. Grumezescu, Editors. 2017, Elsevier. p. 713-740.

90.   Elouahabi A., R.J.M., *Formation and intracellular trafficking of lipoplexes and polyplexes.* Mol Ther Nucleic Acids, 2005. **11**(3): p. 336-47.

91.   Farhood, H., N. Serbina, and L. Huang, *The role of dioleoyl phosphatidylethanolamine in cationic liposome mediated gene transfer.* Biochimica et Biophysica Acta (BBA) - Biomembranes, 1995. **1235**(2): p. 289-295.

92.   Boussif, O., et al., *A versatile vector for gene and oligonucleotide transfer into cells in culture and in vivo: polyethylenimine.* Proc Natl Acad Sci U S A, 1995. **92**(16): p. 7297-301.

93.   Behr, J.-P., *The Proton Sponge: a Trick to Enter Cells the Viruses Did Not Exploit.* CHIMIA International Journal for Chemistry, 1997. **51**(1-2): p. 34-36.

94.   Wightman, L., et al., *Different behavior of branched and linear polyethylenimine for gene delivery in vitro and in vivo.* The Journal of Gene Medicine, 2001. **3**(4): p. 362-372.

95.   Godbey, W.T. and A.G. Mikos, *Recent progress in gene delivery using non-viral transfer complexes.* Journal of Controlled Release, 2001. **72**(1): p. 115-125.

96.   Godbey, W.T., et al., *Improved packing of poly(ethylenimine)/DNA complexes increases transfection efficiency.* Gene Ther, 1999. **6**(8): p. 1380-8.

97.   Zintchenko, A., et al., *Simple modifications of branched PEI lead to highly efficient siRNA carriers with low toxicity.* Bioconjug Chem, 2008. **19**(7): p. 1448-55.

98.   Han, S.E., et al., *Cationic derivatives of biocompatible hyaluronic acids for delivery of siRNA and antisense oligonucleotides.* J Drug Target, 2009. **17**(2): p. 123-32.

99.   Jiang, G., et al., *Hyaluronic acid–polyethyleneimine conjugate for target specific intracellular delivery of siRNA.* Biopolymers, 2008. **89**(7): p. 635-642.

100.   Wood, K.C., et al., *A family of hierarchically self-assembling linear-dendritic hybrid polymers for highly efficient targeted gene delivery.* Angew Chem Int Ed Engl, 2005. **44**(41): p. 6704-8.

101.   Wang, X.L., et al., *Novel polymerizable surfactants with pH-sensitive amphiphilicity and cell membrane disruption for efficient siRNA delivery.* Bioconjug Chem, 2007. **18**(6): p. 2169-77.

102.   Kim, S.H., et al., *Prostate cancer cell-specific VEGF siRNA delivery system using cell targeting peptide conjugated polyplexes.* J Drug Target, 2009. **17**(4): p. 311-7.

103.   Demeneix, B. and J.P. Behr, *Polyethylenimine (PEI)*, in *Advances in Genetics*. 2005, Academic Press. p. 215-230.

104.   Uprichard, S.L., *The therapeutic potential of RNA interference.* FEBS Letters, 2005. **579**(26): p. 5996-6007.

105.   Walsh, S.K., D. *FDA approves first-of-its kind targeted RNA-based therapy to treat a rare disease*. 2018 [cited 2018; Available from: https://www.fda.gov/NewsEvents/Newsroom/PressAnnouncements/UCM616518.htm.

106.   Whitehead, K.A., R. Langer, and D.G. Anderson, *Knocking down barriers: advances in siRNA delivery.* Nat Rev Drug Discov, 2009. **8**(2): p. 129-38.

107.   Kriegel, C., H. Attarwala, and M. Amiji, *Multi-compartmental oral delivery systems for nucleic acid therapy in the gastrointestinal tract.* Adv Drug Deliv Rev, 2013. **65**(6): p. 891-901.

108.   Forbes, D.C. and N.A. Peppas, *Oral delivery of small RNA and DNA.* J Control Release, 2012. **162**(2): p. 438-45.

109.   Parker, N., et al., *Folate receptor expression in carcinomas and normal tissues determined by a quantitative radioligand binding assay.* Anal Biochem, 2005. **338**(2): p. 284-93.

110.   Dohmen, C., et al., *Defined Folate-PEG-siRNA Conjugates for Receptor-specific Gene Silencing.* Molecular therapy. Nucleic acids, 2012. **1**(1): p. e7.

111.   Adrian, J.E., et al., *Targeted delivery to neuroblastoma of novel siRNA-anti-GD2-liposomes prepared by dual asymmetric centrifugation and sterol-based post-insertion method.* Pharm Res, 2011. **28**(9): p. 2261-72.

112.   Han, H.D., et al., *Targeted gene silencing using RGD-labeled chitosan nanoparticles.* Clin Cancer Res, 2010. **16**(15): p. 3910-22.

113.   Yao, Y.D., et al., *Targeted delivery of PLK1-siRNA by ScFv suppresses Her2+ breast cancer growth and metastasis.* Sci Transl Med, 2012. **4**(130): p. 130ra48.

114.   Nolte, A.S., M.; Walker, T.; Wendel, H.P., *Gene-Silencing for Treatment of Cardiovascular Diseases.*, in *Regenerative Medicine and Tissue Engineering-Cells and Biomaterials*, D. Eberli, Editor. 2011: InTech: New York, NY, USA.

115.   Castanotto, D. and J.J. Rossi, *The promises and pitfalls of RNA-interference-based therapeutics.* Nature, 2009. **457**(7228): p. 426-433.

116.   Liu, X., et al., *RNAi functionalized collagen-chitosan/silicone membrane bilayer dermal equivalent for full-thickness skin regeneration with inhibited scarring.* Biomaterials, 2013. **34**(8): p. 2038-48.

117.   San Juan, A., et al., *Development of a functionalized polymer for stent coating in the arterial delivery of small interfering RNA.* Biomacromolecules, 2009. **10**(11): p. 3074-80.

118.   Li, J.M., et al., *Local arterial nanoparticle delivery of siRNA for NOX2 knockdown to prevent restenosis in an atherosclerotic rat model.* Gene Ther, 2010. **17**(10): p. 1279-87.

119.   Kwon, H. and S. Park, *Local Delivery of Antiproliferative Agents via Stents.* Polymers, 2014. **6**(3): p. 755.

120.   Brito, L.A., et al., *Non-viral eNOS gene delivery and transfection with stents for the treatment of restenosis.* Biomed Eng Online, 2010. **9**: p. 56.

121.   Klugherz, B.D., et al., *Gene delivery from a DNA controlled-release stent in porcine coronary arteries.* Nat Biotechnol, 2000. **18**(11): p. 1181-4.

122.   Antunes, J.C., et al., *Layer-by-Layer Self-Assembly of Chitosan and Poly(γ-glutamic acid) into Polyelectrolyte Complexes.* Biomacromolecules, 2011. **12**(12): p. 4183-4195.

123.   Haidar, Z.S., R.C. Hamdy, and M. Tabrizian, *Protein release kinetics for core–shell hybrid nanoparticles based on the layer-by-layer assembly of alginate and chitosan on liposomes.* Biomaterials, 2008. **29**(9): p. 1207-1215.

124.   Meng, S., et al., *The effect of a layer-by-layer chitosan–heparin coating on the endothelialization and coagulation properties of a coronary stent system.* Biomaterials, 2009. **30**(12): p. 2276-2283.

125.   Khademhosseini, A., et al., *Layer-by-layer deposition of hyaluronic acid and poly-l-lysine for patterned cell co-cultures.* Biomaterials, 2004. **25**(17): p. 3583-3592.

126.   Picart, C., et al., *Buildup Mechanism for Poly(l-lysine)/Hyaluronic Acid Films onto a Solid Surface.* Langmuir, 2001. **17**(23): p. 7414-7424.

127.   Lutkenhaus, J.L., K. McEnnis, and P.T. Hammond, *Nano- and Microporous Layer-by-Layer Assemblies Containing Linear Poly(ethylenimine) and Poly(acrylic acid).* Macromolecules, 2008. **41**(16): p. 6047-6054.

128.   Castleberry, S., M. Wang, and P.T. Hammond, *Nanolayered siRNA Dressing for Sustained Localized Knockdown.* ACS Nano, 2013. **7**(6): p. 5251-5261.

129.   Holmes, C.A. and M. Tabrizian, *Substrate-mediated gene delivery from glycol-chitosan/hyaluronic acid polyelectrolyte multilayer films.* ACS Appl Mater Interfaces, 2013. **5**(3): p. 524-31.

130.   Keeney, M., et al., *Mutant MCP-1 protein delivery from layer-by-layer coatings on orthopedic implants to modulate inflammatory response.* Biomaterials, 2013. **34**(38): p. 10287-10295.

131.   Zhi, F., et al., *Functionalized Graphene Oxide Mediated Adriamycin Delivery and miR-21 Gene Silencing to Overcome Tumor Multidrug Resistance In Vitro.* PLOS ONE, 2013. **8**(3): p. e60034.

132.   Wood, K.C., et al., *Controlling interlayer diffusion to achieve sustained, multiagent delivery from layer-by-layer thin films.* Proceedings of the National Academy of Sciences, 2006. **103**(27): p. 10207-10212.

133.   Hossfeld, S., et al., *Bioactive coronary stent coating based on layer-by-layer technology for siRNA release.* Acta Biomater, 2013. **9**(5): p. 6741-52.

134.   Macdonald, M.L., et al., *Tissue integration of growth factor-eluting layer-by-layer polyelectrolyte multilayer coated implants.* Biomaterials, 2011. **32**(5): p. 1446-53.

135.   Williams, D., *Definitions in Biomaterials. Proceedings of a Consensus Conference of the European Society for Biomaterials, Chester, England, March 3–5, 1986*. Vol. 4. 1987, New York: Elsevier.

136.   Elbert, D.L. and J.A. Hubbell, *Surface Treatments of Polymers for Biocompatibility.* Annual Review of Materials Science, 1996. **26**(1): p. 365-394.

137.   Danhier, F., et al., *PLGA-based nanoparticles: an overview of biomedical applications.* J Control Release, 2012. **161**(2): p. 505-22.

138.   Makadia, H.K. and S.J. Siegel, *Poly Lactic-co-Glycolic Acid (PLGA) as Biodegradable Controlled Drug Delivery Carrier.* Polymers (Basel), 2011. **3**(3): p. 1377-1397.

139.   Vert, M., J. Mauduit, and S. Li, *Biodegradation of PLA/GA polymers: increasing complexity.* Biomaterials, 1994. **15**(15): p. 1209-1213.

140.   Houchin, M.L. and E.M. Topp, *Chemical degradation of peptides and proteins in PLGA: a review of reactions and mechanisms.* J Pharm Sci, 2008. **97**(7): p. 2395-404.

141.   Samadi, N., et al., *The effect of lauryl capping group on protein release and degradation of poly(D,L-lactic-co-glycolic acid) particles.* J Control Release, 2013. **172**(2): p. 436-43.

142.   Zolnik, B.S. and D.J. Burgess, *Evaluation of in vivo-in vitro release of dexamethasone from PLGA microspheres.* J Control Release, 2008. **127**(2): p. 137-45.

143.   Jenjob, R., et al., *Recent trend in applications of polymer materials to stents.* gi, 2015. **4**(2): p. 83-88.

144.   Laurent, T.C., U.B. Laurent, and J.R. Fraser, *The structure and function of hyaluronan: An overview.* Immunol Cell Biol, 1996. **74**(2): p. A1-7.

145.   Weissmann, B. and K. Meyer, *The Structure of Hyalobiuronic Acid and of Hyaluronic Acid from Umbilical Cord1,2.* Journal of the American Chemical Society, 1954. **76**(7): p. 1753-1757.

146.   Weigel, P.H., et al., *The role of hyaluronic acid in inflammation and wound healing.* Int J Tissue React, 1988. **10**(6): p. 355-65.

147.   Toole, B.P., *Hyaluronan: from extracellular glue to pericellular cue.* Nat Rev Cancer, 2004. **4**(7): p. 528-39.

148.   Voigt, J. and V.R. Driver, *Hyaluronic acid derivatives and their healing effect on burns, epithelial surgical wounds, and chronic wounds: a systematic review and meta-analysis of randomized controlled trials.* Wound Repair Regen, 2012. **20**(3): p. 317-31.

149.   Hemmrich, K., et al., *Implantation of preadipocyte-loaded hyaluronic acid-based scaffolds into nude mice to evaluate potential for soft tissue engineering.* Biomaterials, 2005. **26**(34): p. 7025-37.

150.   Tashiro, T., et al., *Oral administration of polymer hyaluronic acid alleviates symptoms of knee osteoarthritis: a double-blind, placebo-controlled study over a 12-month period.* ScientificWorldJournal, 2012. **2012**: p. 167928.

151.   Vercruysse, K.P. and G.D. Prestwich, *Hyaluronate derivatives in drug delivery.* Crit Rev Ther Drug Carrier Syst, 1998. **15**(5): p. 513-55.

152.   Kim, E.J., et al., *Hyaluronic acid complexed to biodegradable poly L-arginine for targeted delivery of siRNAs.* J Gene Med, 2009. **11**(9): p. 791-803.

153.   Al-Qadi, S., et al., *Chitosan-hyaluronic acid nanoparticles for gene silencing: the role of hyaluronic acid on the nanoparticles' formation and activity.* Colloids Surf B Biointerfaces, 2013. **103**: p. 615-23.

154.   Park, K., et al., *Target specific tumor treatment by VEGF siRNA complexed with reducible polyethyleneimine-hyaluronic acid conjugate.* Biomaterials, 2010. **31**(19): p. 5258-65.

155.   Raviña, M., et al., *Hyaluronic Acid/Chitosan-g-Poly(ethylene glycol) Nanoparticles for Gene Therapy: An Application for pDNA and siRNA Delivery.* Pharmaceutical Research, 2010. **27**(12): p. 2544-2555.

156.   Trochon, V., et al., *Evidence of involvement of CD44 in endothelial cell proliferation, migration and angiogenesis in vitro.* Int J Cancer, 1996. **66**(5): p. 664-8.

157.   Savani, R.C., et al., *Differential involvement of the hyaluronan (HA) receptors CD44 and receptor for HA-mediated motility in endothelial cell function and angiogenesis.* J Biol Chem, 2001. **276**(39): p. 36770-8.

158.   Takahashi, Y., et al., *Hyaluronan fragments induce endothelial cell differentiation in a CD44- and CXCL1/GRO1-dependent manner.* J Biol Chem, 2005. **280**(25): p. 24195-204.

159.   Pilarski, L.M., et al., *RHAMM, a receptor for hyaluronan-mediated motility, on normal human lymphocytes, thymocytes and malignant B cells: a mediator in B cell malignancy?* Leuk Lymphoma, 1994. **14**(5-6): p. 363-74.

160.   McCourt, P.A., et al., *Intercellular adhesion molecule-1 is a cell surface receptor for hyaluronan.* J Biol Chem, 1994. **269**(48): p. 30081-4.

161.   Minakuchi, Y., et al., *Atelocollagen-mediated synthetic small interfering RNA delivery for effective gene silencing in vitro and in vivo.* Nucleic Acids Res, 2004. **32**(13): p. e109.

162.   Honma, K., et al., *Atelocollagen-based gene transfer in cells allows high-throughput screening of gene functions.* Biochem Biophys Res Commun, 2001. **289**(5): p. 1075-81.

163.   Duarte Campos, D.F., et al., *Supporting Biomaterials for Articular Cartilage Repair.* Cartilage, 2012. **3**(3): p. 205-221.

164.   Monaghan, M., et al., *A collagen-based scaffold delivering exogenous microrna-29B to modulate extracellular matrix remodeling.* Mol Ther, 2014. **22**(4): p. 786-96.

165.   Hanai, K., et al., *Potential of atelocollagen-mediated systemic antisense therapeutics for inflammatory disease.* Hum Gene Ther, 2004. **15**(3): p. 263-72.

166.   Ochiya, T., et al., *Biomaterials for gene delivery: atelocollagen-mediated controlled release of molecular medicines.* Curr Gene Ther, 2001. **1**(1): p. 31-52.

167.   Sano, A., et al., *Atelocollagen for protein and gene delivery.* Adv Drug Deliv Rev, 2003. **55**(12): p. 1651-77.

168.   Takei, Y., et al., *A small interfering RNA targeting vascular endothelial growth factor as cancer therapeutics.* Cancer Res, 2004. **64**(10): p. 3365-70.

169.   Kornowski, R., et al., *In-stent restenosis: contributions of inflammatory responses and arterial injury to neointimal hyperplasia.* J Am Coll Cardiol, 1998. **31**(1): p. 224-30.

170.   Janmey, P.A., et al., *The hard life of soft cells.* Cell Motil Cytoskeleton, 2009. **66**(8): p. 597-605.

171.   Lo, C.-M., et al., *Cell Movement Is Guided by the Rigidity of the Substrate.* Biophysical Journal, 2000. **79**(1): p. 144-152.

172.   Bhana, B., et al., *Influence of substrate stiffness on the phenotype of heart cells.* Biotechnology and Bioengineering, 2010. **105**(6): p. 1148-1160.

173.   Discher, D.E., P. Janmey, and Y.-l. Wang, *Tissue Cells Feel and Respond to the Stiffness of Their Substrate.* Science, 2005. **310**(5751): p. 1139-1143.

174.   Engler, A.J., et al., *Embryonic cardiomyocytes beat best on a matrix with heart-like elasticity: scar-like rigidity inhibits beating.* J Cell Sci, 2008. **121**(Pt 22): p. 3794-802.

175.   Saunders, R.L. and D.A. Hammer, *Assembly of Human Umbilical Vein Endothelial Cells on Compliant Hydrogels.* Cellular and Molecular Bioengineering, 2010. **3**(1): p. 60-67.

176.   Nolte, A., et al., *Impact of polyelectrolytes and their corresponding multilayers to human primary endothelial cells.* J Biomater Appl, 2013. **28**(1): p. 84-99.

177.   Mu, P., et al., *Systemic delivery of siRNA specific to tumor mediated by atelocollagen: combined therapy using siRNA targeting Bcl-xL and cisplatin against prostate cancer.* Int J Cancer, 2009. **125**(12): p. 2978-90.

178.   Nolte, A., et al., *Small-interfering RNA-eluting surfaces as a novel concept for intravascular local gene silencing.* Mol Med, 2011. **17**(11-12): p. 1213-22.

179.   Koenig, O., et al., *RNA-Eluting Surfaces for the Modulation of Gene Expression as A Novel Stent Concept.* Pharmaceuticals (Basel), 2017. **10**(1).

180.   Brewster, L.P., E.M. Brey, and H.P. Greisler, *Cardiovascular gene delivery: The good road is awaiting.* Adv Drug Deliv Rev, 2006. **58**(4): p. 604-29.

181.   Lafont, A. and J. Mensah-Gourmel, *Bioresorbable coronary scaffolds should disappear faster.* The Lancet, 2016. **387**(10025): p. 1275-1276.

182. Fredenberg, S., et al., *The mechanisms of drug release in poly(lactic-co-glycolic acid)-based drug delivery systems--a review.* Int J Pharm, 2011. **415**(1-2): p. 34-52.

183. Nolte, A., et al., *Optimized basic conditions are essential for successful siRNA transfection into primary endothelial cells.* Oligonucleotides, 2009. **19**(2): p. 141-50.

184. Nolte, A., et al., *Small-Interfering RNA–Eluting Surfaces as a Novel Concept for Intravascular Local Gene Silencing.* Molecular Medicine, 2011. **17**(11-12): p. 1213-1222.

185. Gresch, O. and L. Altrogge, *Transfection of difficult-to-transfect primary mammalian cells.* Methods Mol Biol, 2012. **801**: p. 65-74.

186. Hamm, A., et al., *Efficient transfection method for primary cells.* Tissue Eng, 2002. **8**(2): p. 235-45.

187. Koenig, O., et al., *An Atelocollagen Coating for Efficient Local Gene Silencing by Using Small Interfering RNA.* Mol Ther Nucleic Acids, 2017. **6**: p. 290-301.

188. Scheller, B., et al., *A novel drug-coated scoring balloon for the treatment of coronary in-stent restenosis: Results from the multi-center randomized controlled PATENT-C first in human trial.* Catheterization and Cardiovascular Interventions, 2016. **88**(1): p. 51-59.

189. Byrne, R.A., et al., *Paclitaxel-eluting balloons, paclitaxel-eluting stents, and balloon angioplasty in patients with restenosis after implantation of a drug-eluting stent (ISAR-DESIRE 3): a randomised, open-label trial.* The Lancet, 2013. **381**(9865): p. 461-467.

190. Alfonso, F., et al., *Drug-eluting balloons in coronary interventions: the quiet revolution?* Expert Opinion on Drug Delivery, 2017. **14**(7): p. 841-850.

191. McKee, C.M., et al., *Hyaluronan (HA) fragments induce chemokine gene expression in alveolar macrophages. The role of HA size and CD44.* J Clin Invest, 1996. **98**(10): p. 2403-13.

6 Appendix

6.1 Own contribution

Publication I

An Atelocollagen Coating for Efficient Local Gene Silencing by Using Small Interfering RNA

All experiments reported in this publication were planned, performed and evaluated by myself. Dimitrios Nothdurft was involved in the experimental procedure. The ELISAs for the hemocompatibility test were performed by Julia Kurz and Ilka Degenkolbe performed the hemolysis assay. The manuscript was written by myself and Andrea Nolte revised the manuscript. Andrea Nolte was intensively involved in the planning of this study.

Publication II

RNA-Eluting Surfaces for the Modulation of Gene Expression as A Novel Stent Concept

All experiments reported in this publication were equally planned, performed and evaluated by Diane Zengerle and myself. Andreas Behring and Meltem Avci-Adali provided the mRNA. Julia Kurz supported the ELISA performance for the hemocompatibility test. Susanne Hossfeld conducted the 5'-RLM-RACE-PCR experiments. The results of the experiments were statistically evaluated by Diane Zengerle. The manuscript was written by myself and Andrea Nolte revised the manuscript. Andrea Nolte was intensively involved in the planning of this study.

Publication III

Hyaluronic acid/poly(ethylenimine) polyelectrolyte multilayer coatings for siRNA-mediated local gene silencing

All experiments reported in this publication were planned, performed and evaluated by myself. Bernd Neumann was involved in the experimental coating procedure. The manuscript was written by myself and Hans Peter Wendel and Andrea Nolte revised the manuscript. Andrea Nolte was intensively involved in the planning of this study.

6.2   Publication I

An Atelocollagen Coating for Efficient Local Gene Silencing by Using Small Interfering RNA

AMERICAN SOCIETY of
GENE & CELL THERAPY

An Atelocollagen Coating for Efficient Local Gene Silencing by Using Small Interfering RNA

Olivia Koenig,[1] Dimitrios Nothdurft,[1] Nadja Perle,[1] Bernd Neumann,[1] Andreas Behring,[1] Ilka Degenkolbe,[1] Tobias Walker,[1] Christian Schlensak,[1] Hans Peter Wendel,[1] and Andrea Nolte[1]

[1]Department of Thoracic, Cardiac, and Vascular Surgery, University Hospital Tuebingen, Tuebingen, 72076 Baden-Wuerttemberg, Germany

In the last decades, many efforts have been made to counteract adverse effects after stenting atherosclerotic coronary arteries. A breakthrough in better vascular wall regeneration was noted in the new era of drug-eluting stents. A novel personalized approach is the development of gene-eluting stents promising an alteration in gene expression involved in regeneration. We investigated a coating system consisting of the polymer atelocollagen (ATCOL) and a specific small interfering RNA (siRNA) for intercellular adhesion molecule-1 (ICAM-1) found on the surface of defective endothelial cells (ECs). We demonstrated very high cell viability, in which EA.hy926 grew on 0.008% or 0.032% ATCOL layers. Additionally, hemocompatibility assays proved the biocompatibility of this coating. The highest transfection efficiency with EA.hy926 was achieved with 5 μg siRNA immobilized in ATCOL after 2 days. The release of fluorescent-labeled siRNA was about 9 days. Long-term knockdown of ICAM-1 was analyzed by flow cytometry, revealing that the coating with 0.008% ATCOL and 5 μg siICAM-1 provoked gene silencing up to 8 days. 5′-RNA ligase-mediated rapid amplification of cDNA ends PCR (RLM-RACE-PCR) demonstrated the specificity of our established ATCOL gene-silencing coating, meaning that our coating is well suited for further investigations in in vivo studies. Herein, we would like to demonstrate that our ATCOL is well-suited for better artery wall regeneration after stent implantation.

INTRODUCTION

Cardiovascular diseases (CVDs) have long been challenging in modern medicine. This group of diseases accounts for 17.3 million deaths per year and leads the mortality statistics on a global scale.[1] Although age-adjusted mortality rates have decreased throughout the last decades, CVD and especially coronary heart disease (CHD) account for about 20% of deaths in Europe annually and remain highly prioritized fields in medical research.[2,3] Since CHD is mainly caused by atherosclerotic plaques, it is reasonable to tackle the main risk factors for atherosclerosis (namely, hypertension, diabetes mellitus, hyperlipidemia, obesity, smoking, and lack of physical activity) in a secondary preventive therapy.[4,5] The prognosis of CHD can be greatly improved by lifestyle changes (e.g., weight loss, cessation of smoking) and by a variety of drugs (e.g., angiotensin-converting enzyme [ACE] inhibitors, antiplatelet therapy, β blockers).[4,6–8] However, in many cases,

intervention in the form of surgery (e.g., coronary artery bypass surgery [CABG] or percutaneous transluminal coronary angioplasty [PTCA], with or without stent insertion) is unavoidable.[9] While overall mortality with balloon angioplasty did not differ from mortality with CABG, rates of restenosis and reintervention were considerably higher.[10–12] Balloon angioplasty was soon augmented by use of bare metal stents (BMSs). Unfortunately, in-stent restenosis and stent thrombosis (ST) may occur.[13,14] Stent implantation is seen as a trauma to the intimal structure triggering an inflammatory reaction.[15] Endothelial cells (ECs) in the stented area respond to local inflammation through elevated levels of surface-bound adhesion molecules, which facilitate the migration of leukocytes into the intima. The inflammatory reaction mediated through the migrating leukocytes causes a proliferation of intimal smooth muscle cells (SMCs) leading to narrowed vessel lumen.[15,16] Furthermore, overexpression of adhesion molecules promotes a chronification of the inflammatory process.[17] Drug-eluting stents (DESs) were introduced to inhibit neointimal hyperplasia and, hence, slow restenosis of the stented lumen. DESs are essentially BMSs coated with a polymer that releases an antiproliferative agent.[18] The agents as well as the stent design have changed over the course of time, forming two generations of DESs: first-generation (using sirolimus or paclitaxel) and second-generation (using everolimus or zotarolimus) DESs. Both generations show a significant reduction of target-location revascularization compared to BMSs. However, long-term mortality rates remain similar and the risk of late ST and late target-location revascularization persists.[19–22] Inhibition of re-endothelialization could be responsible for late restenosis.[23]

There are new approaches in medical research targeting the mechanism of restenosis on a molecular level to prevent an overexpression of adhesion molecules and thus chronic inflammation. A favorable and elegant method to lower the expression of adhesion molecules is gene silencing, also called gene knockdown. 20- to 25-nucleotide-long RNA strands are used, which are complementary to the mRNA of the target protein. This leads to so-called RNAi: mRNA

OMTN 29

binds the artificial RNA molecule, leading to the degradation of the double-stranded complex and inhibiting the biosynthesis of the target protein. According to their function, these RNA molecules are called small interfering RNAs (siRNAs).[24] However, naked siRNAs have a fairly short half-life and are prone to degradation by endo- and exo-nucleases.[25,26] There are two main working points through which the half-life can be extended: (1) through alteration of the siRNA on a molecular level (e.g., modification of the backbone)[26] or (2) through the use of a carrier substance preventing degradation or binding the negatively charged siRNA.[27] A potent carrier to do so is atelocollagen (ATCOL). ATCOL is basically a modified type I collagen. It is obtained by enzymatic treatment of bovine type I collagen with pepsin leading to the detachment of the telopeptides (N- and C-terminal ends of the collagen molecule), which influence the immunogenicity of the molecule immensely.[28,29] Combined with the natural biocompatibility of collagen, this modification creates a well-tolerated molecule that has many applications in modern medicine (e.g., as a hemostatic agent, bone cartilage substitute, etc.).[30,31] Referring to its use as carrier, there have been several studies demonstrating the usefulness of ATCOL in the delivery of nucleic acids.[31–35] Furthermore, ATCOL has proven to be a viable option in gene silencing, increasing the efficacy of siRNA transduction and offering protection against nucleases.[29] This is mostly achieved through the very stable complexation of the two agents (mostly through hydrogen bonding).[36] Another siRNA carrier is the cationic lipid Lipofectamine 2000 (Invitrogen), which is able to form nanoparticles with nucleic acids due to opposite charges. The negatively charged siRNA causes complexation with the cationic lipid. Consequently, the positively charged siRNA/Lipofectamine 2000 complex can be included in the cell because the electrostatic repulsion of the cell membrane will no longer have an effect.[37] Lipofectamine 2000 is known as a very potent transfection reagent resulting in high transfection efficiencies.

In this study, we focused on developing a bioactive stent coating using siRNA that is complementary to intercellular adhesion molecule-1 (*ICAM-1* or *CD54*). ICAM-1 is prominent on ECs during inflammatory reactions and part of the inflammatory cascade mentioned above and is thus a promising target to break the "vicious cycle" of restenosis. To find an agreeable concentration of ATCOL, we prepared different ATCOL layers and tested cell growth and hemocompatibility. Our siRNA was immobilized in ATCOL layers by drying them on glass slides, followed by cultivation with an immortalized EC line (EA.hy926). The release of embedded fluorescent-labeled siRNA was tested for long-term efficacy with a fluorescent reader. Afterward, we assessed transfection efficiency using Alexa Fluor 488 (AF 488)-labeled siRNA by flow cytometry. In a second approach, we used *ICAM-1* siRNA in a similar setup to evaluate gene knockdown of the ICAM-1 protein in a short- and long-term assay by flow cytometry.

RESULTS

Cell Viability of EA.hy926 on ATCOL Surfaces

Different concentrations of ATCOL coatings were tested for their influence on cell number, morphology, and adherence of EA.hy926.

The evaluation of cell number measurement with a CASY cell counter (Schärfe System) showed no significant alterations in EA.hy926 cell numbers, which were cultivated on 0.008%, 0.016%, and 0.032% ATCOL layers (Figure 1A). A significant cell number reduction of 50% EA.hy926 cultivated on 0.064% ATCOL was seen compared to control glass slides and the other layers. These results could be visually confirmed by microscopic images after 24 hr (Figures 1B–1F) and 48 hr (data not shown) of cultivation. While control slides and concentrations of 0.008%, 0.016%, and 0.032% ATCOL demonstrated adherence of EA.hy926 evenly, the layer with 0.064% ATCOL provoked formation of a boundary line by cells (Figure 1E). Additionally, cells grew mainly one above the other and were round shaped and not fully spread. This phenomenon is also slightly visible with 0.032% and 0.016% ATCOL. In the following experiments, we focused on three concentrations of ATCOL due to excellent cell adhesion and no reduction in cell number: 0.008%, 0.016%, and 0.032%.

Release of siRNA AF 488

The release of immobilized siRNA from ATCOL was observed over a period of 216 hr (9 days). The release was tested with fluorescently labeled siRNA by measuring the supernatant with a fluorescent reader. Within the first 4 hr of incubation, we detected the highest release of siRNA in the supernatant in all tested samples (Figure 2A). The release rate was nearly the same in all samples until the 24-hr time point of the experiment. Afterward, the 0.008% ATCOL layer demonstrated a faster release than the 0.032% ATCOL layer. Here, 0.008% ATCOL layers with 1 μg and 2.5 μg siRNA showed the lowest release values after 9 days (Figure 2B). The 1-μg 0.008% ATCOL coating provoked a decrease up to the 0.032% ATCOL control (without siRNA) at day 4. The same amounts of siRNA embedded in 0.032% ATCOL showed higher release values than 0.008% ATCOL after 9 days. At this time point, the highest release was observed with 5 μg siRNA in 0.032% ATCOL layers with 5,467 relative fluorescence units (RFU) followed by 5 μg siRNA in 0.008% ATCOL. No significant differences in release kinetics could be determined between the two different ATCOL coatings (0.008% and 0.032%) during the duration of the experiment.

Transfection Efficiency of siRNA AF 488 Mediated by ATCOL Coatings

Because ATCOL is used as a transfection reagent in many gene delivery studies,[29,31,32,34–36] we tested the potential of 0.008% and 0.032% ATCOL coatings for transfection efficiency in EA.hy926 with 1, 2.5, and 5 μg siRNA AF 488. After 48 hr of cultivation, the percentage of transfected cells was very low in both ATCOL concentrations but correlated with increased siRNA amounts. The highest transfection efficiency was reached with the combination of 0.008% ATCOL and 5 μg siRNA, with 7.6% positive cells (Figure 3A); 0.032% and 5 μg siRNA showed 3.4% transfected cells (Figure 3B). Considering these unsatisfying transfection efficiencies, we decided to optimize the transfection process by adding Lipofectamine 2000. Here, a remarkable significantly higher amount of transfected cells was observed. The use of Lipofectamine 2000 led to 68.9% positive cells with 0.008% ATCOL and 5 μg siRNA (Figure 3A). The highest
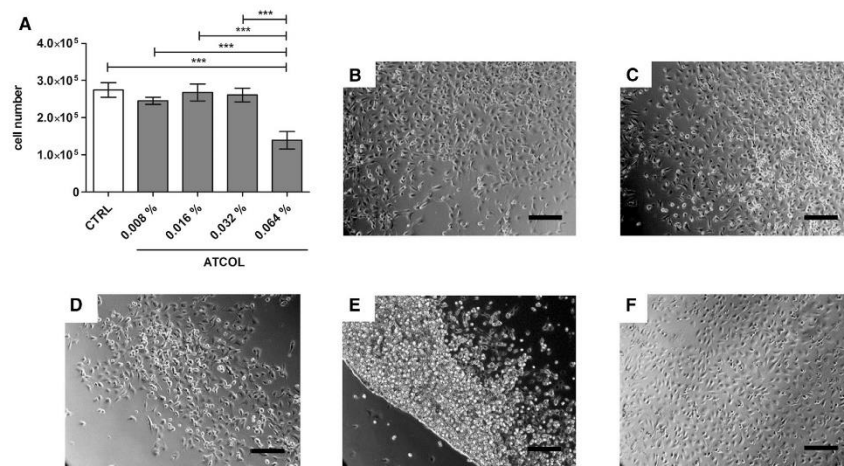
Figure 1. Cell Viability of EA.hy926 Cultured on ATCOL Layers

(A) Cell number analysis of EA.hy926 by CASY measurement. 75,000 cells were seeded onto different ATCOL-coated glass slides in a 24-well plate and cultivated for 48 hr. After cell detachment, the cell number was measured. An uncoated glass slide served as a control. Each bar represents the mean ± SEM (n = 3). ***p < 0.001. (B–F) Microscopy images of EA.hy926 cultivated on different ATCOL layers after 24 hr of cultivation: (B) EA.hy926 on 0.008% ATCOL, (C) EA.hy926 on 0.016% ATCOL, (D) EA.hy926 on 0.032% ATCOL, (E) EA.hy926 on 0.064% ATCOL, and (F) glass slide as a control. Scale bars, 200 μm. CTRL, control.

transfection efficiency (75.2%) was achieved with 0.032% ATCOL and 5 μg siRNA (Figure 3B). Comparing the two different ATCOL concentrations, the coating with 0.032% ATCOL resulted in generally higher transfection efficiencies than did that with 0.008% ATCOL, especially with 1 μg and 2.5 μg siRNA.

Knockdown of ICAM-1

In our study, knockdown of ICAM-1 is defined as the percent removal of the ICAM-1 receptor on EA.hy926 caused by RNAi. Here, siI-CAM-1 is able to bind to the complementary mRNA and to degrade it. First, ICAM-1 knockdown by 0.008% ATCOL and siICAM-1 without Lipofectamine 2000-coated glass slides was tested after 48-hr incubation with EA.hy926. All three amounts of siICAM-1 (1, 2.5, and 5 μg) could not provoke a knockdown (Figure 4A). The values are even slightly higher than the tumor necrosis factor (TNF)-α/antibody (Ab) control. The scrambled siRNA (siSCR) coatings that contained a siRNA that is not complementary to *ICAM-1* mRNA mediated no significant change in ICAM-1 expression compared to the TNF/Ab control and the siICAM-1 samples. The decision to use Lipofectamine 2000 for reinforcement of the transfection efficiency resulted in a higher knockdown of ICAM-1. Both concentrations of ATCOL coatings (0.008% and 0.032%) showed an increase in ICAM-1 knockdown with increasing amounts of siICAM-1 (Figure 4). Furthermore, a significant difference between 5 μg siICAM-1 and the control (5 μg siSCR) was observed with both ATCOL concentrations. While the knockdown provoked with 1 μg siICAM-1 was almost the same with the 0.008% (31.7%) and 0.032% (30.3%)

ATCOL coatings, values differed with 2.5 μg and 5 μg siICAM-1. Here, the 0.032% ATCOL coating resulted in a higher ICAM-1 knockdown with 49.6% (2.5 μg) and 60.4% (5 μg), compared to 0.008% ATCOL with 41.8% (2.5 μg) and 47.9% (5 μg).

Long-Term Knockdown of ICAM-1

Focusing on a long-term release of siRNA for later medical application, we examined the knockdown of ICAM-1 over a period of 8 days by flow cytometry every second day. Therefore, EA.hy926 cells were seeded onto 0.008% or 0.032% ATCOL transfection coatings (ATCOL/Lipofectamine 2000/siICAM-1) to examine the duration of substrate-mediated transfection. Additionally, we tested the knockdown by conventionally transfected cells to compare and reveal the potential for substrate-mediated knockdown. The highest significant ICAM-1 knockdown with 68.9% was reached with siRNA coatings after second day of incubation in the experiment with 0.008% ATCOL (Figure 5A). Very high knockdown was observed after the fourth and sixth days (63.3% and 48.7%), and 11.6% knockdown on the eighth day. Conventional mediated transfection provoked no significant ICAM-1 knockdown compared to the TNF/Ab control. Moreover, conventional transfected cells showed significantly higher ICAM-1 expression compared to the siICAM-1 coating analyzed at days 2, 4, and 6. Similar results were achieved with conventional transfected cells with 0.032% ATCOL and siICAM-1, where the highest knockdown was reached after 2 days with 10.0% and there was a progressive reduction until the eighth day (Figure 5B). siRNA coating-mediated transfection with 0.032% ATCOL provoked significant knockdown
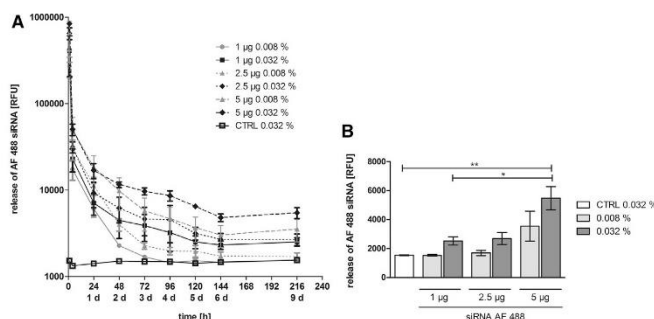
Molecular Therapy: Nucleic Acids

Figure 2. Release of siRNA AF 488 Particles from ATCOL Coatings

(A) Release kinetics of siRNA AF 488 incorporated in ATCOL layers. Glass slides were coated with either 0.008% or 0.032% ATCOL combined with 1, 2.5, or 5 μg siRNA AF 488. Coated slides were set in a 24-well plate and incubated in PBS at 37°C. Supernatants were collected and measured with a fluorescence reader at 485-nm excitation and 535-nm emission wavelengths at different time points. Each bar represents the mean ± SEM (n = 3). (B) RFU of released siRNA of ATCOL layers after 9 days. Final values of release kinetics in (A) are shown in a column diagram for improved distinction of different ATCOL samples. CTRL, control. $^*p < 0.05$; $^{**}p < 0.01$.

after day 2 (41.1%) and day 4 (41%), ending in no knockdown after the sixth and eighth days.

Specific mRNA Degradation Analyzed by RLM-RACE-PCR

The proof of specific mRNA degradation products by transfection reagent-mediated knockdown is mandatory for specific gene silencing in the RNAi mechanism. Consequently, undesired side effects mediated by the biomaterial or transfection reagent provoking knockdown of the targeted protein mRNA can be excluded. The determination of the *ICAM-1* cleavage site by the products of 5′-RNA ligase-mediated rapid amplification of cDNA ends PCR (RLM-RACE-PCR) revealed the correct cleaved mRNA transcript at bp 1,818, based on our expectations (Figure 6). Control coatings such as ATCOL without TNF-α activation, ATCOL, or ATCOL/siSCR with TNF-α activation demonstrated no specific *ICAM-1* mRNA cleavage products (data not shown).

Hemocompatibility

The determination of hemocompatibility is required for all medical devices according to International Organization for Standardization (ISO) standard 10993-4 and applied in our study testing 0.032% ATCOL coatings with incorporated siICAM-1 for later clinical application as a "worst case." First, cell numbers of blood cells were analyzed before incubation (0 hr) and after 1 hr of incubation with coated glass slides. The 1-hr sample served as a control and standard value. Then, coated glass slide samples were analyzed for hemocompatibility: ATCOL, ATCOL/Lipofectamine 2000, and ATCOL/Lipofectamine 2000/siICAM-1. Herein, the cell number of erythrocytes did not show variations in any sample (Figure 7A). Significant decreases (Figures 7B, 7C, 7E, and 7F) or increases (Figure 7D) of cell numbers were encountered comparing the 0-hr sample with most of the other tested samples. Furthermore, uncoated glass slides provoked a significant reduction of cell numbers in leukocytes and granulocytes compared to 1-hr control and ATCOL/Lipofectamine 2000 samples. However, the 1-hr blood control is crucial for the assessment of hemocompatibility and no significant changes in the cell numbers of leukocytes, platelets, lymphocytes, monocytes, and granulocytes were detected herein.

Furthermore, blood parameters (e.g., polymorphonuclear [PMN] elastase) and values of the complement system (e.g., SC5b9 and

C3a) were analyzed, revealing no significant value changes compared to the 1-hr control (Figures 7G–7I). Further investigations for hemocompatibility analysis were made analyzing hemolysis. All coated glass slides revealed significantly higher amounts of free hemoglobin in plasma (Figure 7J). Nevertheless, the standard value of 40 mg/100 mL plasma was been exceeded.

DISCUSSION

The development of new therapeutic strategies for preventing in-stent restenosis after coronary stent placement is a huge challenge. A promising new personalized therapeutic strategy comprises the application of gene-silencing stents that release specific therapeutic siRNAs to the ECs of the vascular wall for its faster regeneration and inhibition of restenosis. Several studies have evaluated the use of siRNAs against different target proteins involved in atherosclerotic processes.[38–42] For therapeutic siRNA release over a period of time, a biomaterial that supports storage features and controlled release and has no adverse effects to cell viability and hemocompatibility should be chosen. Therefore, we decided to use the biocompatible protein ATCOL, which has low toxicity and immunogenicity.

We evaluated the viability of EA.hy926 cells after seeding them onto different ATCOL layers. Our analysis revealed comparable cell counts between 0.008%, 0.016%, and 0.032% ATCOL coatings and the control. However, a significant reduction in cell number was found on the 0.064% ATCOL surface. We assume that higher ATCOL concentrations result in a softer coating surface. It is well known that substrate stiffness plays a pivotal role in cell adhesion, migration, proliferation, and differentiation.[43–48] The majority of EA.hy926 cells grown on 0.064% ATCOL showed a change in cell adhesion with less pseudopodia and a rounded cell shape. These results coincide with the findings of Nolte et al.,[49] in which softer polyelectrolyte multilayers consisting of hyaluronic acid/chitosan caused lower cell viability than the stiffer material (sulfonated polystyrene/polyallylamine hydrochlorite). Additionally, their microscopic images showed the same cell morphology with rounded cells on low rigidity films, like we observed with the 0.064% ATCOL layer.
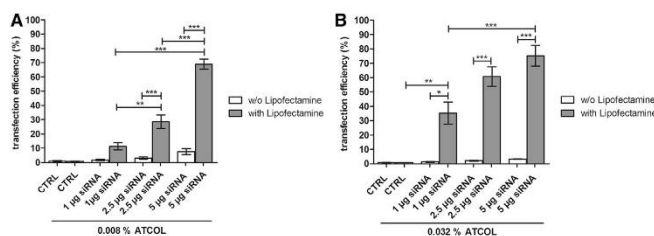
www.moleculartherapy.org

Figure 3. Transfection Efficiency after ATCOL-Mediated Transfection of siRNA AF 488 with or without Lipofectamine 2000

(A) 75,000 EA.hy926 cells were cultivated on 0.008% ATCOL with incorporated siRNA complexed or non-complexed with Lipofectamine 2000. Transfection efficiency was analyzed by flow cytometry after 48 hr of cultivation. (B) 75,000 EA.hy926 cells were cultivated on 0.032% ATCOL with siRNA complexed or noncomplexed with Lipofectamine 2000 and then treated as mentioned previously. Coatings without siRNA and Lipofectamine 2000 served as a control. Each bar represents the mean ± SEM (n = 3, or n = 6 for 0.032% ATCOL with Lipofectamine 2000). *p < 0.05; **p < 0.01; ***p < 0.001. CTRL, control.

A gene-eluting stent coating must fulfill the following requirements: biocompatibility, nucleic acid storage, and controlled release. Furthermore, it is beneficial if the coating supports the delivery of the therapeutic siRNA into cells.

Many previous studies have indicated that ATCOL is a highly potential transfection reagent for gene transfer in vitro and in vivo.[29,31,32,34,35,50,51] In addition, several opportunities for designing an ATCOL gene carrier exist, including minipellets, gels, sponges, or injectable solutions. In this study, we prepared an air-dried siRNA/ATCOL film for surface-mediated therapeutic siRNA delivery for later medical application. We examined the combination of 0.008% or 0.032% ATCOL with 1, 2.5, and 5 μg naked siRNA AF 488 for transfection efficiency in EA.hy926 and revealed unexpectedly few transfected cells (Figure 3). The knockdown experiment showed no ICAM-1 protein reduction, which further provided evidence that the coating is not able to efficiently transfect EA.hy926 cells (Figure 4A). With regard to the results of Minakuchi et al.[29] in preparing 0.008% ATCOL layers with siRNA, our results with 0.008% and 0.032% ATCOL could not achieve transfection efficiencies of 40%–60% (data not shown). Another study by Mu et al.[50] showed successful gene silencing with 0.008% ATCOL/siRNA coating by RT-PCR. Due to their same experimental setup with an ATCOL/siRNA transfection layer in well plates, we assume that the preparation may be a focal point for successful incorporation of siRNA. Both groups prepared their transfection solution by mixing equal volumes of diluted ATCOL and siRNA solution. The solution was rotated at 4°C for 20 min and then air-dried. In contrast, we built the coating by similar mixing and static incubation at room temperature for 30 min. Another reason for the different transfection efficiencies may be the cell type intended for transfection.[52] Whereas the other investigators used human prostate cancer and human testicular tumor cell lines, we transfected a hybrid cell line consisting of primary human umbilical vein cells and a clone of A549. Nevertheless, our approach of encapsulating siRNA into Lipofectamine 2000 led to significant augmented transfection efficiency in EA.hy926. We revealed that the transfection efficiency is dependent on the siRNA amount and ATCOL concentration. As siRNA quantity increased from 1 μg to 5 μg, we noticed significant increases in transfected cells in both ATCOL concentrations.

Transfection efficiency with 5 μg siRNA was comparable between 0.008% (68.9%) and 0.032% (75.2%) ATCOL coatings. Higher values could be achieved by the 0.032% ATCOL coating with 1 and 2.5 μg siRNA compared to the transfection efficiencies of 0.008% ATCOL with the same siRNA amounts (Figure 3).

Gene silencing of cell adhesion molecules (CAMs) in ECs is one key focus of our group as a possible strategy to circumvent and prevent the inflammatory process after stent implantation.[53] While DESs elute cytostatic agents for inhibiting excessive cell growth and migration of SMCs, our RNAi approach intends to interfere in this mechanism before the inflammatory machinery due to vessel injury can take place.[54,55] Therefore, we chose to silence the ICAM-1 adhesion molecule of ECs by local release to prevent the leukocyte adhesion cascade.[17] The coatings we designed with 0.008% or 0.032% ATCOL with 5 μg siICAM-1 and Lipofectamine 2000 were both able to reduce ICAM-1 significantly in our short-term experiment (Figure 4). Consequently, the transfection efficiency and short-term knockdown results led us to conclude that the amount of 5 μg siRNA embedded in 0.008% or 0.032% ATCOL layers is suitable for ICAM-1 knockdown in EA.hy926. 5′-RLM-RACE-PCR demonstrated the functionality of our substrate-mediated gene-silencing system. We detected the correct cleavage site for *ICAM-1* induced by siICAM-1 coating, meaning that siICAM-1 was able to degrade mRNA specifically. The control coatings with siSCR or with ATCOL only did not show typical mRNA degradation products at the cleavage site of *ICAM-1*. Consequently, we can say that the knockdown of ICAM-1 is due to the specific siRNA we used. To successfully prevent an inflammatory process after stent placement, long-term inhibition of leukocyte-endothelial interaction seems to be of crucial importance against in-stent restenosis.[19–22]

The release of fluorescent-labeled siRNA was in line with our knockdown experiments and with our previous studies. The results after 9 days of release revealed that the coating of 0.032% ATCOL with 5 μg siICAM-1 contained the highest siRNA residual amount followed by the combination of 0.008% ATCOL and 5 μg siICAM-1 (Figure 2B). Therefore, we chose these two combinations as delivery coatings in our long-term knockdown experiment. The initial burst
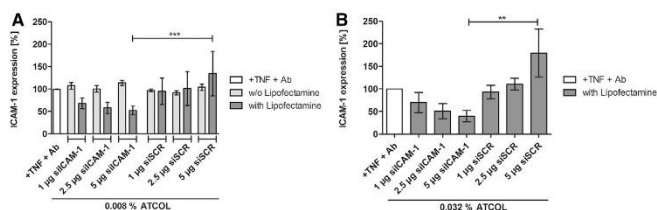
OMTN 29

Figure 4. ICAM-1 Expression after Knockdown with ICAM-1 siRNA with or without Lipofectamine 2000 Mediated by 0.008% and 0.032% ATCOL Transfection Coatings

Glass slides were coated with ATCOL transfection solution and put into a 24-well plate. 75,000 EA.hy926 cells were cultivated on coated glass slides for 48 hr and were then activated with TNF-α. ICAM-1 expression was analyzed by flow cytometry. (A) Coatings consisting of 0.008% ATCOL and 1, 2.5, or 5 μg siICAM-1 with or without Lipofectamine 2000. 0.008% ATCOL coatings with the same amounts of siSCR (scrambled siRNA) and Lipofectamine 2000 served as a control. (B) 0.032% ATCOL coatings with 1, 2.5, and 5 μg siICAM-1 and Lipofectamine 2000. siSCR served as a control. The control (+ TNF + Ab) was set to 100% in (A) and (B). Each bar in (A) and (B) represents the mean ± SEM (n = 3). $^{**}p < 0.01$; $^{***}p < 0.001$.

release within 4 hr seems to be responsible for the excellent ICAM-1 knockdown using 5 μg siICAM-1 embedded in 0.008% and 0.032% ATCOL (Figure 2A). Although the coating with 5 μg siICAM-1 and 0.032% ATCOL showed higher amounts of siRNA release over the 9-day period compared to the same coating with 0.008% ATCOL, we achieved lower knockdown values especially at days 6 and 8. We assume that a faster release of siRNA within the first days of transfection is mandatory for a high and sustained knockdown of the appropriate protein. Data from our two recent studies revealed the same results (O.K., D. Zengerle, N.P., S. Hossfeld, B.N., A.B., M. Avic-Adali, T.W., C.S., H.P.W., and A.N., unpublished data).[53] Comparing the release of coatings with the same siRNA amount but different ATCOL concentrations, we found different release profiles after 24 hr of incubation. Different concentrations of ATCOL are known to influence the density of the collagen matrix and, consequently, the release of molecules. If the collagen concentration is reduced, the collagen matrix shows a lower density leading to a faster escape out of the collagen matrix.[28] Our data underline the findings of Sano et al.,[28] showing that the coatings with the lower ATCOL concentration (0.008%) released the fluorescent-labeled siRNA faster than the higher concentration (0.032%) after day 1.

Analysis of our long-term knockdown experiments with 5 μg siICAM-1 in either 0.008% or 0.032% ATCOL revealed an effective surface-mediated local knockdown compared to transfection particles in suspension. Moreover, ICAM-1 knockdown was extended when the cells were grown on the coatings. In particular, the 0.008% ATCOL coating demonstrated a considerable difference between substrate-mediated transfection and transfection by particles in suspension, showing significance until transfection day 6. Furthermore, we detected a difference in knockdown values between these two transfection methods on day 8, revealing a substrate-mediated knockdown of ICAM-1 with 11.6% and no knockdown in suspension. In comparison, the 0.032% ATCOL coatings could not provoke such considerable ICAM-1 knockdown values as 0.008% did. But we observed a significant ICAM-1 knockdown after the second and fourth days of incubation by ATCOL substrate and no significant differences after transfection in suspension. Additionally, when comparing both knockdown experiments with 0.008% and 0.032% ATCOL coatings, we found that 0.008% provoked an extended knockdown of

ICAM-1 until the end of experiment (day 8), while 0.032% showed gene silencing until day 4. The higher transfection efficiencies and the higher release values of 0.032% ATCOL with 5 μg siICAM-1 compared with the results of the 0.008% ATCOL coating seem to be contradictory to the long-term knockdown results. However, we may find an explanation by taking a closer at the chemistry of our chemicals. Due to the positive charge of ATCOL and Lipofectamine 2000, both chemicals may be in competition with the negatively charged siRNA, especially when the concentration of ATCOL is augmented. Therefore, we expected more naked siRNA in the 0.032% ATCOL coating, which leads to a higher fluorescence signal in transfection efficiency measurement and in the release study. The worse long-term knockdown results may be attributed to the faster degradation of the naked siRNA by nucleases. Because the coating with 5 μg siICAM-1 embedded in 0.008% ATCOL shows better performance than 0.032% ATCOL transfection coating concerning the long-term knockdown of ICAM-1, it would be ideally suited for inhibiting restenosis after stent placement. Furthermore, it is important to emphasize that we expect an even more prolonged gene silencing of ICAM-1 in in vivo experiments than in in vitro experiments, because cell division in tissue culture is much faster than in in vivo ECs. When cells divide, siRNAs are diluted each time and, consequently, the silencing of the protein is diminished.[56]

The examination of the hemocompatibility of our ATCOL coatings proved that the coating of siICAM-1 and Lipofectamine 2000 embedded in ATCOL is biocompatible in contact with blood, leading to a favorable outlook for stent coating. We observed no significant cell number reduction in erythrocytes, leukocytes, platelets, lymphocytes, monocytes, and granulocytes after incubation with coated glass slides compared with the control (Figures 7A–7F). We revealed significant differences comparing the uncoated or coated glass slides with the nonincubated blood control (0 hr), which is mediated most likely due to an interaction between the incubation tube and the blood cells. The results of our blood cell test indicate that blood cells do not accumulate on the ATCOL/siICAM-1 coating, because no reduction in cell number was observed compared to the 1-hr control. Furthermore, we proved the hemocompatibility of our coating system by testing the complement system values of SC5b9 and C3a and the PMN elastase. We noted a significant increase comparing
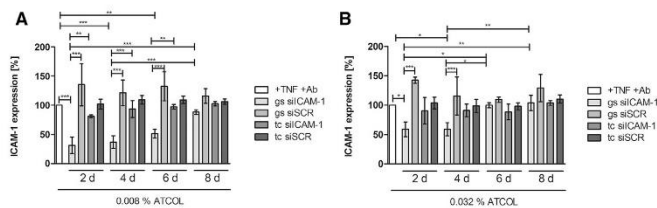
www.moleculartherapy.org

Figure 5. ICAM-1 Expression after Long-Term Knockdown of ICAM-1 Examined by Flow Cytometry

Glass slides were coated with ATCOL/silCAM-1 transfection solution for substrate-mediated transfection and laid in a 24-well plate. For conventional transfection in tissue culture, ATCOL/silCAM-1 transfection solution was added to the cell culture medium, where EA.hy926 cells were seeded 1 day prior. After each time point, cells were activated for 14 hr with TNF-α and analyzed by flow cytometry. ICAM-1 expression was calculated after setting the TNF-α control to 100%. Each bar in (A) and (B) represents the mean ± SEM (n = 3). *p < 0.05; **p < 0.01; ***p < 0.001. gs, glass slide; tc, tissue culture.

0-hr samples to 1-hr samples as described above in all three parameters, but we determined no increase in transfection coating with ATCOL and silICAM-1. Additionally, we found out that none of the coatings provoke hemolysis. In this respect, we suppose that our experiments and results lead the way to a promising new approach in stent development for combating risk after PTCA.

The combination of the biocompatible protein ATCOL with embedded siRNA particles targeting *ICAM-1* seems to be a sophisticated therapeutic approach for the intervention in inflammatory processes after stent placement. The high cell viability of EA.hy926 grown on 0.008%–0.032% ATCOL demonstrated the imperative biocompatibility of the polymer. Furthermore, the coating shows good hemocompatibility, proven by no adsorption of blood cells to the coatings and no hemolysis, inflammation, or complement activation. Unexpectedly, ATCOL with naked siRNA was not able to transfect EA.hy926 sufficiently. As a consequence, we added Lipofectamine 2000 to our ATCOL/siRNA coatings and achieved significantly high transfection efficiencies with 68.9% (0.008% ATCOL) and 75.2% (0.032% ATCOL) positive cells. Our experiments show that the coating consisting of 0.008% ATCOL and 5 μg silICAM-1 is suitable for long-term knockdown of ICAM-1 protein up to 8 days. Because of this excellent performance of ATCOL combined with the personalized approach of using therapeutic siRNA, we consider our coating as a transferable system for in vivo applications that should be further investigated.

MATERIALS AND METHODS
Chemicals for ATCOL Coating
Bovine dermis ATCOLs (3 mg/mL) from Cosmo Bio was diluted under sterile conditions with 5 mM sodium acetate buffer (pH 5.5). Different concentrations of ATCOL were used for coatings: 0.008%, 0.016%, 0.032%, and 0.064%. Sodium acetate was purchased from Sigma-Aldrich and prepared with double distilled water (ddH$_2$O) (Ampuwa; Fresenius Kabi).

siRNAs
The following siRNA (silICAM) was used for gene knockdown: human ICAM-1 with sense strand 5′-GCC UCA GCA CGU ACC-UCU AUU-3′ and antisense 5′-UAG AGG UAC GUG CUG AAG CUU-3′. AF 488-labeled E-selectin siRNA AF 488 was applied

to test the transfection efficiency (sense strand 5′-UUG AGU GGU GCA UUC AAC CUU-3′ and antisense 5′-GGU UGA AUG CAC CAC UCA AUU-3′; both from Eurofins MWG Operon). Control nonsense siRNA (siSCR) was supplied by QIAGEN. QIAGEN does not provide the sequences of their nonsilencing siRNAs but ensures that they have no homology to any known mammalian gene. This nonsilencing siRNA is validated by using Affymetrix GeneChip arrays and a variety of cell-based assays and is shown to ensure minimal nonspecific effects on gene expression and phenotype.

Substrate for ATCOL Coatings
The ATCOL coating was prepared on glass slides from Marienfeld, with a dimension of 10 × 10 × 1 mm. The slides were purified by ultrasonication (Bandelin RK 100H Sonorex; Bandelin Electronic) with 2% Hellmanex solution from Hellma before rinsing with ddH$_2$O. Air-dried slides were sterilized in a heating furnace (Binder) at 200°C for 4 hr prior to their use in the ATCOL coating procedure.

Preparation of ATCOL/siRNA Coatings
The different ATCOL concentrations (0.008%, 0.016%, 0.032%, and 0.064%) were prepared by diluting the stock solution with sodium acetate buffer. siRNA (20 μM) was diluted in 0.15 M NaCl (Fresenius Kabi) and either added to Lipofectamine 2000 or not, depending on the experiment. We mixed different amounts of Lipofectamine 2000 with different amounts of siRNA in the following way: 1 μL Lipofectamine 2000 to 1 μg siRNA, 2 μL to 2.5 μg and 3 μl to 5 μg, respectively. Then, the two solutions (diluted ATCOL and siRNA with or without Lipofectamine 2000) were incubated separately for 10 min and then combined, shortly vortexed, and spun down. Within 20 min, complexes were allowed to form at room temperature. Glass slides were covered with 100 μL of the respective coating solution and air-dried under sterile conditions. ATCOL coatings without siRNA and Lipofectamine 2000 served beside uncoated glass slides as a control in flow cytometry.

ATCOL/siRNA-Mediated Transfection of EA.hy926
Coated glass slides were put in a 24-well plate and a maximum of 75,000 EA.hy926 cells in a 50-μL volume were applied on one glass slide. After 30-min incubation time, 1 mL medium was added to each well and cells were cultivated for 48 hr at 37°C. Thereafter, cells
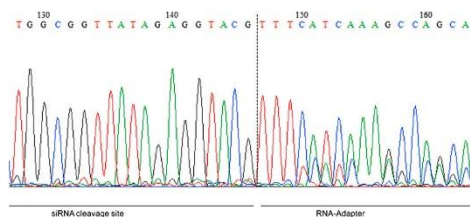
OMTN 29

Figure 6. Sequence of 5′-RLM-RACE-PCR Product after Transfecting EA.hy926 with 0.032% ATCOL-Mediated siICAM-1 Coating

After cultivation of 75,000 cells on coated glass slides, RNA was isolated followed by the 5′-RLM-RACE-PCR procedure. The cleavage site of *ICAM-1* mRNA was detected at 1,818 bp (128–146) with the RNA adaptor sequence (147–163). Each bar represents the mean ± SEM.

were prepared to determine transfection efficiency and knockdown of ICAM-1 protein expression by flow cytometry. The long-term knockdown experiment required adaption of the cell number due to the elongation of cultivation time up to 8 days. The cell number for seeding was reduced from 75,000 EA.hy926 to 30,000 for 4-day cultivation, to 23,000 for 6-day cultivation, and to 15,000 for 8-day cultivation.

To compare the results of the coating-mediated transfection with conventional transfection, cells were seeded 24 hr prior to coating transfection in a 24-well plate. At time point 0 (cultivation of cells on the coating), the same siRNA Lipofectamine 2000 and ATCOL amount that was used for the coating preparation was added to the cells in a solution. After 4 hr of transfection, the complete medium with transfection solution was discarded and cells were washed with cell culture medium. EA.hy926 cells were further cultured with fresh DMEM until the day of flow cytometry analysis. To enable the best cell growth, the medium was changed every second day.

Cultivation of EA.hy926

The immortalized human umbilical vein cell line EA.hy (LGC Standards) was used for all cell experiments. Cells were cultured in high-glucose DMEM containing 10% fetal calf serum, 1% penicillin/streptomycin, and 1% L-glutamine (Gibco, Division of Life Technologies).

Release of AF 488-Labeled E-selectin siRNA AF 488

Coatings of two different concentrations of ATCOL, 0.008% and 0.032%, were tested with 1, 2.5, and 5 µg E-selectin siRNA AF 488 to determine their release profile. Coatings were prepared as mentioned previously and the dried coated glass slides were placed in 24-well plates with 1 mL PBS. Slides were incubated under cell culture conditions at 37°C and supernatant was measured at defined time points with the Mithras LB 940 fluorescent reader (Berthold Technologies) at 485-nm excitation and 535-nm emission. Each sample value was represented in a XY scatter chart. Additionally, the last measured fluorescence intensity values were summed to determine the differences between the samples in a bar chart at day 9.

Flow Cytometry

Transfection efficiency or knockdown of ICAM-1 protein expression was determined by flow cytometry after different cultivation times. Transfection efficiency is shown as the relationship of positive (fluorescent) cells to the total cell amount, given in percentages. In our study, cells were transfected by substrate-mediated transfection with AF 488-labeled siRNA. After cultivation, cells were removed from the substrate by washing and detachment. Cells were subsequently fixed with 2.5% paraformaldehyde (PFA). Flow cytometry analysis was performed with 5,000 cells/measurement (FACScan; Becton Dickinson). The green fluorescence (FL1) signal within the cells was detected by a flow cytometer laser that also recorded forward and side scatter for the detection of viable cells. The results were evaluated with CellQuestPro software (Becton Dickinson), and the number of counts was plotted against the logarithmic scale of FL1. The marker was set at control samples ≤ 1 and transfection efficiency of the transfection samples was determined by this gate. This resulted in the transfection efficiency, given in percentages.

In our study, knockdown of ICMA-1 is defined as the percentage removal of the ICAM-1 receptor on EA.hy926 caused by RNAi. Here, siICAM-1 is able to bind to the complementary mRNA and degrade it. Therefore, surface-mediated siICAM-1 transfection was ended after the defined period and cells were stimulated with 5 ng/mL TNF-α (BD Biosciences) for 14 hr to induce ICAM-1 protein expression. Afterward, immunofluorescence staining with PE mouse anti-human CD54 (BD Biosciences) (30 min at 37°C) was prepared, followed by detachment, PFA fixation, and flow cytometry analysis. Here, the number of counts was plotted against the logarithmic scale of FL2. Geometric mean fluorescence was used to evaluate the results. The control treated with TNF-α and stained with Ab was set to 100%, and transfected cells with siICAM-1 and siSCR were assessed in relation to the control. The figures show the ICAM-1 expression after gene knockdown. Knockdown values are the calculated difference between the control at 100% and the ICAM-1 expression values.

Cell Viability: Cell Counting and Inverted Microscopy

Cell compatibility of EA.hy926 cultivated on ATCOL-coated glass slides was tested by a CASY cell counter and inverted microscopy. Different concentrations of ATCOL were examined: 0.008%, 0.016%, 0.032%, and 0.064%, while uncoated glass slides served as a control. 75,000 EA.hy926 cells were seeded onto the coated glass slides and cultivated for 24 and 48 hr, respectively. Cells were then washed and detached for cell counting with a CASY cell counter to distinguish dead cells from living cells, due to their lower resistance in an electronic pulse area analysis. EA.hy926 morphology and cell behavior were visualized with an Axiovert 135 microscope (Zeiss) and images were captured with the corresponding software.

Hemocompatibility

The development of medical devices requires their verification and qualification in respect tobiocompatibility, primarily cytocompatibility (ISO 10993-5), and hemocompatibility (ISO 10993-4). ISO 10993-4 demands at least one test addressing thrombosis/coagulation,
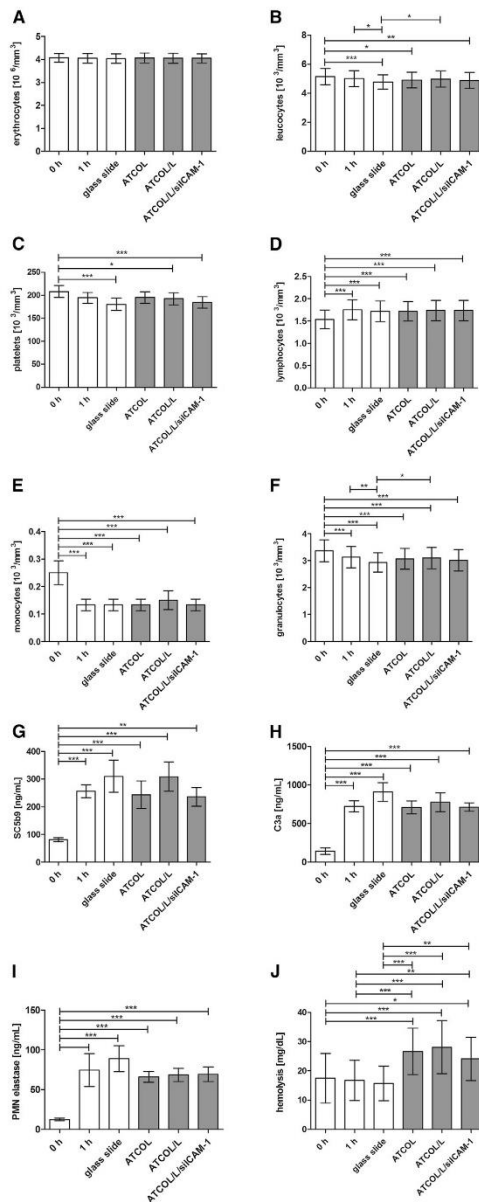
Figure 7. Hemocompatibility Analysis of 0.032% ATCOL/siICAM-1-Coated Glass Slides

Coated slides were incubated with fresh human blood at 37°C under gentle shaking. The 0-hr and 1-hr samples served as the control and the baseline, respectively. After incubation, different blood cell numbers and inflammatory parameters were analyzed by a cell counter or ELISAs: (A) erythrocytes $\times 10^3$ mm^{-3}; (B) leukocytes $\times 10^3$ mm^{-3}; (C) platelets $\times 10^3$ mm^{-3}; (D) lymphocytes $\times 10^3$ mm^{-3}; (E) monocytes $\times 10^3$ mm^{-3}; (F) granulocytes $\times 10^3$ mm^{-3}; (G) SC5b9 (ng mL^{-1}); (H) C3a (ng mL^{-1}); and (I) PMN elastase (ng mL^{-1}). Hemolysis was determined by the detection of free hemoglobin with citrate plasma and a reaction kit: (J) hemolysis (mg dL^{-1}). Each bar represents the mean ± SEM (n = 6). $^*p < 0.05$; $^{**}p < 0.01$; $^{***}p < 0.001$.

hematology, inflammation, and the complement system to determine the compatibility of a medical device with blood.

Therefore, hemocompatibility of different combinations was analyzed with glass slides coated on both sides. Both sides were coated because glass activates blood coagulation. Consequently, we reduced the free glass surfaces, with the exception of their edges. We used 0.032% ATCOL as a worst case in the following sample preparations as coating solution: (1) ATCOL, (2) ATCOL and Lipofectamine 2000, and (3) ATCOL and siICAM-1-Lipofectamine 2000 (5 μg siRNA). Uncoated glass slides with 0-hr and 1-hr blood contact time served as a control and a baseline, respectively. Glass slides were incubated in 14-mL round-bottom tubes (Falcon; Corning Life Sciences) at 37°C under gentle shaking with 13 mL human blood. Six independent blood donors were used for hemocompatibility evaluation. After 1-hr incubation, blood was analyzed with a Micros 60 counter (ABX Diagnostics) for blood cells such as leukocytes, erythrocytes, and platelets. Protein expression of C3a and SC5b9 associated with the complement system was analyzed by ELISAs (both Osteomedical). PMN elastase was tested as a sign of degranulation of leukocytes during an inflammatory reaction (Demeditec Diagnostics). Additionally, β-thromboglobulin expression, associated with activated platelets, was determined by the ASSERA-CHROM β-TG kit (Diagnostica Stago).

Furthermore, a hemoglobin color test (no longer available; Roche) was used to assess coated and uncoated glass slides for their hemolysis capability. In short, defrosted citrated plasma was incubated with a reaction solution (0.6 mM potassium hexacyanoferrate III and 750 nM potassium cyanide) for 3 min at room temperature. Free hemoglobin converts into cyanohemoglobin in the presence of reaction solution and is measured photometrically at 546 nm.

RLM-RACE-PCR

The pivotal point of gene knockdown with siRNA is to prove that RNAi is due to the complementary binding of the siRNA to the respective mRNA and not because of unspecific reactions. In 2004, Soutschek et al.[26] established the 5'-RLM-RACE-PCR technique detecting siRNA-mediated mRNA cleavage. Subsequently, Davis et al.[57] used this technique to verify siRNA-mediated mRNA cleavage in a human phase I clinical trial. Herein, cleaved mRNA products can be detected, meaning that 5'-RLM-RACE-PCR is especially suitable for applications with siRNA transfection, to confirm the mRNA

Table 1. Primer Sequences for 5′-RLM-RACE-PCR

5′-RLM-RACE-PCR	Primer
First strand ICAM-1	5′-AGGTACCATGGCCCCAAATG 3′
ICAM-1 RACE 1	5′-ACTCTGTTCAGTGTGGCACC-3′
ICAM-1 RACE 2	5′-TCTTCCTCGGCCTTCCCATA-3′
ICAM-1 RACE 3	5′-TGGCCCCAAATGCTGTTGTA-3′
RNA adaptor (universally)	5′-GCUGAUGGCGAUGAAUGAACACUGC GUUUGCUGGCUUUGAUGAAA 3′
Outer primer (universally)	5′-GCTGATGGCGATGAATGAACACTG-3′
Inner primer (universally)	5′-CGCGGATCCGAACACTGCGTTTGCT GGCTTTGATG 3′

degradation dependent on the base pair sequence of the siRNA. Coatings of glass slides were produced as mentioned before, with 5 μg silCAM-1, Lipofectamine 2000, and 0.032% ATCOL. 75,000 EA.hy926 cells were cultivated on the coated glass slides for 48 hr. Afterward, cells were stimulated with TNF-α (5 ng/mL) for 14 hr before the RNA was isolated using the Aurum total RNA mini kit (Bio-Rad Laboratories). After quantification of eluted RNA, the RNA was ligated with a 5′-RACE adaptor in presence of T4 RNA ligase, which is commercially available in the First Choice RLM-RACE Kit (Life Technologies). RNA re-isolation was followed by reverse transcription using 200 ng ligated RNA Moloney murine leukemia virus (M-MLV) reverse transcriptase for first-strand cDNA synthesis. Gene-specific primers must be designed for the first-strand synthesis as well as for the outer and inner PCR occurring after first-strand cDNA synthesis. Primers were designed with Primer3[58] and Primer Premier 5 software (PREMIER Biosoft International) and are shown in Table 1. Outer and inner PCR reactions were conducted via qRT-PCR and contained IQ SYBR Green Supermix (Bio-Rad) performed in triplicate. The reaction mixture contained 400 nM forward and reverse primers with 2 ng cDNA in a total volume of 15 μL.

Statistical Analysis

All experiments were conducted at least three times independently, except for the hemocompatibility and hemolysis assay in which the blood of six different donors was used. Comparison of the different samples was done by one-way ANOVA and Bonferroni correction as a post-test.

AUTHOR CONTRIBUTIONS

O.K. designed the experiments and wrote the paper. O.K. and D.N. conducted most of the experiments. N.P. and A.B. provided support to conduct the transfection studies. B.N. provided technical support for the hemocompatibility assays. I.D. performed the hemolysis experiment. T.W., C.S., and H.P.W. supported the work with their clinical expertise and revised the manuscript. A.N. supervised the work.

CONFLICTS OF INTEREST

The authors declare no conflict of interest.

ACKNOWLEDGMENTS

REFERENCES

1. Laslett, L.J., Alagona, P., Jr., Clark, B.A., 3rd, Drozda, J.P., Jr., Saldivar, F., Wilson, S.R., Poe, C., and Hart, M. (2012). The worldwide environment of cardiovascular disease: prevalence, diagnosis, therapy, and policy issues: a report from the American College of Cardiology. J. Am. Coll. Cardiol. 60 (Suppl), S1–S49.

2. Roth, G.A., Huffman, M.D., Moran, A.E., Feigin, V., Mensah, G.A., Naghavi, M., and Murray, C.J. (2015). Global and regional patterns in cardiovascular mortality from 1990 to 2013. Circulation 132, 1667–1678.

3. Nichols, M., Townsend, N., Scarborough, P., and Rayner, M. (2014). Cardiovascular disease in Europe 2014: epidemiological update. Eur. Heart J. 35, 2950–2959.

4. Winniford, M.D., Jansen, D.E., Reynolds, G.A., Apprill, P., Black, W.H., and Hillis, L.D. (1987). Cigarette smoking-induced coronary vasoconstriction in atherosclerotic coronary artery disease and prevention by calcium antagonists and nitroglycerin. Am. J. Cardiol. 59, 203–207.

5. Wilson, P.W. (1994). Established risk factors and coronary artery disease: the Framingham Study. Am. J. Hypertens. 7, 7S–12S.

6. Thompson, P.D. (2005). Exercise prescription and proscription for patients with coronary artery disease. Circulation 112, 2354–2363.

7. Smith, S.C., Jr., Benjamin, E.J., Bonow, R.O., Braun, L.T., Creager, M.A., Franklin, B.A., Gibbons, R.J., Grundy, S.M., Hiratzka, L.F., Jones, D.W., et al.; World Heart Federation and the Preventive Cardiovascular Nurses Association (2011). AHA/ACCF secondary prevention and risk reduction therapy for patients with coronary and other atherosclerotic vascular disease: 2011 update: a guideline from the American Heart Association and American College of Cardiology Foundation. Circulation 124, 2458–2473.

8. Eckel, R.H., Jakicic, J.M., Ard, J.D., de Jesus, J.M., Houston Miller, N., Hubbard, V.S., Lee, I.M., Lichtenstein, A.H., Loria, C.M., Millen, B.E., et al.; American College of Cardiology/American Heart Association Task Force on Practice Guidelines (2014). 2013 AHA/ACC guideline on lifestyle management to reduce cardiovascular risk: a report of the American College of Cardiology/American Heart Association Task Force on Practice Guidelines. Circulation 129 (Suppl 2), S76–S99.

9. Windecker, S., Kolh, P., Alfonso, F., Collet, J.P., Cremer, J., Falk, V., Filippatos, G., Hamm, C., Head, S.J., Jüni, P., et al.; Authors/Task Force members (2014). 2014 ESC/EACTS Guidelines on myocardial revascularization: The Task Force on Myocardial Revascularization of the European Society of Cardiology (ESC) and the European Association for Cardio-Thoracic Surgery (EACTS)Developed with the special contribution of the European Association of Percutaneous Cardiovascular Interventions (EAPCI). Eur. Heart J. 35, 2541–2619.

10. Henderson, R.A., Pocock, S.J., Sharp, S.J., Nanchahal, K., Sculpher, M.J., Buxton, M.J., and Hampton, J.R. (1998). Long-term results of RITA-1 trial: clinical and cost comparisons of coronary angioplasty and coronary-artery bypass grafting. Randomised Intervention Treatment of Angina. Lancet 352, 1419–1425.

11. Hamm, C.W., Reimers, J., Ischinger, T., Rupprecht, H.J., Berger, J., and Bleifeld, W. (1994). A randomized study of coronary angioplasty compared with bypass surgery in patients with symptomatic multivessel coronary disease. German Angioplasty Bypass Surgery Investigation (GABI). N. Engl. J. Med. 331, 1037–1043.

12. RITA-2 Trial Participants (1993). Coronary angioplasty versus coronary artery bypass surgery: the Randomized Intervention Treatment of Angina (RITA) trial. Lancet 341, 573–580.

13. Daemen, J., Boersma, E., Flather, M., Booth, J., Stables, R., Rodriguez, A., Rodriguez-Granillo, G., Hueb, W.A., Lemos, P.A., and Serruys, P.W. (2008). Long-term safety and efficacy of percutaneous coronary intervention with stenting and coronary artery bypass surgery for multivessel coronary artery disease: a meta-analysis with 5-year patient-level data from the ARTS, ERACI-II, MASS-II, and SoS trials. Circulation 118, 1146–1154.

14. Cutlip, D.E., Chauhan, M.S., Baim, D.S., Ho, K.K., Popma, J.J., Carrozza, J.P., Cohen, D.J., and Kuntz, R.E. (2002). Clinical restenosis after coronary stenting: perspectives from multicenter clinical trials. J. Am. Coll. Cardiol. 40, 2082–2089.

OMTN 29

www.moleculartherapy.org

15. Kornowski, R., Hong, M.K., Tio, F.O., Bramwell, O., Wu, H., and Leon, M.B. (1998). In-stent restenosis: contributions of inflammatory responses and arterial injury to neointimal hyperplasia. J. Am. Coll. Cardiol. 31, 224–230.

16. Kearney, M., Pieczek, A., Haley, L., Losordo, D.W., Andres, V., Schainfeld, R., Rosenfield, K., and Isner, J.M. (1997). Histopathology of in-stent restenosis in patients with peripheral artery disease. Circulation 95, 1998–2002.

17. Ley, K., Laudanna, C., Cybulsky, M.I., and Nourshargh, S. (2007). Getting to the site of inflammation: the leukocyte adhesion cascade updated. Nat. Rev. Immunol. 7, 678–689.

18. Serruys, P.W., Kutryk, M.J.B., and Ong, A.T.L. (2006). Coronary-artery stents. N. Engl. J. Med. 354, 483–495.

19. Kimura, T., Morimoto, T., Nakagawa, Y., Kawai, K., Miyazaki, S., Muramatsu, T., Shiode, N., Namura, M., Sone, T., Oshima, S., et al.; j-Cypher Registry Investigators (2012). Very late stent thrombosis and late target lesion revascularization after sirolimus-eluting stent implantation: five-year outcome of the j-Cypher Registry. Circulation 125, 584–591.

20. Bangalore, S., Kumar, S., Fusaro, M., Amoroso, N., Attubato, M.J., Feit, F., Bhatt, D.L., and Slater, J. (2012). Short- and long-term outcomes with drug-eluting and bare-metal coronary stents: a mixed-treatment comparison analysis of 117 762 patient-years of follow-up from randomized trials. Circulation 125, 2873–2891.

21. Fajadet, J., Wijns, W., Laarman, G.J., Kuck, K.H., Ormiston, J., Münzel, T., Popma, J.J., Fitzgerald, P.J., Bonan, R., and Kuntz, R.E.; ENDEAVOR II Investigators (2006). Randomized, double-blind, multicenter study of the Endeavor zotarolimus-eluting phosphorylcholine-encapsulated stent for treatment of native coronary artery lesions: clinical and angiographic results of the ENDEAVOR II trial. Circulation 114, 798–806.

22. Stettler, C., Wandel, S., Allemann, S., Kastrati, A., Morice, M.C., Schömig, A., Pfisterer, M.E., Stone, G.W., Leon, M.B., de Lezo, J.S., et al. (2007). Outcomes associated with drug-eluting and bare-metal stents: a collaborative network meta-analysis. Lancet 370, 937–948.

23. Douglas, G., Van Kampen, E., Hale, A.B., McNeill, E., Patel, J., Crabtree, M.J., Ali, Z., Hoerr, R.A., Alp, N.J., and Channon, K.M. (2013). Endothelial cell repopulation after stenting determines in-stent neointima formation: effects of bare-metal vs. drug-eluting stents and genetic endothelial cell modification. Eur. Heart J. 34, 3378–3388.

24. Dorsett, Y., and Tuschl, T. (2004). siRNAs: applications in functional genomics and potential as therapeutics. Nat. Rev. Drug Discov. 3, 318–329.

25. Dowler, T., Bergeron, D., Tedeschi, A.L., Paquet, L., Ferrari, N., and Damha, M.J. (2006). Improvements in siRNA properties mediated by 2′-deoxy-2′-fluoro-beta-D-arabinonucleic acid (FANA). Nucleic Acids Res. 34, 1669–1675.

26. Soutschek, J., Akinc, A., Bramlage, B., Charisse, K., Constien, R., Donoghue, M., Elbashir, S., Geick, A., Hadwiger, P., Harborth, J., et al. (2004). Therapeutic silencing of an endogenous gene by systemic administration of modified siRNAs. Nature 432, 173–178.

27. Boussif, O., Lezoualc'h, F., Zanta, M.A., Mergny, M.D., Scherman, D., Demeneix, B., and Behr, J.P. (1995). A versatile vector for gene and oligonucleotide transfer into cells in culture and in vivo: polyethylenimine. Proc. Natl. Acad. Sci. USA 92, 7297–7301.

28. Sano, A., Maeda, M., Nagahara, S., Ochiya, T., Honma, K., Itoh, H., Miyata, T., and Fujioka, K. (2003). Atelocollagen for protein and gene delivery. Adv. Drug Deliv. Rev. 55, 1651–1677.

29. Minakuchi, Y., Takeshita, F., Kosaka, N., Sasaki, H., Yamamoto, Y., Kouno, M., Honma, K., Nagahara, S., Hanai, K., Sano, A., et al. (2004). Atelocollagen-mediated synthetic small interfering RNA delivery for effective gene silencing in vitro and in vivo. Nucleic Acids Res. 32, e109.

30. Rubin, A.L., Miyata, T., and Stenzel, K.H. (1969). Collagen: medical and surgical applications. J. Macromol. Sci. Chem. 3, 113–118.

31. Ochiya, T., Nagahara, S., Sano, A., Itoh, H., and Terada, M. (2001). Biomaterials for gene delivery: atelocollagen-mediated controlled release of molecular medicines. Curr. Gene Ther. 1, 31–52.

32. Honma, K., Ochiya, T., Nagahara, S., Sano, A., Yamamoto, H., Hirai, K., Aso, Y., and Terada, M. (2001). Atelocollagen-based gene transfer in cells allows high throughput screening of gene functions. Biochem. Biophys. Res. Commun. 289, 1075–1081.

33. Hirai, K., Sasaki, H., Sakamoto, H., Takeshita, F., Asano, K., Kubota, Y., Ochiya, T., and Terada, M. (2003). Antisense oligodeoxynucleotide against HST-1/FGF-4 suppresses tumorigenicity of an orthotopic model for human germ cell tumor in nude mice. J. Gene Med. 5, 951–957.

34. Hanai, K., Kurokawa, T., Minakuchi, Y., Maeda, M., Nagahara, S., Miyata, T., Ochiya, T., and Sano, A. (2004). Potential of atelocollagen-mediated systemic antisense therapeutics for inflammatory disease. Hum. Gene Ther. 15, 263–272.

35. Monaghan, M., Browne, S., Schenke-Layland, K., and Pandit, A. (2014). A collagen-based scaffold delivering exogenous microRNA-29B to modulate extracellular matrix remodeling. Mol. Ther. 22, 786–796.

36. Svintradze, D.V., and Mrevlishvili, G.M. (2005). Fiber molecular model of atelocollagen-small interfering RNA (siRNA) complex. Int. J. Biol. Macromol. 37, 283–286.

37. Dalby, B., Cates, S., Harris, A., Ohki, E.C., Tilkins, M.L., Price, P.J., and Ciccarone, V.C. (2004). Advanced transfection with Lipofectamine 2000 reagent: primary neurons, siRNA, and high-throughput applications. Methods 33, 95–103.

38. San Juan, A., Bala, M., Hlawaty, H., Portes, P., Vranckx, R., Feldman, L.J., and Letourneur, D. (2009). Development of a functionalized polymer for stent coating in the arterial delivery of small interfering RNA. Biomacromolecules 10, 3074–3080.

39. Li, J.M., Newburger, P.E., Gounis, M.J., Dargon, P., Zhang, X., and Messina, L.M. (2010). Local arterial nanoparticle delivery of siRNA for NOX2 knockdown to prevent restenosis in an atherosclerotic rat model. Gene Ther. 17, 1279–1287.

40. Che, H.L., Bae, I.H., Lim, K.S., Song, I.T., Lee, H., Muthiah, M., Namgung, R., Kim, W.J., Kim, D.G., Ahn, Y., et al. (2012). Suppression of post-angioplasty restenosis with an Akt1 siRNA embedded coronary stent in a rabbit model. Biomaterials 33, 8548–8556.

41. Hlawaty, H., San Juan, A., Jacob, M.P., Vranckx, R., Letourneur, D., and Feldman, L.J. (2007). Inhibition of MMP-2 gene expression with small interfering RNA in rabbit vascular smooth muscle cells. Am. J. Physiol. Heart Circ. Physiol. 293, H3593–H3601.

42. Shyu, K.G., Wang, B.W., Kuan, P., and Chang, H. (2008). RNA interference for discoidin domain receptor 2 attenuates neointimal formation in balloon injured rat carotid artery. Arterioscler. Thromb. Vasc. Biol. 28, 1447–1453.

43. Janmey, P.A., Winer, J.P., Murray, M.E., and Wen, Q. (2009). The hard life of soft cells. Cell Motil. Cytoskeleton 66, 597–605.

44. Lo, C.-M., Wang, H.-B., Dembo, M., and Wang, Y.L. (2000). Cell movement is guided by the rigidity of the substrate. Biophys. J. 79, 144–152.

45. Bhana, B., Iyer, R.K., Chen, W.L.K., Zhao, R., Sider, K.L., Likhitpanichkul, M., Simmons, C.A., and Radisic, M. (2010). Influence of substrate stiffness on the phenotype of heart cells. Biotechnol. Bioeng. 105, 1148–1160.

46. Discher, D.E., Janmey, P., and Wang, Y.L. (2005). Tissue cells feel and respond to the stiffness of their substrate. Science 310, 1139–1143.

47. Engler, A.J., Carag-Krieger, C., Johnson, C.P., Raab, M., Tang, H.Y., Speicher, D.W., Sanger, J.W., Sanger, J.M., and Discher, D.E. (2008). Embryonic cardiomyocytes beat best on a matrix with heart-like elasticity: scar-like rigidity inhibits beating. J. Cell Sci. 121, 3794–3802.

48. Saunders, R.L., and Hammer, D.A. (2010). Assembly of human umbilical vein endothelial cells on compliant hydrogels. Cell. Mol. Bioeng. 3, 60–67.

49. Nolte, A., Hossfeld, S., Schroeppel, B., Mueller, A., Stoll, D., Walker, T., Wendel, H.P., and Krastev, R. (2013). Impact of polyelectrolytes and their corresponding multilayers to human primary endothelial cells. J. Biomater. Appl. 28, 84–99.

50. Mu, P., Nagahara, S., Makita, N., Tarumi, Y., Kadomatsu, K., and Takei, Y. (2009). Systemic delivery of siRNA specific to tumor mediated by atelocollagen: combined therapy using siRNA targeting Bcl-xL and cisplatin against prostate cancer. Int. J. Cancer 125, 2978–2990.

51. Takeshita, F., Minakuchi, Y., Nagahara, S., Honma, K., Sasaki, H., Hirai, K., Teratani, T., Namatame, N., Yamamoto, Y., Hanai, K., et al. (2005). Efficient delivery of small interfering RNA to bone-metastatic tumors by using atelocollagen in vivo. Proc. Natl. Acad. Sci. USA 102, 12177–12182.

52. Kim, T.K., and Eberwine, J.H. (2010). Mammalian cell transfection: the present and the future. Anal. Bioanal. Chem. 397, 3173–3178.

53. Nolte, A., Walker, T., Schneider, M., Kray, O., Avci-Adali, M., Ziemer, G., and Wendel, H.P. (2011). Small-interfering RNA-eluting surfaces as a novel concept for intravascular local gene silencing. Mol. Med. *17*, 1213–1222.

54. Khan, W., Farah, S., and Domb, A.J. (2012). Drug eluting stents: developments and current status. J. Control Release *161*, 703–712.

55. Sluiter, W., Pietersma, A., Lamers, J.M., and Koster, J.F. (1993). Leukocyte adhesion molecules on the vascular endothelium: their role in the pathogenesis of cardiovascular disease and the mechanisms underlying their expression. J. Cardiovasc. Pharmacol. *22* (*Suppl 4*), S37–S44.

56. Dykxhoorn, D.M., Novina, C.D., and Sharp, P.A. (2003). Killing the messenger: short RNAs that silence gene expression. Nat. Rev. Mol. Cell Biol. *4*, 457–467.

57. Davis, M.E., Zuckerman, J.E., Choi, C.H., Seligson, D., Tolcher, A., Alabi, C.A., Yen, Y., Heidel, J.D., and Ribas, A. (2010). Evidence of RNAi in humans from systemically administered siRNA via targeted nanoparticles. Nature *464*, 1067–1070.

58. Rozen, S., and Skaletsky, H. (2000). Primer3 on the WWW for general users and for biologist programmers. Methods Mol. Biol. *132*, 365–386.

6.3 Publication II

RNA-Eluting Surfaces for the Modulation of Gene Expression as A Novel Stent Concept

pharmaceuticals

MDPI

Article

RNA-Eluting Surfaces for the Modulation of Gene Expression as A Novel Stent Concept

Olivia Koenig †, Diane Zengerle †, Nadja Perle, Susanne Hossfeld, Bernd Neumann, Andreas Behring, Meltem Avci-Adali, Tobias Walker, Christian Schlensak, Hans Peter Wendel * and Andrea Nolte

Department of Thoracic, Cardiac, and Vascular Surgery, University of Tuebingen, Calwerstraße 7/1, 72076 Tuebingen, Germany; olivia.koenig@gmx.de (O.K.); diane.zengerle@icloud.com (D.Z.); nadja.perle@gmx.de (N.P.); susanne.hossfeld@nexgo.de (S.H.); b.neumann.71@web.de (B.N.); behring.andi@googlemail.com (A.B.); meltem.avci.adali@gmail.com (M.A.-A.); tobias.walker@med.uni-tuebingen.de (T.W.); christian.schlensak@med.uni-tuebingen.de (C.S.); andrea.nolte-karayel@gmx.de (A.N.)
* Correspondence: hans-peter.wendel@med.uni-tuebingen.de; Tel.: +49-7071-2986-605
† These authors contributed equally to this work.

Abstract: Presently, a new era of drug-eluting stents is continuing to improve late adverse effects such as thrombosis after coronary stent implantation in atherosclerotic vessels. The application of gene expression–modulating stents releasing specific small interfering RNAs (siRNAs) or messenger RNAs (mRNAs) to the vascular wall might have the potential to improve the regeneration of the vessel wall and to inhibit adverse effects as a new promising therapeutic strategy. Different poly (lactic-*co*-glycolic acid) (PLGA) resomers for their ability as an siRNA delivery carrier against intercellular adhesion molecule (ICAM)-1 with a depot effect were tested. Biodegradability, hemocompatibility, and high cell viability were found in all PLGAs. We generated PLGA coatings with incorporated siRNA that were able to transfect EA.hy926 and human vascular endothelial cells. Transfected EA.hy926 showed significant silCAM-1 knockdown. Furthermore, co-transfection of siRNA and enhanced green fluorescent protein (eGFP) mRNA led to the expression of eGFP as well as to the siRNA transfection. Using our PLGA and siRNA multilayers, we reached high transfection efficiencies in EA.hy926 cells until day six and long-lasting transfection until day 20. Our results indicate that siRNA and mRNA nanoparticles incorporated in PLGA films have the potential for the modulation of gene expression after stent implantation to achieve accelerated regeneration of endothelial cells and to reduce the risk of restenosis.

Keywords: atherosclerosis; drug eluting stents; PLGA films; gene delivery; local transfection; silCAM-1; gene knockdown; mRNA

---

1. Introduction

In 2012 more than 17.5 million people died from cardiovascular diseases (CVD), representing 31% of all global deaths. Atherosclerosis represents the most common cause for CVD and is especially represented in industrial nations [1]. The main causes of death among CVDs are the coronary artery diseases triggering stroke and heart attack. Herein, the blockage of blood flow leads to the interruption of oxygen supply, and finally the death of myocardial and brain cells, respectively. During the inflammatory process of atherosclerosis, low density lipoprotein (LDL) cholesterol causes the accumulation of lipids within the artery wall, followed by several events such as lesion initiation, plaque rupture, and thrombotic vessel occlusion [1–3]. Different therapeutic approaches for the

treatment of coronary artery stenosis exist, e.g., bypass surgery or percutaneous transluminal coronary angioplasty (PTCA), which was performed in 1977 for the first time [4]. The method of choice is the minimally invasive introduction of a coronary stent by a balloon catheter during the PTCA. Nevertheless, the insertion of a stent harbors the risk of in-stent restenosis (ISR) and stent thrombosis and is of tremendous significance in daily clinical life [5]. Coronary stent implantation may cause atherosclerotic plaque rupture and the damage of the endothelial layer, resulting in the activation of a cascade of wound-healing mechanisms, known as neointimal hyperplasia [6,7]. Besides a cascade of various events taking place, such as medial smooth muscle cell proliferation and migration, platelet aggregation, release of growth factors, and extracellular matrix remodeling, inflammatory cell infiltration is the first response in neointimal hyperplasia [6]. After the deposition of activated platelets and fibrin on the de-endothelialized vessel wall, the recruitment and infiltration of leukocytes occurs due to inflammatory mediators and chemoattractant factors [8,9]. Therefore, endothelial cells (ECs) start with an enhanced expression of cell adhesion molecules (CAMs) such as intercellular adhesion molecule (ICAM)-1 (specific to T lymphocytes), P-selectin (specific to monocytes and neutrophils), E-selectin (specific to monocytes and granulocytes), and vascular cell adhesion molecule (VCAM)-1 (specific to monocytes) [8,10,11]. The CAMs enable the adhesion of leukocytes and subsequently the migration of the cells into the intima via diapedesis. As a consequence, the vascular smooth muscle cells (VSMCs) proliferate and migrate from the media into the neointima and a chronic inflammatory process is evoked [12,13]. Substantial progress against ISR was made with the development of drug-eluting stents (DES) replacing bare metal stents (BMS), with a reduction of ISR rates to 60%–80% [7]. Both the first-generation of DESs containing paclitaxel or sirolimus and also the second-generation DESs with zotarolimus or everolimus show adverse effects leading to delayed re-endothelialization and consequently to a prolonged antiplatelet therapy [14,15]. Nevertheless, the new DES era revealed promising efforts to eradicate these drawbacks [16]. For example, new drug-coated stents rely on the capture of endothelial progenitor cells with specific antibodies such as anti-CD34 for accelerated re-endothelialization after stent implantation [17–20]. Another promising therapeutic strategy is the coating of stents with agents at the molecular level. Gene-silencing stents containing small interfering RNA (siRNA) have the potential to inhibit inflammatory processes on the vessel wall by blocking the transcription of cytokine receptors or adhesion molecule proteins [9]. The short double-stranded 21- to 23-nucleotide-long siRNAs interfere with its complementary messenger RNA (mRNA) which is subsequently degraded [12]. This powerful and conserved self-defense mechanism in *Eukarya* has a threefold biological meaning: (1) it helps prevent infections by viral RNA, (2) it regulates and alters gene expression and (3) it controls a certain type of transposon. It is hence worthwhile pursuing this mechanism with respect to an elementary potential therapeutic strategy in humans. Therefore, siRNAs get designed and stabilized for therapeutic applications, overcoming the degradation of free siRNA by endo- and exonucleases in blood, in serum, and in living cells [13,14]. The liposome or lipid protection strategy is common for in vitro and in vivo siRNA transfection. Cationic lipids such as Lipofectamine® 2000 are able to form nanoparticles (NPs) with siRNA as well as with mRNA, another transient gene delivery approach, which has gained increasing interest in the treatment of several diseases [15,16]. The mRNA delivered into the cell uses the cell's own translational machinery to produce the protein it encodes. Recently, we showed the potency of a CD39 mRNA coating in reducing complications after stent angioplasty [17]. The pivotal point in designing a drug delivery system is the choice of the material where the NPs can be embedded. Both biocompatibility and hemocompatibility are equally important to ensure not only cell proliferation and viability but also a possible therapeutic application. Additionally, the release of drugs with long-term effects, controlled delivery and efficacy is of no lesser importance. One of the most popular Food and Drug Administration (FDA)- and European Medicines Agency (EMA)-approved biomaterials in drug delivery carrier systems is poly (lactic-*co*-glycolic acid) (PLGA), a copolymer of poly lactic acid (PLA) and poly glycolic acid (PGA) [21,22]. During the hydrolysis of PLGA, these two monomers emerge again with the metabolic products carbon dioxide and water. PLGA seems to provoke less systemic cytotoxicity, considering PLA and PGA naturally

form in the human body via the Krebs cycle [21–23]. However, the production of acids upon polymer degradation is seen as a disadvantage of PLGA [24]. The degradation of commercially available PLGA is determined by the physico-chemical properties of the polymers such as the molecular weight, end groups (capped or uncapped) and PLA:PGA ratio, and it is degraded slowly over months to years in the body [25–27]. With a higher content of PGA in PLGA, the degradation time is increased, except for 50:50 (PLA:PGA) having the fastest degradation of one to two months (PLGA 75:25, four to five months; PLGA 85:15, five to six months) [28,29]. Therefore, PLGA is a promising biodegradable polymer for coating cardiovascular stents as a drug carrier in either thin coatings or PLGA NPs. Commercially available DESs such as Nevo™ (Johnson & Johnson) and Supralimus™ (Sahajanand Medical) consist of PLGA as a coating material for cobalt-chromium or stainless steel with sirolimus as a drug to prevent ISR [30]. Furthermore, a study by Klugherz et al. demonstrated the importance and effectiveness of plasmid DNA-loaded PLGA NPs by successfully transfecting pig arteries in vivo for the first time [31]. In 2010, Brito et al. clarified the long-term effect of PLGA in a rabbit iliac artery restenosis model with endothelial nitric oxide synthase (eNOS) expressing plasmid DNA lipoplexes, while restenosis was significantly reduced [32].

Our study deals with the development of a biodegradable coating consisting of PLGA that releases RNAs over a distinct period. Different PLGA derivatives are used to immobilize Lipofectamine® 2000–encapsulated siRNA against ICAM-1 and reporter mRNA (eGFP). First, PLGA coatings were tested for pH value changes during incubation in media. Afterwards, the cell viability, transfection efficiency, and knockdown in EA.hy926 cells and human vascular endothelial cells (hVECs) were analyzed. Furthermore, the release duration of PLGA coatings and co-transfection of EA.hy926 cells with eGFPmRNA and siRNA were determined. We tested the immune response of immortalized and primary endothelial cells as well as ICAM-1 expression by quantitative RT-PCR after incubation on PLGA coatings. Additionally, the cleavage site of ICAM-1 mRNA was demonstrated by 5′-RLM-RACE-PCR. The hemocompatibility of PLGA coatings was analyzed with regard to later medical applications.

2. Results

2.1. Stability of the pH Value

The presence of an aqueous solution is responsible for the degradation of PLGA. In this case, hydrolysis provokes the biodegradation of esterase linkage into D,L-Lactic acid and glycolic acid. Consequently, the pH changes in a different manner when different PLGA monomer ratios of lactic acid and glycolic acid are used [33]. We decided to use cell culture medium instead of a simple saline solution to correspond more to in vivo conditions.
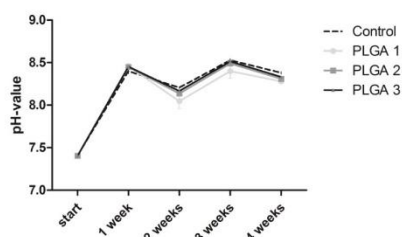

Figure 1. Change of pH values in cell culture media during incubation with PLGA 1-, 2-, and 3-coated coverslips. Slides were incubated in media for one, two, three, and four weeks. The supernatants were used to measure the pH values. An uncoated coverslip served as a control. The analysis was done with two equally coated coverslips of each PLGA and two measurements for each supernatant.

The pH value showed an increase in the first week for all PLGAs analyzed (Figure 1). Lower pH values were observed for PLGA 1 after two, three, and four weeks and for PLGA 2 after two and four weeks compared to PLGA 3.

2.2. Influence of PLGA on Cell Viability

The influence of PLGA degradation products on cell viability was analyzed after 48 h cultivation. In advance, PLGA-coated slides were incubated with medium for different time points. The cells were grown using these supernatants. The cell viability was measured by MTT assay (Figure 2) and CASY® (Supplementary Figure S1). Both techniques showed similar cell viability results for the whole observation period of four weeks. No changes in the cell viability occurred after incubation with one- and two-week-old supernatants of the different PLGAs. However, a slight but not significant decrease of viability was recognized when cells were cultivated with three-week-old supernatants. Herein, PLGA 2 and 3 reduced the viability to 85%, while PLGA 1 caused a slight reduction to 90% viability. The four-week-old supernatants of PLGA 2 and 3 reduced the cell viability to a lesser extent.
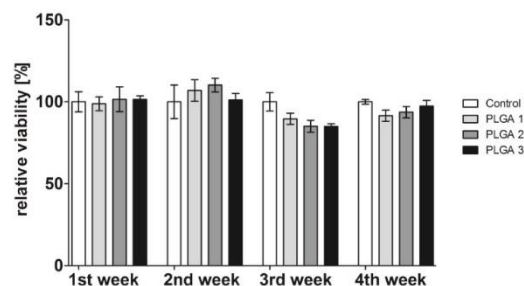

Figure 2. Relative viability of EA.hy926 cells analyzed by MTT assay after incubation with supernatant of incubated PLGA 1–, 2– or 3–coated coverslips. Therefore, 100,000 EA.hy926 cells were seeded in one well of a 24-well plate and cultivated with the supernatant of the respective cultivated PLGA slides for 48 h. For the control group, medium was incubated with coverslips and supernatant added to the cells. The control was set to 100%, each bar represents the mean ± standard error (SEM) of $n = 1$.

2.3. Hemocompatibility

With regard to the requirements of hemocompatibility tests for medical devices, different parameters concerning white and red blood cells, platelets, coagulation, and parameters of the immune system were analyzed. None of the different blood cells analyzed showed a significant reduction of their cell number in comparison to the controls (0 h and 1 h). However, it has to be mentioned that the cell numbers of platelets (Figure 3b), leukocytes (Figure 3c), lymphocytes (Figure 3d), monocytes (Figure 3e) and granulocytes (Figure 3f) were reduced after 1 h incubation in the control, whereby incubation with PLGA resulted in a similar cell number compared to the 0 h control (Figure 3a–e). Assessing the blood parameters β-Thromboglobulin, Thrombin-Antithrombin III-complex (TAT), and polymorphnuclear granulocyte (PMN)-elastase as well as the values of the complement system C3a and SC5b9, a significant increase appeared between the 0 h control and samples that were incubated for 1 h (Figure 3g–k). There was no difference between blood incubated with or without PLGA for 1 h, suggesting that no activation of the complement system as well as no activation of platelets occurred. Additionally, coated slides provoked a slight decrease of the PMN-elastase in comparison to the 1 h control, and therefore a decrease of the inflammatory reaction (Figure 3h). It has to be mentioned that PLGAs triggered a slight increase of the coagulation activity determined by TAT expression; however, this was not significant (Figure 3i).
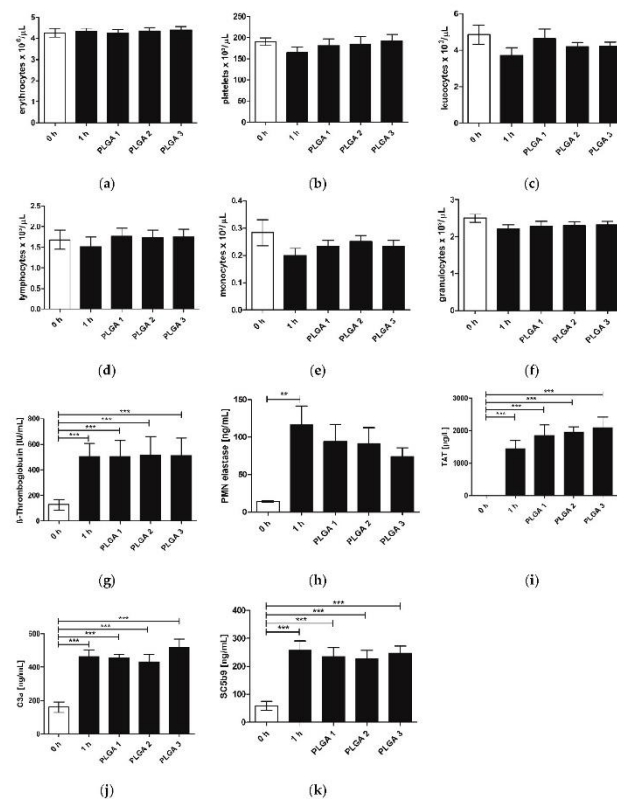
Figure 3. Hemocompatibility of PLGA 1–3–coated slides. Slides were incubated with fresh human blood at 37 °C for 1 h under gentle shaking. The 0 h control was fresh blood without incubation and served as a baseline. Different blood cells, inflammatory and thrombogenic parameters were determined by a cell counter (**a**) erythrocytes $\times 10^3$ μL^{-1}; (**b**) platelets $\times 10^3$ μL^{-1}; (**c**) leukocytes $\times 10^3$ μL^{-1}; (d) lymphocytes $\times 10^3$ μL^{-1}; (**e**) monocytes $\times 10^3$ μL^{-1}; (**f**) granulocytes $\times 10^3$ μL^{-1} or appropriate ELISAs (**g**) β-Thromboglobulin (IU·mL^{-1}); (**h**) PMN elastase (ng·mL^{-1}); (**i**) TAT (μg·L^{-1}); (**j**) C3a (ng·mL^{-1}); (**k**) SC5b9 (ng·mL^{-1}), respectively. The comparison between the uncoated slides and the PLGA-coated slides shed light on the hemocompatibility of the polymer. Each bar represents the mean ± standard error (SEM) of $n = 6$. ** indicates statistical significance at a level of $p < 0.01$; *** indicates statistical significance at a level of $p < 0.001$.

2.4. Immune Response of hVECs to Different PLGAs

Biomaterials and external molecules such as RNAs may trigger an immune response in cells which is not desirable, especially for medical devices. Therefore, the expression of different inflammatory markers such as CXCL-7, CXCL-10, OAS, and STAT-1 was determined after the incubation of hVECs with PLGA 1–3 coatings in combination with Lipofectamine® 2000, siICAM-1 and control nonsense siRNA (scrRNA), or the transfection of poly (IC) double-stranded RNA (dsRNA) with Lipofectamine® 2000. The dsRNA induced the mRNA expression of CXCL-10, OAS, and STAT-1 mRNA to a greater extent than siICAM-1 or scrRNA PLGA coatings (Figure 4). When looking at the results in detail, all three PLGAs in combination with Lipofectamine® 2000 alone or siICAM-1 or scrRNA provoked the same slight increase in the mRNA level. However, PLGA without transfection solution and

transfection complexes showed almost no augmentation in the expression level (Figure 4a) or even a lower level than the control (Figure 4b–d). The addition of Lipofectamine® 2000 alone to the PLGAs caused a remarkable increase of the inflammatory markers, which was further intensified by siICAM-1 or scrRNA.
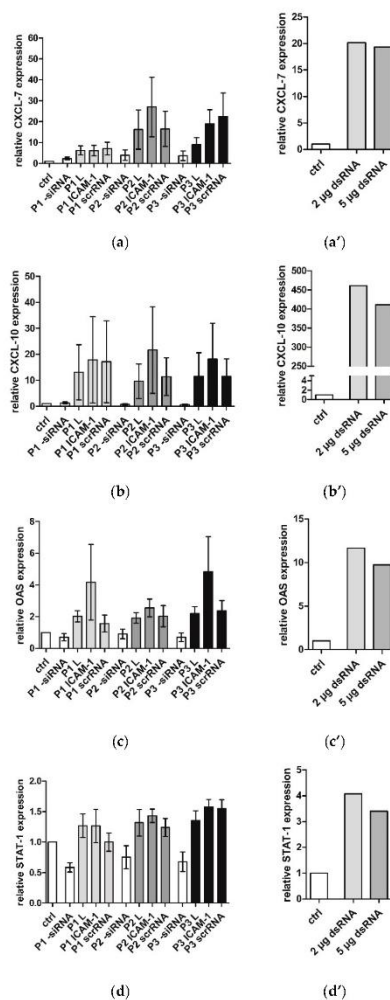

Figure 4. Immune response of hVECs analyzed by qRT-PCR after incubation with siICAM-1, scrRNA or Lipofectamine® 2000 alone, PLGA 1–3 coatings and PLGA 1-3 alone. After 24 h incubation of coated slides with hVECs, RNA was isolated for qRT-PCR. The relative expression of (**a**) CXCL-7, (**b**) CXCL-10, (**c**) OAS, and (**d**) STAT-1 was compared to untreated cells. Another assay was the transfection of hVECs with dsRNA (2 and 5 µg): (**a′**) relative expression of CXCL-7, (**b′**) relative expression of CXCL-10, (**c′**) relative expression of OAS, and (**d′**) relative expression of STAT-1. The expression of untreated cells was set to one. Each bar represents the mean ± standard error (SEM) of $n = 4$. The dsRNA was tested only once, $n = 1$. p = PLGA.

2.5. Short-Term Uptake of siRNA AF488

The three different PLGAs were tested for their ability to release siRNA complexes for transfecting EA.hy926. The transfection efficiency was determined by three siRNA AlexaFluor (AF) 488 amounts: 1, 3, and 6 µg. The cultivation of EA.hy926 with the functional polymer coating yielded the following results (Figure 5). The increase of the siRNA amount correlated with the transfection efficiency, independently of the kind of PLGA. For two-way ANOVA, we grouped the samples of different amounts of siRNA and the respective PLGAs. Comparing the group of 1 µg and 3 µg siRNA, we recognized that significantly higher uptake rates were reached with 3 µg. The application of 6 µg siRNA could not cause a significantly higher transfection efficiency anymore. 96% positive cells were observed with PLGA 2 and 95% positive cells with PLGA 1. However, PLGA 3 mediated the lowest uptake rate of 92% in comparison with the other PLGA coatings. Hence, in subsequent experiments, 3 µg siRNA was introduced in combination with PLGA 1–3. Furthermore, PLGA 1–3 showed significant distinctions in siRNA complex uptake using 1 µg and 3 µg siRNA. Herein, PLGA 3 yielded the lowest uptake in EA.hy926 with 53% (1 µg siRNA) and with 77% using 3 µg siRNA. The transfection efficiency by PLGA 1 and 2 was significantly higher except between PLGA 2 and 3 with 3 µg siRNA. The comparison of PLGA 1–3 showed that PLGA 1 was significantly more successful for the transfection efficiency than PLGA 2 and 3.
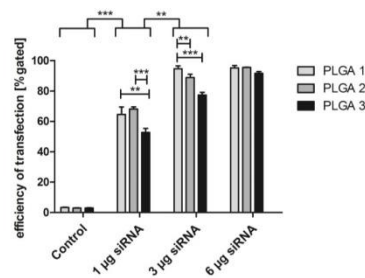

Figure 5. Uptake of siRNA AF 488 by PLGA coatings in EA.hy926. Different amounts of siRNA were combined with PLGA 1–3 and tested for transfection efficiency. Cells were incubated 24 h with respective coated glass slide and afterwards analyzed by flow cytometry. PLGA-coated slides without siRNA served as a control. Statistical analysis was prepared by two-way ANOVA. Each bar represents the mean ± standard error of $n = 3$. ** indicates statistical significance at a level of $p < 0.01$; *** indicates statistical significance at a level of $p < 0.001$

2.6. ICAM-1 Knockdown and mRNA Levels of EA.hy926 and hVECs

The transfection of EA.hy926 and hVECs was investigated with the three different PLGA coatings including 3 µg silCAM-1 and scrRNA complexes, respectively. The protein expression of the adhesion molecule ICAM-1 expressed by EA.hy926 and hVECs was analyzed by flow cytometry (Figure 6) as well as its mRNA levels analyzed by qRT-PCR (Supplementary Figure S2). All three PLGA coatings were able to reduce the ICAM-1 protein expression significantly in EA.hy926 compared to the control group, activated by TNF-α. The highest knockdown of 36% was reached with PLGA 1 combined with silCAM-1. This reduction was also significant compared to scrRNA and the TNF-α control. Similar significant reductions were achieved with PLGA 2 and 3 compared to the TNF-α control. Furthermore, a significant reduction was also mediated by silCAM-1 PLGA 2 compared to the TNF-α control. Additionally, these results were paralleled by the mRNA level of ICAM-1 (Supplementary Figure S2). The knockdown experiment was also carried out with hVECs and a reduction of the ICAM-1 expression of 22% (PLGA 1), 10% (PLGA 3), and 5% (PLGA 2) could be achieved. PLGA alone and the scrRNA PLGA coating with TNF-α stimulation revealed no reduction of the examined protein.

Nevertheless, comparing the results of EA.hy926 and hVECs, significant gene knockdown could not be detected with primary cells.
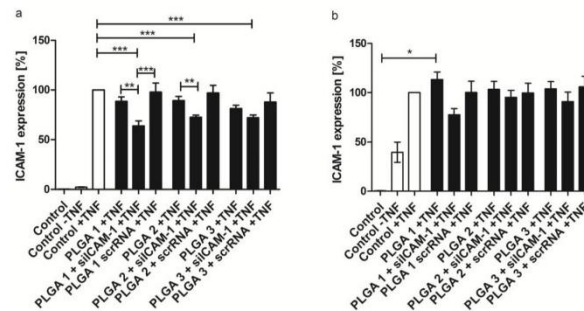

Figure 6. Gene knockdown of ICAM-1 after 48 h transfection by PLGA-coated slides examined by flow cytometry. (**a**) Expression of ICAM-1 in EA.hy926; (**b**) Expression of ICAM-1 in hVECs. EA.hy926 and hVECs were seeded one day before transfection with PLGA 1–3–coated glass slides in combination with either siICAM-1 or scrRNA or without additives, which served as a control. ICAM-1 expression was calculated after setting the TNF-α control to 100%. Each bar represents the mean $\pm$ standard error of $n = 5$. * Statistical significance $p < 0.05$; ** statistical significance $p < 0.01$; *** statistical significance $p < 0.001$.

2.7. Specific mRNA Degradation Analyzed by 5'-RLM-RACE-PCR

The analysis of specific mRNA degradation products is very important to distinguish between the desired specific RNA interference (RNAi) mechanism and the undesired effects that are mediated by the biomaterial, transfection reagent, etc. These undesired effects may also lead to a knockdown of the targeted ICAM-1 mRNA. With the usage of 5'-RLM-RACE-PCR we could prove that the RNAi mechanism occurred in EA.hy926 cells at the siRNA cleavage site of the mRNA (Figure 7). Our analysis revealed that the mRNA transcript was cleaved at bp 1818 as anticipated by us. PLGA-scrRNA or PLGAs without siRNA did not show specific ICAM-1 mRNA cleavage products (data not shown).
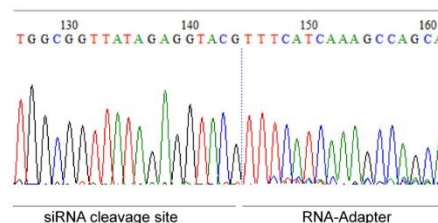

Figure 7. Sequence of 5'-RLM-RACE-PCR product (Inner PCR with Inner Primer and RACE1) of PLGA-ICAM-1 siRNA–treated EA.hy926 cells. The sequence shows the siRNA cleavage site of the ICAM-1 mRNA at bp 1818 (126–144) and the RNA Adapter sequence (145–161).

2.8. Long-Term Release of siRNA Complexes

With respect to the requirements of long-term release coatings for medical devices, we developed and analyzed a multilayer buildup. During the first two days of transfection by PLGA-coated glass slides with siRNA AF 488, a very high transfection efficiency of at least 80% on day one and 85% on day two could be achieved (Figure 8). The highest value was reached with PLGA 1 (96%). From the third day on, the uptake of fluorescent siRNA decreased continuously until day six, where a baseline was

reached with 1%–2% transfection efficiency. PLGA 1 showed a slight increase of transfection efficiency from day seven until day nine, which was not significant compared to PLGA 2 and 3. Release of siRNA AF 488 was tested until day 20. The transfection efficiency was slightly but continuously increased by PLGA 2 and 3 from day 12 to day 18. PLGA control slides showed baseline values except for day 18.
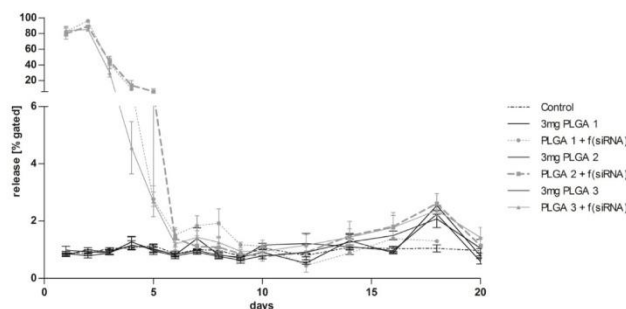

Figure 8. Long-term release of siRNA AF 488 complexes and the conditional transfection efficiency in EA.hy926. Glass slides were coated four times with alternating layers of 0.5 mg PLGA and 3 µg siRNA AF 488 with a capping layer of 1 mg PLGA. In the first 10 days, slides were transferred to new confluent cells every day. From day 11, slides were changed every second day. As control samples, cells without a slide and slides coated with 3 mg PLGA only were used. Uptake of siRNA was measured by flow cytometry. f(siRNA) = fluorescence-labeled siRNA. Statistical analysis was performed by an outlier test (alpha = 0.05) and test for normal distribution before the ANOVA. Each bar represents the mean ± standard error of $n = 4$.

2.9. Co-Transfection of eGFPmRNA and siRNA AF 555 in EA.hy926

Gene silencing by RNAi is not the only way to alter protein expression. Also, the transfection of mRNA is capable of changing the protein expression pathway. In our approach we wanted to ascertain if the PLGA coating is capable of releasing and transfecting both transfection complexes with eGFPmRNA and siRNA AF 555 simultaneously. Different combinations of PLGA 1 (which was the most efficient PLGA in the former experiments) and RNAs were tested. The co-transfection achieved 11% transfected cells that were positive for both eGFPmRNA and siRNA AF 555 (Table 1). Furthermore, the values of eGFP expression and cells positive for AF 555 separately showed 7.90% positive cells for mRNA and 6.25% positive cells for siRNA when both siRNA and mRNA were immobilized in the coating. As a control, coatings with only one complexed RNA were tested for transfection efficiency. Regarding the combination of PLGA and siRNA, 26% transfected cells could be achieved, while the PLGA/mRNA coating also provoked 11% positive cells. Table 1 shows an overview of the transfection efficiency values. The analysis of the mRNA and siRNA transfection was also done by fluorescence microscopy (Supplementary Figure S3), with which it was visible that some cells efficiently expressed eGFP or/and were transfected with siAF555 simultaneously.

Table 1. Transfection efficiency values of co-transfection with eGFPmRNA and siRNA AF 555. (++): without Lipofectamine® 2000 and PLGA 1; (+): without Lipofectamine® 2000; *: without; + with. Ctrl = control.

Positive Cells (%)	Ctrl (++)	*mRNA* siRNA (+)	*mRNA* siRNA	*-mRNA +siRNA	+mRNA *siRNA	+mRNA +siRNA
siRNA positive	0.03	0.05	0.08	26.03	0.01	6.25
mRNA positive	0.94	2.19	2.86	0.26	10.91	7.90
siRNA + mRNA positive	1.02	1.72	3.18	4.33	2.84	11.01

3. Discussion

The placement of stents by PTCA is a common treatment of narrowed arteries in atherosclerosis. Nowadays, DES releasing paclitaxel or sirolimus is the treatment of choice to circumvent restenosis, although adverse effects such as late ISR may occur. Huge efforts are being made to improve the re-endothelialization of stented arteries and new delivery systems are constantly being developed. Some of the new inventions use biodegradable biomaterials for stent coating, to incorporate pharmacological agents in a depot for controlled and sustained release. However, such a biomaterial has to be carefully selected regarding its biodegradability without toxic degradation products, stabilization of the incorporated drug, controlled drug release, bioresorbability, hemocompatibility, and inappropriate immune response. Peng et al. revealed in a porcine coronary model that PLGA-coated stents showed a long-term biocompatibility of three months and the degradation products led to fewer reactions compared to BMS [34]. In this respect, we used the biocompatible and biodegradable FDA- and EMA-approved biomaterial PLGA with different lactide:glycolide ratios, different molecular weights, and either end-capped or non-end-capped polymers. We determined the biocompatibility of PLGA 1, 2, and 3 by looking at the pH value shift and the cell viability over four weeks. Hereby, we observed a pH value rise from the beginning until the first week that might be due to the pH augmentation of the cell culture medium in which the coatings were incubated. It is well known that the pH of a cell culture medium shifts towards basic conditions after refrigerator storage. Additionally, we assume that the cell culture medium was capable of buffering the pH value, resulting in no decrease of the pH due to the hydrolysis of PLGA. The cell viability showed no reduction after the first two weeks, indicating that the increase of the pH value from 7.4 to 8.4 has no influence (Figure 1). Furthermore, cell viability was only slightly but not significantly decreased after the third and fourth weeks. This leads to the conclusion that PLGA does not cause cytotoxicity, since the reduction of the cell viability was less than 30% (determined value according to EN ISO 10993-5) (Figure 2).

The comparison of the three PLGAs regarding the pH value is in line with the literature stating that free carboxylic acid end groups of PLGA 1 and a low molecular weight are responsible for faster degradation as compared to PLGA 2 and 3 with capped carboxyl end groups [26,27]. With free carboxylic acid end groups, the polymer is becoming more hydrophilic, leading to increased water uptake and consequently to hydrolysis. Hence, the carboxylic acid end groups explain the decreased pH value of PLGA 1 from week two until week four compared with the other PLGAs and the control (Figure 1).

The excellent hemocompatibility of PLGA is essential for future medical device applications. In contrast to the 1 h control, all three PLGA samples caused no reduction in the number of platelets, leukocytes, lymphocytes, monocytes, and granulocytes after incubation (Figure 3). A reduction of their numbers would indicate the adherence to the PLGA surface, which was not observed. Therefore, we conclude that there is no adverse adhesion of blood cells onto the polymer coatings. Furthermore, the hemocompatibility of PLGAs was verified by the unchanged parameters ß-Thromboglobulin, TAT, PMN-elastase and complement C3a and SC5b9 after incubation. This confirmed that no activation of the complement system as well as no activation of platelets occurred, reducing the risk of thrombus formation after PTCA.

The expression of inflammatory and interferone response markers was not increased by PLGA. When Lipofectamine was added, the markers increased. Lipofectamine is a cationic lipid which forms nanoparticles that are taken up by the cell. In a previous study we could also observe the activation of inflammatory markers when using Lipofectamine [35]. The addition of siRNAs to this experimental setup led to a still-higher inflammatory marker increase.

Although it is thought/intended that siRNAs are specific and only interact with the RNA-induced silencing complex and do not lead to any increase in inflammatory markers, we can assume that siRNAs can facilitate a certain activation of inflammatory markers. This effect belongs to the dsRNA of 21 nucleotides or longer that can bind directly to Toll-like receptor 3. This results in receptor dimerization and activation of an intracellular pathway, leading to the expression of inflammatory

markers. It must be noted, however, that the use of a long dsRNA leads to a much higher activation of the inflammatory markers.

In our study, we generated drug delivery particles consisting of ICAM-1 siRNA and Lipofectamine and embedded them in thin PLGA films. The therapeutic approach of RNAi holds a lot of promise in combating CVD by preventing the inflammatory process. Several studies provided substantial evidence that the knockdown of CAMs such as ICAM-1, VCAM-1, and E-selectin is an excellent tool to prevent the inflammatory process by leukocyte infiltration within different cell types of the artery wall [36–41]. Based on this available evidence, we successfully transfected EA.hy926 cells with siRNA AF 488 released from PLGA 1–3 thin films. Even 3 μg of siRNA was sufficient to achieve a transfection efficiency of 95% which could not be significantly augmented with a higher amount of siRNA. Therefore, we conclude that cells are saturated at 3 μg siRNA. However, only PLGA 1 was capable of reaching such an efficiency, convincing us again that PLGA 1 is the fastest in degradation. In our previous studies with different materials, it turned out that fast-degrading materials often show the highest transfection efficiency [42,43]. Additionally, a DES for long-term release of siRNA NPs from PLGA multilayer coatings was conducted and confirmed by their uptake in EA.hy926 cells for 20 days. The rationale of generating several alternating layers is: (1) decelerating the NPs' release due to several PLGA films that have to be passed and (2) the immobilization of mRNA and siRNA into different layers to yield the gradual release of both. Within the first two days, we demonstrated a very high uptake of siRNA NPs, demonstrating a burst release mainly by diffusion of the water-soluble NPs. However, from days three to six, cells showed a decreasing uptake of siRNA NPs, which indicates the beginning of the slow degradation of PLGA films (Figure 8). Additionally, a progressively low uptake of siRNA NPs was seen until day 20, indicating that a sustained release of NPs from PLGA multilayers is guaranteed. The in vitro experimental setup, relocating the coated slides on new EA.hy926 cells until day 10 for every day and until the end of the experiment for every second day, simulated a very high turnover of endothelial cells in vivo. Considering that the endothelium is only renewed once after stent implantation, not every (second) day, the transfection duration and efficiency would be significantly higher in vivo compared to our results.

Several PLGA degradation mechanisms are described in the literature which might lead to the release of our embedded siRNA NPs: (1) diffusion through the polymer barrier, (2) erosion (physical) and degradation (chemical) of the polymer material or (3) a combination of diffusion and erosion/degradation [44,45]. An enzymatic degradation of PLGA besides the proven hydrolysis is still debated [46,47]. Therefore, we presume that in our case, siRNA NPs were released by diffusion (for the first two days) through the polymer, by degradation (hydrolysis), and by erosion.

A further advantage of our multilayered coating approach is the possibility of co-transfecting eGFPmRNA and siRNA AF 555 for long-term release. This is, to our knowledge, the first description of this mechanism and its feasibility has been proven. The simultaneous transfection of EA.hy926 cells with mRNA and siRNA convinced us of the novel concept to build up several layers with different RNAs (Table 2). Our results indicate the possibility that two contrary mechanisms in the protein expression machinery occur concurrently in EA.hy926: (1) gene knockdown by siRNA transfection and (2) protein expression by mRNA transfection.

The effectiveness of PLGA carrier-mediated transfection was extensively confirmed by the gene knockdown of adhesion molecule ICAM-1 in EA.hy926 cells and hVECs. The highest knockdown was observed with the combination of PLGA 1 and siICAM-1 in the cell line and primary cells, leading to the assumption that faster degradation of PLGA leads to faster release of siICAM-1 and consequently to a significant (EA.hy926) ICAM-1 knockdown (Figure 6a). Additionally, we confirmed decreased ICAM-1 expression with PLGA 2 and 3 by flow cytometry. We thus suppose that PLGA 1 is the most suitable coating for significant ICAM-1 gene silencing or for co-transfection. The results of the qRT-PCR underline our assumptions, where the lowest ICAM-1 mRNA level with 53% (in EA.hy926 cells) was achieved with the PLGA 1 coating (Supplementary Figure S2). To assure that our siICAM-1 was able to specifically degrade target mRNA, 5′-RLM-RACE-PCR was performed. The correct cleavage

site seen with ICAM-1, but not with the scrRNA coating or PLGA alone, confirmed the functionality. In conclusion, siICAM-1 in combination with PLGA 1 was fully functional and the side effects of PLGA or scrRNA could be excluded.

Comparing the ICAM-1 expressions of EA.hy926 cells and hVECs, our data are in accordance with the literature that efficient gene transfer is more difficult to manage in primary cells than in cell lines [48,49]. In our view, too few siRNA NPs reached the cell cytoplasm for effective gene silencing or an unwanted effect of Lipofectamine was responsible for the lower knockdown in primary cells. A different transfection reagent, higher amounts of the transfection reagent or increased RNA amounts could achieve improvements of the transfection. We could show in our previous work that other transfection reagents might be more suitable for the transfection of primary cells [35]. Moreover, using different transfection reagents for siRNA and mRNA would equally be possible as they can be incorporated into different layers.

4. Materials and Methods

4.1. Chemicals for PLGA Coating

Three different PLGAs were purchased from Sigma-Aldrich (Steinheim, Germany): PLGA (1) Resomer® RG 752 H, 75:25, acid terminated, 4,000–15,000 Da; PLGA (2) PLGA, 85:15, ester terminated, 50,000–75,000 DA; PLGA (3) Resomer® RG 756 S, 75:25, ester terminated, 76,000–115,000 Da. Subsequently, PLGAs are named with PLGA 1, PLGA 2, and PLGA 3. Ethyl acetate from Sigma-Aldrich (Steinheim, Germany) was used for preparing PLGA solutions.

4.2. SiRNAs

The following siRNA was used for gene knockdown: intercellular adhesion molecule (ICAM)-1 hum with sense strand 5′-GCC UCA GCA CGU ACC-UCU ATT-3′′, antisense 5′-UAG AGG UAC GUG CUG AAG CTT-3′. Alexa Fluor 488 labeled E-selectin siRNA was applied to test the transfection efficiency: sense strand 5′-UUG AGU GGU GCA UUC AAC CTT-3′, antisense 5′-GGU UGA AUG CAC CAC UCA ATT-3′ (both from Eurofins MWG Operon, Ebersberg, Germany), and scrRNA (Qiagen, Hilden, Germany) without labeling and with AF 488 and AF 555 labeling, respectively. Qiagen does not provide the sequence of their nonsilencing siRNAs but ensure that they have no homology to any known mammalian gene. This nonsilencing siRNA is validated by using Affymetrix GeneChip arrays and a variety of cell-based assays and shown to ensure minimal nonspecific effects on gene expression and phenotype. Additionally, scrRNA AF488 from Qiagen was used for long-term release experiment.

4.3. Synthesis of eGFPmRNA

The production of modified mRNA was performed as described by Avci-Adali et al. [50]. Coding DNA sequence (CDS) with known flanking sequences was amplified by PCR using specific primers. PCR product was then purified and the quality of the generated DNA was determined. Using the in vitro transcription (IVT) process, mRNA was generated from the DNA product. Subsequently, the product was purified and treated with phosphatase to remove 5′-triphosphates. After the additional purification and quality control of generated mRNA, transfection experiments were performed.

4.4. Substrate for PLGA Coatings

PLGA films were build-up on glass slides from Paul Marienfeld GmbH (Lauda-Königshofen, Germany). The dimension of the slides was $10 \times 10 \times 1$ mm. They were purified by ultrasonication (Bandelin RK 100H Sonorex, Bandelin electronic, Germany) with 2% Hellmanex solution from Hellma (Müllheim, Germany) before rinsing with ddH$_2$O. Air-dried slides were sterilized by steam sterilization for 20 min at 121 °C (systec dx-23, systec GmbH, Linden, Germany) prior coating.

4.5. Build-Up of PLGA/RNA Coatings

PLGA 1, 2, and 3 were dissolved in ethyl acetate with a concentration of 1 µg/µL. For every experiment, PLGA solutions were daily prepared. The complexation of Lipofectamine® 2000 and siRNA was obtained by diluting them in medium (DMEM) for 30 min at RT. In this connection, Lipofectamine amounts varied in relation to increasing siRNA amounts: 1 µg siRNA and 1 µL Lipofectamine, 3 µg and 2 µL, and 6 µg and 4 µL. PLGA/Lipofectamine coatings without siRNA served as a control. PLGA and Lipofectamine/siRNA complexes were mixed with a 1:1 ratio and 100 µL of coating solution consisting of Lipofectamine complexed siRNA and PLGA were pipetted onto the glass slides.

For analysis of the long-term transfection efficiency, a multilayer build-up of PLGA and Lipofectamine/siRNA particles was deposited onto glass slides. Then 3 µg AllStars Neg. siRNA AF 488 (Qiagen, Hilden, Germany) was complexed with Lipofectamine. The multilayered coatings were alternately dried with 500 µg PLGA and 3 µg siRNA complexes for four times, resulting in 2 mg PLGA and 12 µg siRNA for one glass slide. To prevent fast degradation of layers, a capping layer of 1 mg PLGA was deposited on top. For the control, slides were coated with a single layer of 3 mg PLGA.

The co-transfection analysis was done with PLGA 1, eGFPmRNA, and siRNA AF 555 (Qiagen). Nunc™ Thermanox™ Coverslips, dia. 13 mm (Thermo Fisher Scientific, Waltham, MA, USA) were used for coating. Therefore, PLGA solution (50 µg in 50 µL/coverslip) was mixed with a transfection mix consisting of 10 µg eGFPmRNA, 3 µg siRNA and 2 µL Lipofectamine® 2000. Afterwards the transfection solution was pipetted and dried on coverslips for one night. Then, the slides were laid down on confluent EA.hy926 cells for 48 h in 12-wells and later analyzed by FACS or fluorescence microscopy.

4.6. Cultivation of EA.hy926 and Human Primary Endothelial Cells (hVECs)

The human umbilical vein cell line EA.hy926 (LGC Standards GmbH, Wesel, Germany) was used for cell experiments. Cells were cultured in Dulbecco's Modified Eagle's Medium (DMEM) high glucose containing 10% fetal bovine serum (FBS), 1% Penicillin/Streptomycin, and 1% L-glutamine.

Human primary endothelial cells (hVECs) were isolated from saphenous vein specimens obtained from patients undergoing elective coronary artery bypass grafting (CABG). The patients' statement of agreement and the permit of the Clinical Ethics Committee of the University of Tuebingen authorized the handling. ECs were isolated by collagenase digestion as described by Walker et al. [51]. Cells were cultivated in VascuLife™ EnGS cell culture medium (Lifeline Cell Technology, Walkersville, MD, USA), a basal medium with a supplemental kit: 0.2% EnGS, 5 ng/mL rh epidermal growth factor (EGF), 50 µg/mL Ascorbic Acid, 10 mM L-Glutamine, 1 µg/mL Hydrocortisone Hemisuccinate, 0.75 Units/mL Heparin Sulfate, 2% FBS, 100 U/mL Penicillin, 100 µg/mL Streptomycin, and 10 ng/mL Amphotericin. Passages from four to seven were used for experiments.

4.7. Measurement of pH Value

PLGA degrades into lactic acid and glycolic acid by hydrolysis, whereby pH value shift is possible. Thus, environment for cells could change and influence them negatively in cell proliferation right up to cell death. Therefore, coverslips (15 mm diameter) were coated with 50 µg of three different PLGA solutions: (1) RG 752 H 75:25, (2) PLGA 85:15, and (3) RG 756 S 75:25. Slides were air-dried overnight and incubated 2 mL in medium each slide under standard cultivation conditions. Uncoated glass slides served as a control. Medium was measured at time zero which served as a baseline. The first pH value was determined by measuring the supernatant of each sample after one week and continued for four weeks.

4.8. PLGA/RNA Mediated Transfection of EA.hy926 and hVECs

First, 100,000 EA.hy926 or 120,000 hVECs were seeded one day before in 24-well plates. For co-transfection approach 130,000 EA.hy926 were seeded in one well of a 12-well plate. We decided us to use this amount of cells to reach 80% confluency on the next day. Previous experiments showed that the highest transfection efficiencies are achieved with this amount of cells. PLGA coatings were dried overnight and glass slides or coverslips were laid down with the coated side on the medium refreshed cell layer. This so called reverse assay was first described by Wintermantel et al. and applied in our laboratory for many substrate-mediated transfection tests [52]. Transfection time of EA.hy926 mediated by PLGA/RNA coatings was: 24 h for transfection efficiency and 48 h for (a) knockdown experiments, (b) immune response tests (plus hVECs), and (c) 5'-RNA ligase mediated rapid amplification of cDNA-ends PCR assay. The incubation time for knockdown evaluation was reduced to 24 h for hVECs in knockdown experiments due to their sensitivity. After transfection, cells were prepared for flow cytometry or quantitative Real-Time PCR (qRT-PCR). In the long-term transfection efficiency approach, the coated glass slides were laid down on always newly prepared EA.hy926 for 24 h until day 10. At later time points, the cells were incubated for 48 h with the slides. Herein, we always used the initially coated glass slides from day one to the last day. If cells were cultured for 48 h, medium was replaced every 24 h. After 24 h (days 1–10) or 48 h (days 12–20), cells were analyzed by flow cytometry. For co-transfection of mRNA and siRNA, cells were transfected for 48 h and subsequently analyzed by flow cytometry or fluorescence microscopy.

4.9. Cell Viability Assay

The three different polymers were tested for cell compatibility by MTT-assay and by CASY® cell counter (Schärfe System, Reutlingen, Germany). For both tests, coverslips were coated as mentioned before (measurement of pH-value). Coated slides were incubated in medium for one, two, three, and four weeks at standard culture conditions and supernatants were used for cell cultivation. Then 100,000 EA.hy926 were seeded in a 24-well plate and cultivated for 48 h with the obtained supernatants. Then, cells were detached for cell count measurement with CASY® cell counter, which detects living cells by an electronic pulse area analysis. For the MTT-assay, used medium was removed and replaced by 300 μL RPMI without phenol red and supplemented with 10% MTT (5 mg/mL). After 4 h incubation, MTT solution was aspirated and 200 μL dimethyl-sulfoxide was added to each well and gently shaked. Absorbance was measured at wavelength 540 nm by a microplate reader (Mithras LB 940, Berthold Technologies, Bad Wildbad, Germany).

4.10. Hemocompatibility Testing

Medical devices must be verified in respect of biocompatibility which is separated in two fields: cytocompatibility and hemocompatibility. The EN ISO 10993–4 demands for at least one test addressing thrombosis/coagulation, hematology, inflammation, and complement system to determine the compatibility of a medical device in combination with blood.

Hemocompatibility of PLGA 1–3 was tested with polymer-coated coverslips as described in measurement of pH-value. Coverslips were incubated in 12-well plates at 37 °C under gentle shaking with 3 mL human blood from six independent blood donors. After 1 h incubation, blood was pooled for blood cells analysis like leukocytes, erythrocytes, and platelets. A Micros 60 counter (ABX Diagnostics, Montpellier, France) counted the blood cell numbers. Protein expression of C3a and SC5b9 which were associated with the complement system was analyzed by ELISAs (both Osteomedical GmbH, Bünde, Germany). Additionally, polymorphonuclear-Elastase (PMN-elastase) was tested as a sign of degranulation of leukocytes during an inflammatory reaction (Demeditec Diagnostics, Kiel, Germany). β-Thromboglobulin expression, associated with activated platelets, was determined by ASSERA-CHROM® β-TG kit (Diagnostica Stago, Asnieres, France). The measurement of thrombin-antithrombin complex (TAT) with ELISA based Enzygnost® TAT micro

enzyme immunoassay (Dade Behring, Marburg, Germany) gives information about the alteration of coagulation activity.

4.11. Flow Cytometry

Transfection efficiency or knockdown of PLGA/RNA coatings was determined by flow cytometry after 24 h or 48 h, respectively. Glass slides were removed after incubation time and cells were washed, detached and fixed with 2.5% paraformaldehyde (PFA). For knockdown experiments, cells were additionally stimulated with 5 ng/mL tumor necrosis factor (TNF)-α (BD Biosciences, Germany) for 12 h to induce ICAM-1 expression after the washing step. Immunofluorescence staining was prepared with PE mouse anti-human CD54, diluted in a 0.5% FBS/PBS solution, (BD Bioscience, Germany) for 30 min at 37 °C with following detachment and fixation of the cells as stated above. Flowcytometric analysis was performed with 10,000 cells/measurement (FACScan™, Becton Dickinson GmbH, Heidelberg, Germany) and evaluated with CellQuestPro software (version 4, Becton Dickinson GmbH). The geometric mean served for evaluating the results.

4.12. Quantitative Real-Time PCR (qRT-PCR)

First of all, total RNA from PLGA/RNA transfected EA.hy926 and hVECs was isolated using Aurum™ total RNA mini kit (Bio-Rad Laboratories, Inc., Hercules, CA, USA). RNA was quantified and 200 ng of each RNA sample was utilized for the iScript™ cDNA Synthesis Kit from (Bio-Rad) according to the manufacturer's instructions for reverse transcription. Primer design was done with NCBI primer-blast, the primer sequences in Table 2, synthesized by Operon (Köln, Germany), were used for qRT-PCR. Poly (IC) dsRNA from R&D systems (Minneapolis, MN, USA) served as positive control for immune stimulation. PCR mixes contained IQ™SYBR®Green Supermix (Bio-Rad), 400 nM forward and reverse primer, and 2 ng of cDNA in a total volume of 15 µL. All samples were performed in triplicates. Normalized gene expression was calculated by the threshold cycle (ΔCt) method using GAPDH as a reference.

Table 2. Primer sequences for qRT-PCR and primer sequences for 5'-RLM-RACE PCR purchased from MWG Operon (Ebersberg, Germany).

qRT-PCR Primer	Sequence
OAS	forward: 5'-GGAGACAGCTGGAAGCCTGTC-3' reverse: 5'-TGACCCAGGGCATCAAAGG-3'
STAT-1	forward: 5'-TGGAAGCGGAGACAGCAGAG-3' reverse: 5'-AGGTGTATTTCTGTTCCAATTCCTC-3'
CXCL-10	forward: 5'-AAGTGGCATTCAAGGAGTACC-3' reverse: 5'-ACGTGGACAAAATTGGCTTGC-3'
ICAM-1	forward: 5'-CTTGAGGGCACCTACCTCTGTC-3' reverse: 5'-CGGCTGCTACCACAGTGATG-3'
ß-Actin	forward: 5'-GAGCACAGAGCCTCGCCTTT-3' reverse: 5'-TCATCATCCATGGTGAGCTGG-3'
5'-RLM-RACE PCR	**sequence**
ICAM-1 first strand	5'-AGGTACCATGGCCCCAAATG-3'
ICAM-1 RACE 1	5'-ACTCTGTTCAGTGTGCCACC-3'
ICAM-1 RACE 2	5'-TCTTCCTCGGCCTTCCCATA-3'
ICAM-1 RACE 3	5'-TGGCCCCAAATGCTGTTGTA-3'
RNA-Adapter (universally)	5'-GCUGAUGGCGAUGAAUGAACACUGCGUUUGCUGGCUUUGAUGAAA-3'
Outer Primer (universally)	5'-GCTGATGGCGATGAATGAACACTG-3'
Inner Primer (universally)	5'-CGCGGATCCGAACACTGCGTTTGCTGGCTTTGATG-3'

4.13. 5'-RNA Ligase–Mediated Rapid Amplification of cDNA-Ends PCR (5'-RLM-RACE-PCR)

This technique which was established to detect siRNA-mediated mRNA cleavage was first described by Soutschek et al. in 2004 [53]. Later Davis et al. used this technique to verify siRNA-mediated mRNA cleavage in a human phase I clinical trial [54]. This technique detects cleaved mRNA and is especially suitable to confirm the mRNA degradation dependent on the base

pair sequence of the siRNA in transfection assays. Therefore, 50 µg of PLGA and 3 µg ICAM-siRNA were dried on glass slides, the glass slides were laid down on confluent EA.hy926 cells for 48 h and cells were stimulated for 12 h with the above stated TNF-α concentration. Subsequently, the RNA was isolated as described above. For our study we used components of the commercially available First Choice® RLM-RACE Kit from Life technologies (Darmstadt, Germany). The kit is delivered with RNA-Adapter and T4 RNA Ligase to conduct the 5′ RACE Adapter Ligation. We used 2 µg of isolated RNA for ligation. Also the kit contains M-MLV Reverse Transcriptase for first strand cDNA synthesis where we used 200 ng of ligated RNA. The user has to design gene-specific primers for the first strand synthesis and also for the PCR of the Outer and Inner PCR which are following after first strand cDNA synthesis. Primer design was done again with the software 'Primer3' [55] and Primer Premier 5 (PREMIER Biosoft International). Primer sequences that were used for 5-RLM-RACE-PCR are shown in Table 1. All PCR reactions (Outer and Inner PCR) were conducted as a qRT-PCR and contained IQ™SYBR®Green Supermix from Bio-Rad (Hercules, CA, USA), 400 nM forward and reverse primer and 2 ng of cDNA in a total volume of 15 µL. All PCR reactions were performed in triplicates. For better understanding of this technique we also designed an illustration (Figure 9).
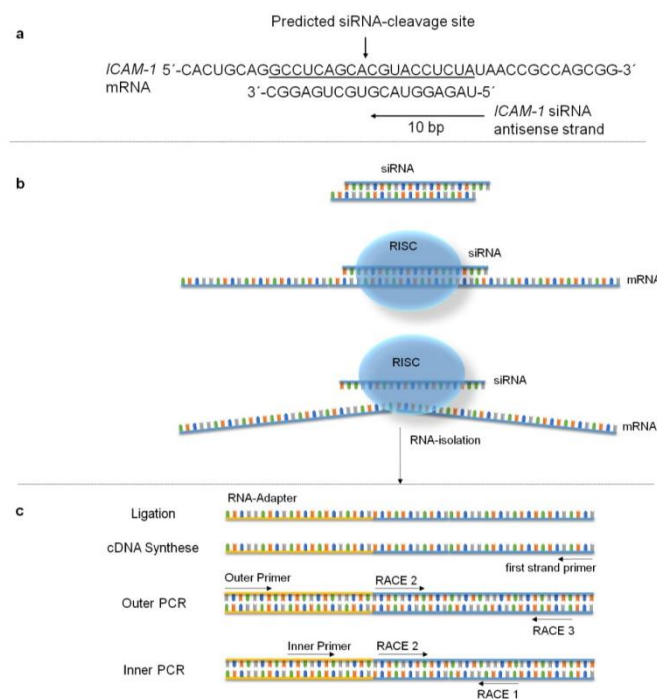

Figure 9. Illustration of the RNA Interference mechanism and the 5′-RLM-RACE PCR technique. (**a**) Shows the predicted siRNA cleavage site in the ICAM-1 mRNA. (**b**) Illustrates the RNAi mechanism in the cytoplasm of EA.hy926 cells. (**c**) Demonstrates the 5′-RLM RACE PCR technique, starting with total RNA Isolation, then the RNA adapter is ligated to cleaved mRNA strands. Afterwards RNA is reverse transcribed gene-specifically, with specific first-strand synthesis primers for ICAM-1. Subsequently, Outer PCR and Inner PCR with gene-specific primers (RACE 1, 2, and 3) and adapter-specific primers (Outer and Inner Primer) are conducted. Only if siRNA-mediated cleavage occurs specific products are produced with primer combinations of Inner Primer and RACE 1. These PCR products are then sequenced to prove siRNA-specific degradation.

4.14. Statistics

All experiments described in this work were done at least three times independently. Values showing variation were analyzed by an outlier test with a significance value of 0.05. The comparison of different samples was done by ANOVA and Bonferroni correction as a Post-test.

5. Conclusions

PLGA seems to be an excellent biodegradable and hemocompatible RNA NP delivery carrier, especially regarding the challenge for innovative improvements in DES. In combination with the powerful mechanism of RNAi, the gene silencing of undesired CAMs during inflammation could be achieved. All three PLGA resomers were non-toxic to EA.hy926 cells and proved hemocompatible with no adherence of blood cells on the PLGA coatings, a crucial point with respect to preventing thrombosis after stent implantation. The siRNA NPs incorporated in the PLGA 1–3 coatings were released and able to transfect EA.hy926 cells, where PLGA 1 with 3 μg siRNA was the best combination with 95% transfection efficiency. Furthermore, siICAM-1 NPs in PLGA 1 provoked the highest ICAM-1 knockdown of 36%. These findings and the results of pH stability indicated that PLGA 1 is degraded the fastest. With our novel multilayer build-up of PLGA 1 and siRNA NPs, we demonstrated the co-transfection of eGFPmRNA and siRNA. Furthermore, our multilayer coating with siRNA has the potential to transfect cells with high efficiency in the first two days, with a burst release until day six, and with a sustained slow release thereafter. Considering our results, we finally summarize that the delivery carrier PLGA combined with siICAM-1 NPs has great potential for the development of new a era of stents preventing ISR.

References

1. Mendis, S.; Puska, P.; Norrving, B. Global atlas on cardiovascular disease prevention and control. World Health Organization, 2011.
2. Espinola-Klein, C.; Rupprecht, H.J.; Bickel, C.; Lackner, K.; Schnabel, R.; Munzel, T.; Blankenberg, S. Inflammation, atherosclerotic burden and cardiovascular prognosis. *Atherosclerosis* **2007**, *195*, e126–e134. [CrossRef] [PubMed]
3. Ross, R. Atherosclerosis—An inflammatory disease. *N. Engl. J. Med.* **1999**, *340*, 115–126. [CrossRef]
4. Grüntzig, A. Transluminal dilatation of coronary-artery stenosis. *The Lancet* **1978**, *311*, 263. [CrossRef]
5. Byrne, R.A.; Joner, M.; Kastrati, A. Stent thrombosis and restenosis: What have we learned and where are we going? The Andreas Grüntzig Lecture ESC 2014. *Eur. Heart J.* **2015**, *36*, 3320–3331. [CrossRef] [PubMed]
6. Tahir, H.; Bona-Casas, C.; Hoekstra, A.G. Modelling the effect of a functional endothelium on the development of in-stent restenosis. *PLoS ONE* **2013**, *8*, e66138. [CrossRef] [PubMed]
7. Otsuka, F.; Finn, A.V.; Yazdani, S.K.; Nakano, M.; Kolodgie, F.D.; Virmani, R. The importance of the endothelium in atherothrombosis and coronary stenting. *Nat. Rev. Cardiol.* **2012**, *9*, 439–453. [CrossRef] [PubMed]

8.   Sluiter, W.; Pietersma, A.; Lamers, J.M.; Koster, J.F. Leukocyte adhesion molecules on the vascular endothelium: Their role in the pathogenesis of cardiovascular disease and the mechanisms underlying their expression. *J. Cardiovasc. Pharmacol.* **1993**, *22*, S37–S44. [CrossRef] [PubMed]

9.   Inoue, T.; Node, K. Molecular basis of restenosis and novel issues of drug-eluting stents. *Circ. J.* **2009**, *73*, 615–621. [CrossRef] [PubMed]

10. Binnerts, M.E.; van Kooyk, Y.; Simmons, D.L.; Figdor, C.G. Distinct binding of T lymphocytes to ICAM-1, -2 or -3 upon activation of LFA-1. *Eur. J. Immunol.* **1994**, *24*, 2155–2160. [CrossRef] [PubMed]

11. Koedam, J.A.; Cramer, E.M.; Briend, E.; Furie, B.; Furie, B.C.; Wagner, D.D. P-selectin, a granule membrane protein of platelets and endothelial cells, follows the regulated secretory pathway in ATT-20 cells. *J. Cell Biol.* **1992**, *116*, 617–625. [CrossRef] [PubMed]

12. Welt, F.G.; Rogers, C. Inflammation and restenosis in the stent era. *Arterioscler. Thromb. Vasc. Biol.* **2002**, *22*, 1769–1776. [CrossRef] [PubMed]

13. Ley, K.; Laudanna, C.; Cybulsky, M.I.; Nourshargh, S. Getting to the site of inflammation: The leukocyte adhesion cascade updated. *Nat. Rev. Immun.* **2007**, *7*, 678–689. [CrossRef] [PubMed]

14. Inoue, T.; Croce, K.; Morooka, T.; Sakuma, M.; Node, K.; Simon, D.I. Vascular inflammation and repair: Implications for re-endothelialization, restenosis, and stent thrombosis. *JACC Cardiovasc. Interv.* **2011**, *4*, 1057–1066. [CrossRef] [PubMed]

15. Khan, W.; Farah, S.; Domb, A.J. Drug eluting stents: Developments and current status. *J. Control. Release* **2012**, *161*, 703–712. [CrossRef] [PubMed]

16. Martin, D.M.; Boyle, F.J. Drug-eluting stents for coronary artery disease: A review. *Med. Eng. Phys.* **2011**, *33*, 148–163. [CrossRef] [PubMed]

17. Wendel, H.P.; Avci-Adali, M.; Ziemer, G. Endothelial progenitor cell capture stents–hype or hope? *Int. J. Cardiol.* **2010**, *145*, 115–117, author reply 117–118. [CrossRef] [PubMed]

18. Nakazawa, G.; Granada, J.F.; Alviar, C.L.; Tellez, A.; Kaluza, G.L.; Guilhermier, M.Y.; Parker, S.; Rowland, S.M.; Kolodgie, F.D.; Leon, M.B.; et al. Anti-CD34 antibodies immobilized on the surface of sirolimus-eluting stents enhance stent endothelialization. *JACC Cardiovasc. Interv.* **2010**, *3*, 68–75. [CrossRef] [PubMed]

19. Yang, F.; Feng, S.-C.; Pang, X.-J.; Li, W.-X.; Bi, Y.-H.; Zhao, Q.; Zhang, S.-X.; Wang, Y.; Feng, B. Combination coating of chitosan and anti-CD34 antibody applied on sirolimus-eluting stents can promote endothelialization while reducing neointimal formation. *BMC Cardiovasc. Disord.* **2012**, *12*, 1–8. [CrossRef] [PubMed]

20. Tan, A.; Goh, D.; Farhatnia, Y.; G, N.; Lim, J.; Teoh, S.H.; Rajadas, J.; Alavijeh, M.S.; Seifalian, A.M. An anti-CD34 antibody-functionalized clinical-grade poss-PCU nanocomposite polymer for cardiovascular stent coating applications: A preliminary assessment of endothelial progenitor cell capture and hemocompatibility. *PLoS ONE* **2013**, *8*, e77112. [CrossRef] [PubMed]

21. Danhier, F.; Ansorena, E.; Silva, J.M.; Coco, R.; Le Breton, A.; Preat, V. PLGA-based nanoparticles: An overview of biomedical applications. *J. Control. Release* **2012**, *161*, 505–522. [CrossRef] [PubMed]

22. Makadia, H.K.; Siegel, S.J. Poly lactic-*co*-glycolic acid (PLGA) as biodegradable controlled drug delivery carrier. *Polymers* **2011**, *3*, 1377–1397. [CrossRef] [PubMed]

23. Kumari, A.; Yadav, S.K.; Yadav, S.C. Biodegradable polymeric nanoparticles based drug delivery systems. *Colloid. Surface B* **2010**, *75*, 1–18. [CrossRef] [PubMed]

24. Fredenberg, S.; Wahlgren, M.; Reslow, M.; Axelsson, A. The mechanisms of drug release in poly(lactic-*co*-glycolic acid)-based drug delivery systems—A review. *Int. J. Pharm.* **2011**, *415*, 34–52. [CrossRef] [PubMed]

25. Vert, M.; Mauduit, J.; Li, S. Biodegradation of PLA/GA polymers: Increasing complexity. *Biomaterials* **1994**, *15*, 1209–1213. [CrossRef]

26. Samadi, N.; Abbadessa, A.; Di Stefano, A.; van Nostrum, C.F.; Vermonden, T.; Rahimian, S.; Teunissen, E.A.; van Steenbergen, M.J.; Amidi, M.; Hennink, W.E. The effect of lauryl capping group on protein release and degradation of poly(D,L-lactic-co-glycolic acid) particles. *J. Control. Release* **2013**, *172*, 436–443. [CrossRef] [PubMed]

27. Houchin, M.L.; Topp, E.M. Chemical degradation of peptides and proteins in PLGA: A review of reactions and mechanisms. *J. Pharm. Sci.* **2008**, *97*, 2395–2404. [CrossRef] [PubMed]

28.   Zolnik, B.S.; Burgess, D.J. Evaluation of in vivo-in vitro release of dexamethasone from PLGA microspheres. *J. Control. Release* **2008**, *127*, 137–145. [CrossRef] [PubMed]

29.   Jenjob, R.; Taranamai, P.; Na, K.; Yang, S.-G. Recent trend in applications of polymer materials to stents. *Gastrointest. Interv.* **2015**, *4*, 83–88. [CrossRef]

30.   Kwon, H.; Park, S. Local delivery of antiproliferative agents via stents. *Polymers* **2014**, *6*, 755–775. [CrossRef]

31.   Klugherz, B.D.; Jones, P.L.; Cui, X.; Chen, W.; Meneveau, N.F.; DeFelice, S.; Connolly, J.; Wilensky, R.L.; Levy, R.J. Gene delivery from a DNA controlled-release stent in porcine coronary arteries. *Nat. Biotechnol.* **2000**, *18*, 1181–1184. [PubMed]

32.   Brito, L.A.; Chandrasekhar, S.; Little, S.R.; Amiji, M.M. Non-viral enos gene delivery and transfection with stents for the treatment of restenosis. *Biomed. Eng. Online* **2010**, *9*, 56. [CrossRef] [PubMed]

33.   Wu, X.S.; Wang, N. Synthesis, characterization, biodegradation, and drug delivery application of biodegradable lactic/glycolic acid polymers. Part II: Biodegradation. *J. Biomater. Sci. Polym. Ed.* **2001**, *12*, 21–34. [CrossRef] [PubMed]

34.   Peng, H.Y.; Chen, M.; Zheng, B.; Wang, X.G.; Huo, Y. Long-term effects of novel biodegradable, polymer-coated, sirolimus-eluting stents on neointimal formation in a porcine coronary model. *Int. Heart J.* **2009**, *50*, 811–822. [CrossRef] [PubMed]

35.   Nolte, A.; Raabe, C.; Walker, T.; Simon, P.; Ziemer, G.; Wendel, H.P. Optimized basic conditions are essential for successful siRNA transfection into primary endothelial cells. *Oligonucleotides* **2009**, *19*, 141–150. [CrossRef] [PubMed]

36.   San Juan, A.; Bala, M.; Hlawaty, H.; Portes, P.; Vranckx, R.; Feldman, L.J.; Letourneur, D. Development of a functionalized polymer for stent coating in the arterial delivery of small interfering RNA. *Biomacromolecules* **2009**, *10*, 3074–3080. [CrossRef] [PubMed]

37.   Qu, Y.; Shi, X.; Zhang, H.; Sun, W.; Han, S.; Yu, C.; Li, J. VCAM-1 siRNA reduces neointimal formation after surgical mechanical injury of the rat carotid artery. *J. Vasc. Surg.* **2009**, *50*, 1452–1458. [CrossRef] [PubMed]

38.   Pluvinet, R.; Petriz, J.; Torras, J.; Herrero-Fresneda, I.; Cruzado, J.M.; Grinyo, J.M.; Aran, J.M. RNAi-mediated silencing of CD40 prevents leukocyte adhesion on CD154-activated endothelial cells. *Blood* **2004**, *104*, 3642–3646. [CrossRef] [PubMed]

39.   Wang, B.; Qian, H.; Yang, H.; Xu, L.; Xu, W.; Yan, J. Regression of atherosclerosis plaques in apolipoprotein e−/− mice after lentivirus-mediated RNA interference of cd40. *Int. J. Cardiol.* **2013**, *163*, 34–39. [CrossRef] [PubMed]

40.   Walker, T.; Wendel, H.P.; Tetzloff, L.; Heidenreich, O.; Ziemer, G. Suppression of ICAM-1 in human venous endothelial cells by small interfering RNAS. *Eur. J. Cardiothorac. Surg.* **2005**, *28*, 816–820. [CrossRef] [PubMed]

41.   Walker, T.; Wendel, H.P.; Tetzloff, L.; Raabe, C.; Heidenreich, O.; Simon, P.; Scheule, A.M.; Ziemer, G. Inhibition of adhesion molecule expression on human venous endothelial cells by non-viral siRNA transfection. *J. Cell. Mol. Med.* **2007**, *11*, 139–147. [CrossRef] [PubMed]

42.   Hossfeld, S.; Nolte, A.; Hartmann, H.; Recke, M.; Schaller, M.; Walker, T.; Kjems, J.; Schlosshauer, B.; Stoll, D.; Wendel, H.P.; et al. Bioactive coronary stent coating based on layer-by-layer technology for siRNA release. *Acta Biomater* **2013**, *9*, 6741–6752. [CrossRef] [PubMed]

43.   Nolte, A.; Walker, T.; Schneider, M.; Kray, O.; Avci-Adali, M.; Ziemer, G.; Wendel, H.P. Small-interfering RNA-eluting surfaces as a novel concept for intravascular local gene silencing. *Mol. Med.* **2011**, *17*, 1213–1222. [CrossRef] [PubMed]

44.   Jain, R.A. The manufacturing techniques of various drug loaded biodegradable poly(lactide-co-glycolide) (PLGA) devices. *Biomaterials* **2000**, *21*, 2475–2490. [CrossRef]

45.   Zhu, X.; Braatz, R.D. A mechanistic model for drug release in PLGA biodegradable stent coatings coupled with polymer degradation and erosion. *J. Biomed. Mater. Res. A* **2015**, *103*, 2269–2279. [CrossRef] [PubMed]

46.   Cai, Q.; Shi, G.; Bei, J.; Wang, S. Enzymatic degradation behavior and mechanism of poly(lactide-co-glycolide) foams by trypsin. *Biomaterials* **2003**, *24*, 629–638. [CrossRef]

47.   Zhou, X.; Cai, Q.; Yan, N.; Deng, X.; Yang, X. In vitro hydrolytic and enzymatic degradation of nestlike-patterned electrospun poly(D,L-lactide-co-glycolide) scaffolds. *J. Biomed. Mater. Res. A* **2010**, *95A*, 755–765. [CrossRef] [PubMed]

48.   Gresch, O.; Altrogge, L. Transfection of difficult-to-transfect primary mammalian cells. *Methods Mol. Biol.* **2012**, *801*, 65–74. [PubMed]

49. Hamm, A.; Krott, N.; Breibach, I.; Blindt, R.; Bosserhoff, A.K. Efficient transfection method for primary cells. *Tissue Eng.* **2002**, *8*, 235–245. [CrossRef] [PubMed]

50. Avci-Adali, M.; Behring, A.; Keller, T.; Krajewski, S.; Schlensak, C.; Wendel, H.P. Optimized conditions for successful transfection of human endothelial cells with in vitro synthesized and modified mRNA for induction of protein expression. *J. Biol. Eng.* **2014**, *8*, 8. [CrossRef] [PubMed]

51. Walker, T.; Wendel, H.P.; Raabe, C.; Wiechnik, P.; Spranger, L.; Heidenreich, O.; Scheule, A.M.; Nordheim, A.; Ziemer, G. Graft protection in bypass surgery: siRNA-mediated silencing of adhesion molecules. *Oligonucleotides* **2009**, *19*, 15–21. [CrossRef] [PubMed]

52. Minuth, W.W.; Schumacher, K.; Strehl, R.; de Vries, U. Mikroreaktortechnik für Tissue Engineering. In *Medizintechnik mit biokompatiblen werkstoffen und verfahren*, 3rd ed.; Wintermantel, E., Ha, S.-W., Eds.; Springer: Berlin, Germany, 2002.

53. Soutschek, J.; Akinc, A.; Bramlage, B.; Charisse, K.; Constien, R.; Donoghue, M.; Elbashir, S.; Geick, A.; Hadwiger, P.; Harborth, J.; et al. Therapeutic silencing of an endogenous gene by systemic administration of modified siRNAs. *Nature* **2004**, *432*, 173–178. [CrossRef] [PubMed]

54. Davis, M.E.; Zuckerman, J.E.; Choi, C.H.; Seligson, D.; Tolcher, A.; Alabi, C.A.; Yen, Y.; Heidel, J.D.; Ribas, A. Evidence of RNAi in humans from systemically administered siRNA via targeted nanoparticles. *Nature* **2010**, *464*, 1067–1070. [CrossRef] [PubMed]

55. Rozen, S.; Skaletsky, H. Primer3 on the www for general users and for biologist programmers. *Methods Mol. Biol.* **2000**, *132*, 365–386. [PubMed]

6.4 Publication III

Hyaluronic acid/poly(ethylenimine) polyelectrolyte multilayer coatings for siRNA-mediated local gene silencing

PLOS ONE

Hyaluronic acid/poly(ethylenimine) polyelectrolyte multilayer coatings for siRNA-mediated local gene silencing

Olivia Koenig, Bernd Neumann, Christian Schlensak, Hans Peter Wendel ⓘ *, Andrea Nolte

Department of Thoracic, Cardiac, and Vascular Surgery, University of Tuebingen, Tuebingen, Baden-Wuerttemberg, Germany

* hans-peter.wendel@med.uni-tuebingen.de

Abstract

Local gene delivery systems utilizing RNA interference technology are a promising approach for therapeutic applications where site-specific release of agents is desired. Poly-electrolyte multilayers (PEMs) can be constructed using the layer-by-layer (LbL) technique and serve as a depot for bioactive substances, which can then be released in a controlled manner. Multilayers of hyaluronic acid/poly(ethylenimine) HA/PEI were built up with different numbers of bilayers and PEI-siRNA particles were embedded in bioactive layers for gene silencing. The increase of the bilayers and the release of siRNA particles were demonstrated by fluorescence intensity measurement with a fluorescence reader. Two different LbL techniques were tested for the reduction of ICAM–1 expression in EA.hy926: PEM build-up by dipping or drying steps, respectively. Herein, the drying technique of the bioactive layers with ICAM siRNA mediated a significant reduction of the ICAM–1 expression from 3 to 24 bilayers. The fluorescent siRNA release study and the re-culturing of the HA/PEI films demonstrated a release of the transfection particles within the first hour. The advantage of dried built-up PEMs compared to a dried monolayer of PEI-siRNA particles with the same siRNA concentration was a significant higher amount of viable cells.

1 Introduction

The RNA interference (RNAi) mechanism is a powerful and specific technique in molecular biology and shows high potential for therapeutic applications, including cardiovascular diseases (CVD), infectious diseases and cancer [1–8]. RNAi was first discovered by Fire *et. al* in 1998 in *C. elegans* with double-stranded RNA causing the silence of complementary messenger RNA sequence [9]. This self-defense mechanism in *Eukarya* is known for preventing infections and following gene integrity by pathogens and regulating gene expression processes. The ability to artificially produce short interfering RNA (siRNA) with 21–23 nucleotides which binds specific to the target mRNA is a promising approach for various therapeutic applications with the aim of transient gene silencing [10]. Despite promising therapeutic options, the delivery of siRNA to the target tissue or cells is one of the major challenges. Systemic delivery of siRNA is preferred when the target of interest is quite difficult to access and especially in

cancer therapy approaches [11–14]. However, if targeted silencing is desired, such as e.g. for vascular stents or general implants, local application of siRNA is essential to avoid the occurrence of systemic off targets and to reduce the amount of active substances, while locally a high release can be guaranteed [1, 3, 15–17].

Vascular cell adhesion molecule 1 (VCAM–1), E-selectin, and Intercellular Adhesion Molecule 1 (ICAM–1) are cell adhesion molecules on endothelial cells which are increasingly expressed in inflammation. Inflammatory processes can be observed in atherosclerotic lesions or after vascular intervention like coronary artery stenting, which in the last case is called in-stent restenosis. This adverse side effect of a neointimal hyperplasia should be avoided in atherosclerotic therapy. A promising approach is the reduction of the inflammatory process by siRNA gene silencing of the above mentioned involved adhesion proteins [18–20]. Reducing inflammation is thought to decrease the probability of restenosis, avoid re-surgeries, and reduce the duration of antithrombotic drug use.

The complexation of the siRNA with transfection agents for better stability benefits the approach of substrate-mediated transfection. These complexes can be incorporated in large quantities in coatings and act as a depot. Herein, the use of polyelectrolyte multilayers (PEMs) is a promising approach in the field of substrate-mediated active substance delivery [1, 21–26]. The ability to incorporate drugs into the PEMs makes this system interesting for siRNA release and the desired gene silencing [1, 27, 28]. A simple technique for the deposition of PEMs is the versatile layer-by-layer (LbL) technique, in which polyelectrolytes are alternately deposited to a substrate. The alternation of positive and negative charged materials creates electrostatic interactions that stabilize the structure. Popular materials for cell biomaterial interaction were used in many PEM research works like the cationic polyelectrolytes: poly(L-lysine), chitosan, and poly(ethylenimine), and the anionic ones: alginate, hyaluronic acid, and polyacrylic acid [29–34]. Among the cationic polymers, the poly(ethylenimine) (PEI) is much favored for the complexation of negatively charged siRNA, as it forms a non-covalent bond with its strong cationic charge density. By complexing siRNA, the limiting factors of nucleic acid transfection, such as negative charge, degradation by nucleases, stimulation of the immune system, can be avoided. PEI has nitrogen on every third atom and is hence protonable in an endosome [35]. Due to its buffer capacity, chloride anions flow into the endosome which causes an influx of water and consequently an osmotic swelling. This so called "proton-sponge-effect" causes the endosome to burst and releases the PEI-siRNA complexes into the cytoplasm [36]. For successful transfection, the choice of molecular weight, chemical structure and nitrogen phosphate (N/P) ratio is important. The N/P ratio is defined as the quotient of the moles of the amine groups of cationic polymer to the phosphate groups of DNA or RNA and is crucial for efficient gene delivery. The ratio determines the size of the particles for transfection and is therefore an important measure for cell experiments [37–39].

Hyaluronic acid (HA) is a negatively charged glycosaminoglycan which occurs naturally like in the extracellular matrix, synovial fluid, umbilical cord, and in blood [40, 41]. The biopolymer properties like biocompatibility, biodegradability, and no immunogenicity make hyaluronic acid a suitable material in wound healing, treatment of knee osteoarthritis or for tissue-engineered scaffolds [42–44]. Crucial for this is the molecular weight of the hyaluronic acid which is responsible for the properties of the polymer. The high molecular weight hyaluronic acid has anti-inflammatory effects during tissue injury, while the low molecular weight hyaluronic acid is responsible for the activation of pro-inflammatory chemokines and cytokines [45]. Although HA is not a typical transfection agent due to its negative charge, it is often used in nucleic acid delivery in combination with chitosan or poly-L-arginine [46, 47]. The combined use of HA with the transfection agent PEI has the great advantage that HA can reduce the cytotoxic effects of PEI [48].

The well considered choice of biomaterials is of particular importance for the success of transfection and the necessary cell adhesion. In addition to parameters such as thickness, roughness, and viscoelasticity of the substrate, stiffness is of great importance for cell adhesion [49, 50]. The cultivation of primary cells on soft biomaterials from natural origin causes low adhesion on the substrate and thus leads to apoptosis in *in vitro* assays [51]. As a result, soft PEM layers cannot be properly assessed for toxicity. It is indistinguishable whether the apoptosis occurs due to the cytotoxicity of the polymer or because of low stiffness. The 'reverse assay' is a suitable method to avoid possible influence by the stiffness where coated substrates can be placed on pre-cultured cells [51].

In this study we describe the potential of a PEM system that might be used as a coating for medical devices which is capable to release siRNA from HA/PEI multilayers for ICAM–1 gene knockdown in EA.hy926 in vitro. Bilayers from 3 to 24 were tested in an 'reverse assay' for gene knockdown and transfection efficiency using two different LbL techniques, wet or dried layers, on ICAM–1 silencing. The build-up of the $(HA/PEI)_n$ multilayers and the release of siRNA particles were determined by fluorescence intensity as a scan of the coated substrates and of the supernatant, respectively. A possible influence of the polymer on cell growth was investigated with the determination of cell viability.

2 Materials and methods

2.1 Polyelectrolyte solutions for PEM build-up

Branched polyethylenimines (PEI), (molecular weight (MW) = 750 kDa and 25 kDa) were purchased from Sigma-Aldrich (Steinheim, Germany) and prepared in ddH$_2$O (Ampuwa, Fresenius Kabi, Bad Homburg, Germany). The concentration of 750 kDa PEI was 1 µM and of 25 kDa 100 µM. Sodium hyaluronate 95% (MW = 1500–2200 kDa) was obtained from Acros Organics (Fisher Scientific, Schwerte, Germany) and 1 mg/mL was dissolved in 5 mM sodium acetate buffer (pH 5.5). All solutions were sterilized by sterile filtration.

2.2 SiRNAs

The following siRNA was used for gene knockdown: intercellular adhesion molecule (ICAM)–1 human with sense strand 5'-GCC UCA GCA CGU ACC UCU AUU-3', antisense 5'-UAG AGG UAC GUG CUG AAG CUU-3'. E-selectin siRNA AF 488 was applied to test the transfection efficiency: with sense strand 5'-UUG AGU GGU GCA UUC AAC CUU-3', antisense 5'-GGU UGA AUG CAC CAC UCA AUU-3' (both from Eurofins MWG Operon, Ebersberg, Germany), and control nonsense siRNA (siSCR) (Qiagen, Hilden, Germany). Qiagen does not provide the sequence of their nonsilencing siRNAs but ensure that they have no homology to any known mammalian gene. This nonsilencing siRNA is validated by using Affymetrix GeneChip arrays and a variety of cell-based assays and shown to ensure minimal nonspecific effects on gene expression and phenotype.

2.3 Glass slide as a substrate for PEM build-up

PEMs were built-up on glass slides from Marienfeld GmbH (Lauda-Königshofen, Germany). The dimension of the slides was 10 x 10 x 1 mm. They were purified by ultrasonication (Bandelin RK 100H Sonorex, Bandelin electronic, Germany) with 2% Hellmanex solution from Hellma (Müllheim, Germany) before rinsing with ddH$_2$O. Air-dried slides were sterilized in a heating furnace (Binder, Germany) at 200° C for 4 h prior using in PEM films build-up procedure.

2.4 Cultivation of EA.hy926

The human umbilical vein cell line EA.hy926 (LGC Standards GmbH, Wesel, Germany) was used for all cell experiments. Cells were cultured in Dulbecco's Modified Eagle's Medium (DMEM) high glucose containing 10% fetal calf serum, 1% Penicillin/Streptomycin, and 1% L-glutamine (gibco® by Life Technologies, Carlsbad, California). Cell number and viability was tested by a CASY cell counter (Schärfe System).

2.5 Complexation of PEI-siRNA particles

PEI-siRNA particles were formed by diluting siRNA (20 µM) and PEI 25 kDa in 0.15 M NaCl (Fresenius Kabi, Bad Homburg, Germany) each. For PEM-mediated transfection, 0.5 µg siRNA was used for one layer. After 10 min incubation the two solutions were mixed, shortly vortexed and span down. Within 20 min, the PEI-siRNA particles were allowed to form at RT. All PEI-siRNA particles used in the PEM build-up had an mN/P ratio of 18.75. The N/P ratio is determined by the amount of moles of primary amine groups (PEI) and the number of moles of phosphate groups of siRNA.

2.6 Build-up of PEM films

PEMs were built-up manually with increasing number of bilayers: PEI(HA/PEI)$_2$(HA/PEI-siRNA)$_{3,5,7,10,12,24}$. Therefore, purified and sterilized glass slides were coated using the layer-by-layer technique. Layers of HA/PEI are designated as precursor layers, whereas HA/PEI-siRNA layers are designated as bioactive layers throughout this manuscript. The first precursor layer of 750 kDa PEI was deposited by dipping the glass slide for 10 min in PEI solution. After extensively rinsing for 3 x 2 min in 0.15 M NaCl, two further precursor bilayers of HA and 25 kDa PEI (HA/PEI)$_2$ were alternately added (dipping time: 10 min). Between each deposition, a washing step (3 x 2 min) with sodium acetate buffer and NaCl solution was held. Following this, bioactive layers were produced in two different ways. In the layer-by-layer method, the desired number of active layers (HA/PEI-siRNA) was deposited on precursor layers as follows: Glass slides were dipped in HA and PEI-siRNA particle solution for 10 min with washing steps as described above. In the modified layer-by-layer coating method, glass slides were dipped in HA for 20 sec and air-dried. Subsequently, PEI/siRNA particles (0.5 µg siRNA) were pipetted and not dipped onto the slide and air-dried, too. The coated slides were used for substrate mediated delivery in transfection experiments with EA.hy926 and for the release study.

2.7 Build-up of monolayer films

As described in the chapter before, prepared glass slides served as a substrate for the monolayer coatings in cell culture experiments. PEI-siRNA particles with either siICAM−1 or siSCR were complexed with PEI 25 kDa as described in chapter 2.5. The 10-fold amount of siRNA, PEI and NaCl was used for the total amount of 5 µg siRNA, which was also present in the 10 bilayers. The transfection solution was pipetted onto the glass slides and air-dried. Monolayer films were tested in cell culture experiments for the comparison of cell viability with PEMs.

2.8 PEM-mediated transfection

Cell seeding with 1 x 10^5 cells in a 24−well plate was prepared 48 h before transfection with PEM- or monolayer-coated glass slides. After media exchange, the coated glass slides with siRNA AF 488 and siSCR were deposited onto the cells in a so called reverse assay [52]. This assay is illustrated in Fig 1. After deposition of the glass slides 1 mL medium was added into each well and incubated for 24 h at 37°C with 5% CO$_2$. Uncoated glass slides served as a negative control.
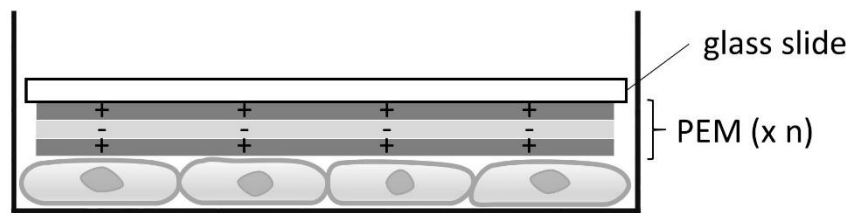
Hyaluronic acid/poly(ethylenimine) polyelectrolyte multilayers for gene silencing

Fig 1. Reverse assay for cell transfection. The coated glass slide is placed on the previously seeded and cultured cells to transfect them.

2.9 Flow cytometry

Transfection efficiency was determined by flow cytometry after 24 h cultivation. Glass slides were removed from the cells and they were washed and detached from cell culture plate before fixing them with 2.5% paraformaldehyde (PFA) in round-bottom special tubes for flow cytometry applications (Falcon®). Flow cytometry analysis was performed with 5000 cells/measurement (FACScan™, Becton Dickinson GmbH) and evaluated with CellQuestPro software (Becton Dickinson GmbH). Knockdown of ICAM−1 protein expression was examined as follows, cells were stimulated with 5 ng/mL tumor necrosis factor (TNF)-α (BD Biosciences, Germany) for 14 h to induce ICAM−1 expression. Immunofluorescence staining with PE mouse anti-human CD54 (BD Bioscience, Germany) was prepared before paraformaldehyde (PFA) fixing and flow cytometry analysis for 30 min at 37° C.

2.10 Release of PEI-siRNA AF 488 particles

Testing the PEM-mediated release of PEI-siRNA particles, complexes with 0.5 µg siRNA AF488 were formed with a mN/P ratio of 18.75. PEMs with 3, 5, 7, and 10 bilayers were built-up as described before. An uncoated glass slide and a 10 bilayer coated slide without siRNA served as controls. The slides were incubated in a 24-well plate with 500 µL PBS at 37° C. At different time points (1 h, 4 h, 24 h, and 48 h), the fluorescence intensity of the supernatant was measured with the fluorescence reader Mithras LB 940 (Berthold Technologies, Germany) with an excitation wavelength of 485 nm and an emission wavelength of 535 nm. Additionally, coated glass slides were scanned after buffer removal with 25 x 25 horizontal and vertical steps by rows, a rectangular scanning mode and a point displacement at 0.65 mm.

2.11 Statistics

The experiments were performed three times independently and the resulting values were tested and proven for Gaussian distribution. The values were compared by One-way ANOVA and Bonferroni correction as a Post-test. Difference between different treatment groups were determined as significant, if $p < 0.05$.

The analysis were performed with the statistic program GraphPad Prism 5 (GraphPad Software, La Jolla, USA).

3 Results

3.1 Reduction of ICAM−1 expression by polyelectrolyte multilayers

PEMs were prepared by incubating in the respective solution without drying PEI-siRNA particles on the preceding layers as described in the method for modified PEMs. The PEI(HA/

PEI$_2$(HA/PEI-siRNA)$_{3,10}$ coating showed a minimal decrease of ICAM−1 expression with remaining 89% and 86% but was not significant compared to the control (Fig 2). Only the PEI (HA/PEI)$_2$(HA/PEI-siRNA)$_{10}$ and PEI(HA/PEI)$_2$(HA/PEI-siSCR)$_{10}$ coatings differed significantly from each other with 86% ICAM−1 expression and 102%, respectively.

3.2 Transfection efficiency of EA.hy926 mediated by PEI-siRNA AF488 modified polyelectrolyte multilayers

The efficient uptake of agents into cells is mandatory for their effectiveness and the following response of the cells. Fluorescent labeled siRNA is a suitable and smart device determining the uptake of siRNA into the cells by flow cytometry. Therefore, we examined the transfection efficiency of PEI(HA/PEI)$_2$(HA/PEI-siRNA$_f$)$_{3,10}$ with incorporated siRNA AF488 and EA.hy926 cells. After 24 h incubation of coated slides on pre-cultured EA.hy926, the uptake of siRNA AF 488 particles was evaluated by flow cytometry. A transfection efficiency of 21% was measured with PEM PEI(HA/PEI)$_2$(HA/PEI-siRNA$_f$)$_3$ and 50% with PEM PEI(HA/PEI)$_2$(HA/PEI-siRNA$_f$)$_{10}$ (Fig 3). Both active PEMs with siRNA AF 488 showed significant higher transfection efficiency values than the control slides PEI(HA/PEI)$_2$(HA/PEI)$_{3,10}$. Furthermore, the PEM PEI(HA/PEI)$_2$(HA/PEI-siRNA$_f$)$_{10}$ with 10 bilayers achieved a significantly higher transfection efficiency than PEI(HA/PEI)$_2$(HA/PEI$_f$)$_3$.

3.3 ICAM−1 expression after transfection with modified polyelectrolyte multilayers

To determine the most effective amount of bilayers for gene knockdown, we tested 3, 5, 7, 10, 12 bilayers of (HA/PEI-siRNA)$_n$. The results show that the desired ICAM−1 expression decrease was achieved in the samples with increasing number of layers and amount of siICAM−1. PEI(HA/PEI)$_2$(HA/PEI-siICAM−1)$_{3,5,7,10,12}$ showed significant reduction of ICAM−
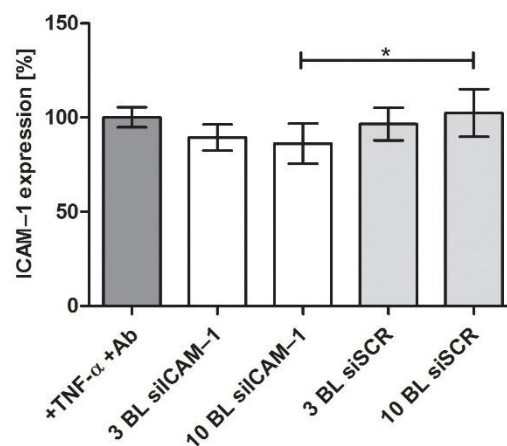
Fig 2. ICAM−1 expression of EA.hy926 after cultivation with PEMs. The multilayers were prepared by the dip and wash method without drying the PEI-siRNA particles as in the modified method. After 24 h of cultivation using the reverse assay, ICAM−1 expression was determined by flow cytometry and untreated but TNF-α stimulated cells were set to 100%. BL = bilayer, Ab = antibody. Each bar represents the mean ± standard error (SEM) of n = 6. * Statistical significance at p < 0.05.

Hyaluronic acid/poly(ethylenimine) polyelectrolyte multilayers for gene silencing
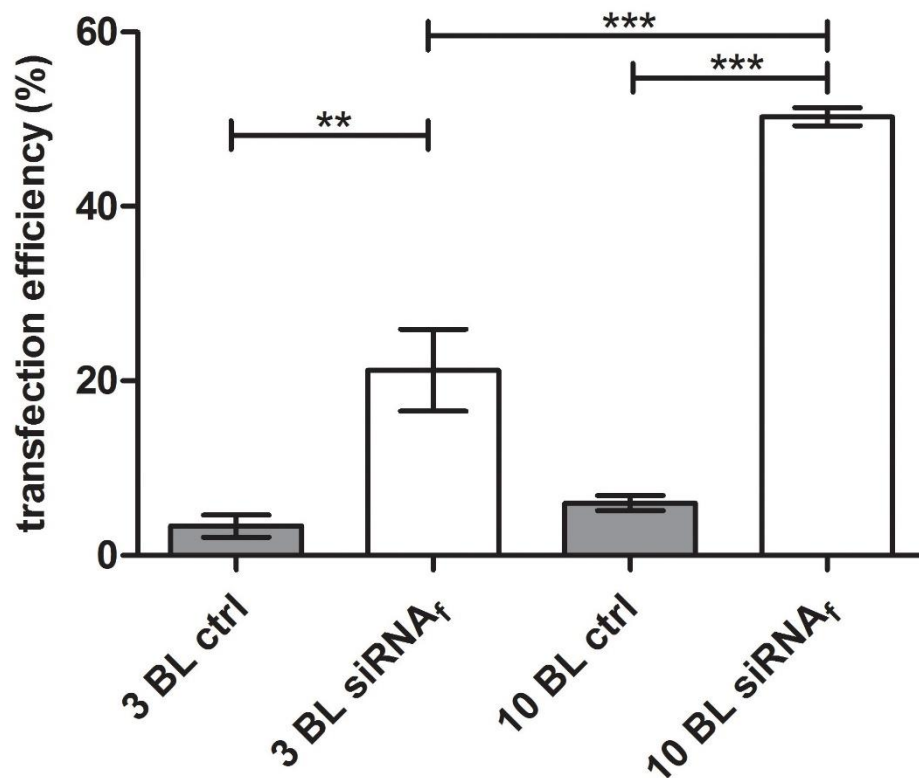
Fig 3. Evaluation of the siRNA uptake in EA.hy926 by flow cytometry. Cells were incubated with PEI(HA/PEI)$_2$(HA/PEI-siRNA$_f$)$_{3,10}$ coated slides in the reverse assay for 24 h. The fluorescence signal of transfected cells was measured by flow cytometry. Control slides were prepared without siRNA AF 488. BL = bilayer; ctrl = control. Each bar represents the mean ± standard error (SEM) of n = 3. *** Statistical significance at p < 0.001, ** statistical significance at p < 0.01.

https://doi.org/10.1371/journal.pone.0212584.g003

1 expression in comparison to control cells which were stimulated with TNF-α and antibody treated. The highest knockdown was achieved with 10 bilayers and remaining 44% ICAM–1 expression (Fig 4). 7 and 12 bilayer revealed similar ICAM–1 expression levels with 49% and 48% respectively. The ICAM–1 expression of control PEMs with siSCR were at the expression level of the control cells.

3.4 The effectiveness of modified polyelectrolyte multilayers for ICAM–1 knockdown

Two sizes of PEM bilayers PEI(HA/PEI)$_2$(HA/PEI-siICAM–1)$_{10,24}$ were evaluated for the delivery of siICAM–1 and the following knockdown of the ICAM–1 receptor in EA.hy926. 10 bilayers were chosen due to the results in 2.3 where 10 bilayers provoked the highest ICAM–1 knockdown. Additionally, a high amount of PEMs with 24 bilayers was tested to verify if a significant increase in bilayers and thus total siRNA levels could result in higher knockdown or
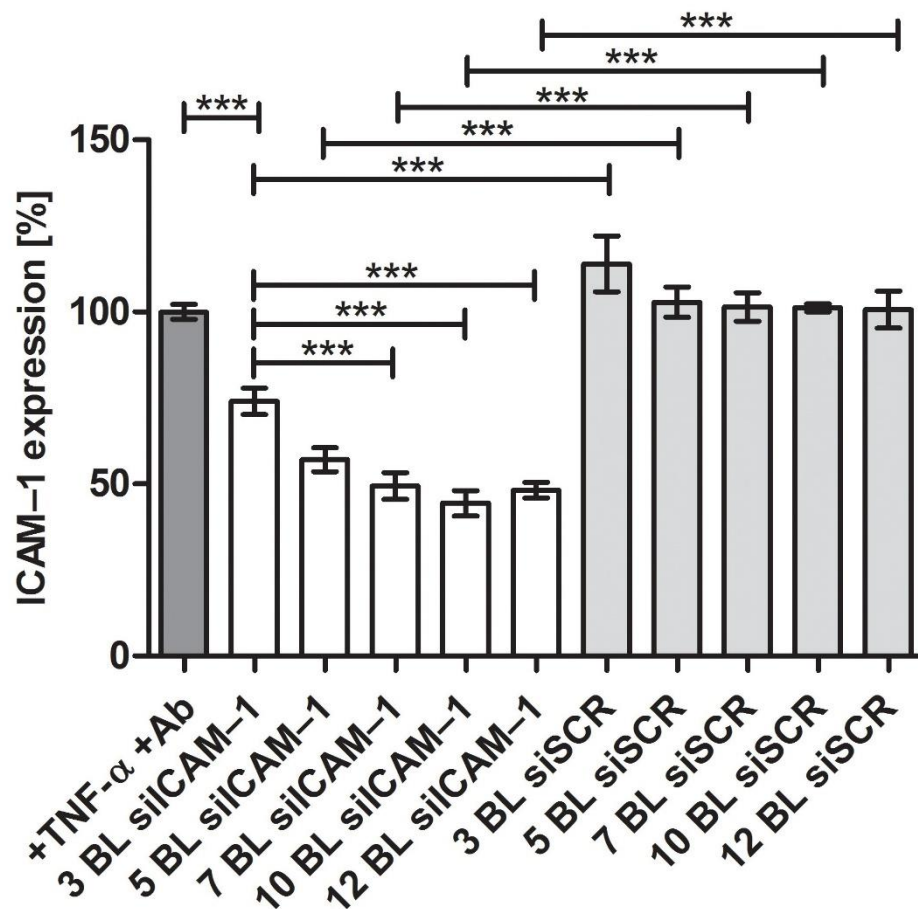
Fig 4. ICAM–1 expression after 24 h reverse assay with EA.hy926. Cells were cultivated with PEI(HA/PEI)$_2$(HA/PEI-siRNA)$_{3,5,7,10,12}$ coated glass slides for 24 h. Thereafter cells were stimulated with TNF-α for 14 h. After ICAM–1 antibody staining, fluorescence signal was determined by flow cytometry. Untreated but TNF-α stimulated cells were set to 100% and the results of the treatment groups represent the expression of ICAM–1 receptor in %. Ab = antibody, BL = bilayer. Each bar represents the mean ± standard error (SEM) of n = 5. *** Statistical significance at p < 0.001.

https://doi.org/10.1371/journal.pone.0212584.g004

prolonged release. First, cells were incubated with PEI(HA/PEI)$_2$(HA/PEI-siICAM–1)$_{10,24}$ and PEI(HA/PEI)$_2$(HA/PEI-siSCR)$_{10,24}$ for 24 h. Afterwards the same PEM coated glass slides were incubated with new pre-cultured cells for another 24 h.

The ICAM–1 expression was significant reduced by 10 and 24 bilayers after the first 24 h of incubation (Fig 5A). The 10 bilayers achieved a slightly higher ICAM–1 knockdown (5%) compared to 24 bilayers. Re-cultivation of the same PEMs for 24 h did not cause any significant knockdown of the ICAM–1 receptor in fresh cultured cells (Fig 5B).
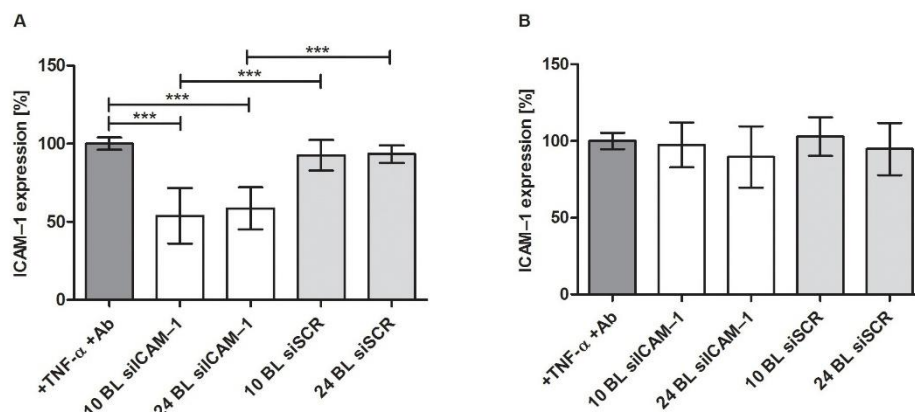
Hyaluronic acid/poly(ethylenimine) polyelectrolyte multilayers for gene silencing

Fig 5. ICAM–1 expression after 24 h and following 24 h after re-cultivation of the same PEMs with new seeded EA.hy926. A: After 24 h reverse assay with 10 and 24 bilayers, cells were analyzed by flow cytometry and untreated but with TNF α stimulated cells were set to 100%. B: The same 10 and 24 bilayer were cultivated for another 24 h with new pre-cultivated EA.hy926 and analyzed as described in A. Ab – antibody, BL – bilayer. Each bar represents the mean ± standard error (SEM) of n = 6. *** Statistical significance at p < 0.001.

https://doi.org/10.1371/journal.pone.0212584.g005

3.5 Release of siRNA AF 488 from modified polyelectrolyte multilayers

The release of siRNA AF 488 (siRNA$_f$) from PEMs PEI(HA/PEI)$_2$(HA/PEI-siRNAf)$_{3,5,7,10}$ was determined after 1, 4, 24, and 48 hours incubation in PBS (Fig 6A). The supernatant was measured with a fluorescent reader. After 1 h of incubation, the highest relative fluorescence unit (RFU) signal (16,899) was measured with 10 bilayers. The values of the RFU were getting less with the decrease of bilayers: 14,409 RFU with 7 bilayers, 13,325 RFU with 5 bilayers and 10,184 with 3 bilayers. Both control glass slides, the uncoated and the PEI(HA/PEI)$_2$(HA/PEI-siSCR)$_{10}$, showed low fluorescence signals with 1,874 and 2,034 RFU, respectively. After 4 hours incubation, the fluorescence signals of PEI(HA/PEI)$_2$(HA/PEI-siRNAf)$_{3,5,7,10}$ decreased into the range of both controls with 2,900, 2,779, 2,731, and 2,444 RFU for 10, 7, 5, and 3 double layers, respectively. The following RFU values of PEI(HA/PEI)$_2$(HA/PEI-siRNAf)$_{3,5,7,10}$ glass slides were on the RFU level of the control and uncoated glass slides after 24 and 48 h.

In order to determine the total amount of siRNA AF 488 applied during PEM coating, the glass slides were scanned immediately after the coating procedure (time point 0 h) and the fluorescence was analyzed. Furthermore, the glass slides were scanned after the incubation times (1 h, 4 h, 24 h, and 48 h) after removal of the supernatants (Fig 6B). Highest fluorescence intensity sum was found at timepoint zero directly after PEM coating with 2.6 x 10^7 RFU for 3 bilayers, 3.2 x 10^7 RFU for 5 bilayers, 3.5 x 10^7 RFU for 7 bilayers, and 4.1 x 10^7 RFU 10 bilayers. After 1 h incubation all intensity values of 3, 5, 7, and 10 bilayers were significantly reduced to 1.7 x 10^7 and 1.8 x 10^7 RFU and were nearly at control level, which was 1.5 x10^7 RFU. From the time point 4 h there was no significant change in the fluorescence intensity of siRNA AF 488-containing PEM and all samples had similar RFU values.

3.6 Influence of different siRNA coatings on cell viability

Polyelectrolyte multilayers, siRNA and transfection agents may influence the cell viability during the cultivation. The influence of these parameters was tested by determination of cell number and viability of EA.hy926 with a CASY cell counter. It is of interest whether the PEMs are

Hyaluronic acid/poly(ethylenimine) polyelectrolyte multilayers for gene silencing
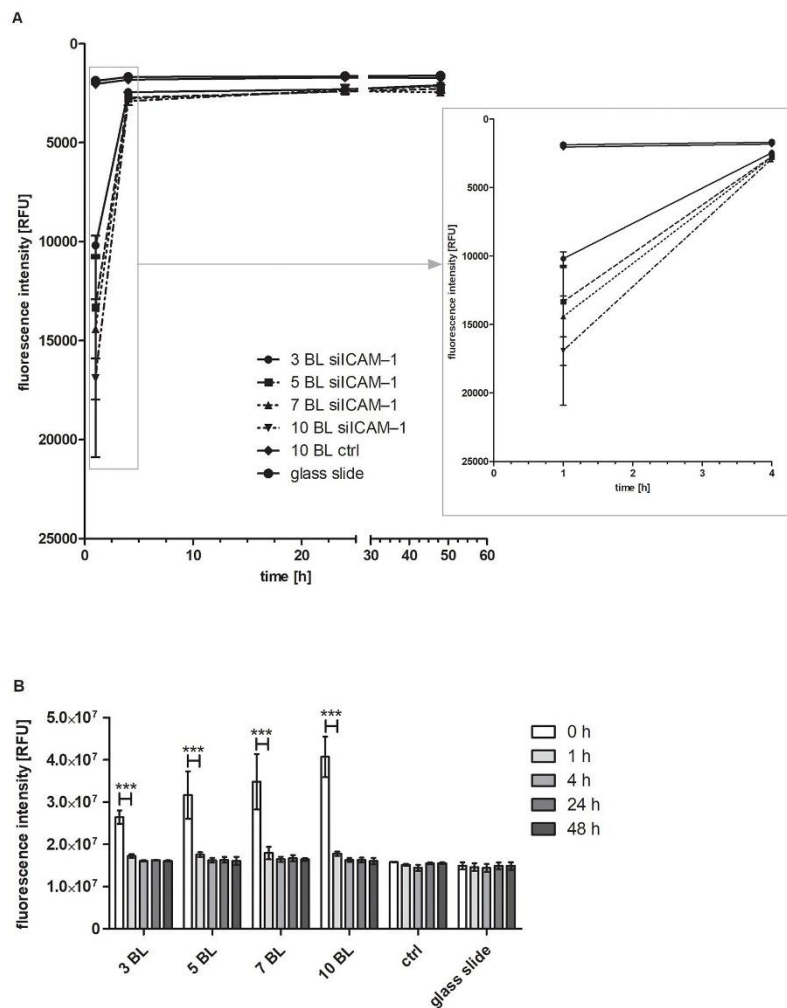
Fig 6. Release of siRNA AF 488 from PEMs within 48 h. A: Release of siRNA AF 488 by measurement of the supernatant. The fluorescence intensity of the supernatants was measured after 1, 4, 24, and 48 h incubation in PBS with a fluorescence reader at 485 nm excitation and 535 nm emission wavelength. In the right box an enlarged section of the period 1 to 4 h is shown. Each bar represents the mean ± standard error (SEM) of n = 3. B: Glass slide scan for release control. After the removal of the supernatant, glass slides were scanned with a resolution of 25 x 25 measurement points, at the same wavelengths as described before. The sum of all measurement points = fluorescence intensity, was determined at different timepoints. BL = bilayer; ctrl = control. Each bar represents the mean ± standard error (SEM) of n = 3. *** Statistical significance at p < 0.001.

https://doi.org/10.1371/journal.pone.0212584.g006

superior to the monolayer system in terms of cell viability. To determine the compatibility of PEM-coated slides in comparison to the same amount of PEI-siRNA in a monolayer system (hereby, the same amount of siRNA and PEI which was used for 10 bilayers was used to dry into a monolayer), cells were analyzed after 24 h reverse assay. PEM of $PEI(HA/PEI)_2(HA/PEI-siICAM-1)_{10}$ showed a significant higher cell number of 3.2×10^5 in comparison to the monolayer with the same siICAM-1 amount and the cell number 1.7×10^5 (Fig 7). The same result can be seen in the samples with siSCR. Again, the cell numbers are significantly different from each other and the PEM of $PEI(HA/PEI)_2(HA/PEI-siSCR)_{10}$ had a significantly higher number on 3.9×10^5 cells than the monolayer with 1.7×10^5 cells. The control sample where cells were cultivated with uncoated glass slides showed a cell number of 2.6×10^5 and is even lower than the cell number of PEMS.

4 Discussion

Substrate-mediated gene silencing by RNAi has great potential for therapeutic approaches where local effect is desired. A sophisticated and today well developed method is the LbL
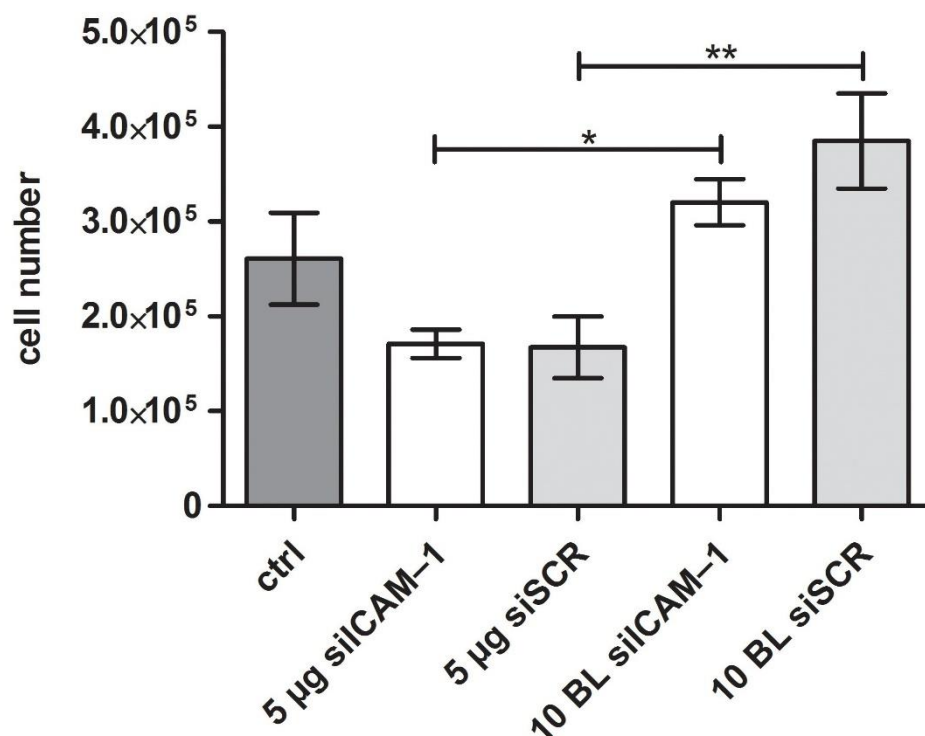
Fig 7. Cell number of EA.hy926 after incubation with PEI-siRNA particles and PEMs. EA.hy926 were incubated with different coated glass slides for 24 h and then tested for cell number after detachment with a CASY cell counter. Cells cultivated with an uncoated glass slide served as a control. 10 BL PEMs were compared with the monolayer of PEI siRNA with the same siRNA amount (5 μg). BL = bilayer, ctrl = control. Each bar represents the mean ± standard error (SEM) of n = 3. *** Statistical significance at $p < 0.001$, ** statistical significance at $p < 0.01$, * statistical significance at $p < 0.005$.

https://doi.org/10.1371/journal.pone.0212584.g007

technique, where a multilayer system can be built with different biomaterials of natural or synthetic origin with opposite charges. The structure of these PEMs allows the embedding of siRNA nanoparticles for gene silencing. To transport the siRNA, a cationic polymer like PEI can be used so that the siRNA, protected from enzymatic degradation, enters the cell for transfection.

The purpose of this study was the development of an siRNA-eluting coating using the LbL technique for gene silencing of the adhesion molecule ICAM–1 that plays a key role in the adhesion of leukocytes during leukocyte diapedesis at inflammatory sites [53]. Two different build-up methods with either dipping or drying (modified PEMs) steps were tested for HA/PEI PEMs. The PEMs were characterized for siRNA release, for cell viability, for transfection efficiency and ICAM–1 knockdown. Therefore, the reverse assay [51, 54] was applied for all cell culture assays to evade the possible influence of mechanical properties of the biomaterials HA and PEI on cell growth.

The build-up of PEMs PEI(HA/PEI)$_2$(HA/PEI-siRNA)$_n$ was initially prepared by the dip and wash method. The ICAM–1 expression results showed that neither 3 bilayers (1.5 μg siRNA) nor 10 dipped bilayers (5 μg siRNA) could induce uptake of siRNA after 24 h (Fig 2). The small decrease in ICAM–1 expression with 3 and 10 bilayers suggests that only small amounts of siRNA particles were incorporated into PEMs which results in a low transfection efficiency. We suppose that during the dipping step with PEI-siRNA particles, the incubation time was insufficient to bind to the hyaluronic acid. A recent study of Holmes and Tabrizian showed an efficient LbL system with glycol-chitosan/HA PEMs where DNA lipoplexes were adsorbed for 2 h followed washing and further adsorption steps. Herein, NIH3T3 and HEK293 cells were successfully transfected with different amount of DNA (2; 4; 6 μg) [22].

Consequently, we modified the process of the LbL method by omitting the washing steps after the precursor layers and dried the functional bilayers of PEI-siRNA and HA on the platelets. The purpose of the modification was to change the build-up of the PEMs as little as possible. With the modified drying method of PEM assembly, a coating could be established that released PEI-siRNA particles which were taken up by the cells through substrate-mediated transfection. The transfection efficiency showed the significant uptake of siRNA with 3 and 10 bilayers compared to control, moreover 10 bilayers provoked with 50% a significantly higher transfection efficiency compared with 3 bilayers with 21% (Fig 3). The results of ICAM–1 expression underlined the effectiveness of the modified method, where ICAM–1 expression could be significantly reduced up to 44% with 10 bilayers in comparison to the TNF-α/Ab control and the associated siSCR control (Fig 4). The 3, 5, 7, and 12 bilayers also showed significant ICAM–1 reduction in comparison to both controls. Within the experimental siICAM–1 series, there was also a significant difference between the 3 bilayers and the 7, 10 and 12 bilayers. This result indicates that an augmentation of bilayers up to 10 is meaningful for reaching the highest reduction of ICAM–1 expression. This was also proved with the knockdown experiment with 10 and 24 bilayers in comparison (Fig 5A). An increase in the number of bilayers, and the associated additional increase of siICAM–1 in the layers cause no further reduction in ICAM–1 expression. We might suppose with regard to this result either transfected cells were saturated with siRNA particles from the bilayers and consequently were no longer capable for siRNA uptake or the build-up of PEMs has reached its maximum after 10 bilayers in our study. In a previous preliminary study it was observed that also the application of 15 bilayers had no higher reduction of the ICAM–1 expression, and the value was between that of the 10 and 12 bilayers.

The decrease of the ICAM–1 expression (Fig 4) in response to the increase in the number of layers indicates that the layer build-up has taken place successfully using the drying method. The glass slide scanning dates at time point zero corroborate these results showing an increase

in fluorescence intensity with an increase in bilayers (Fig 6B) as well as the release results after 1 h incubation (Fig 6A). Consequently, these results suggest that the amount of $siRNA_f$-PEI has been incorporated in every bilayer.

The duration of siRNA release for substrate-mediated transfection is of particular importance for the transfer of the system to medical devices, such as stents or balloon catheters in atherosclerosis therapy. For long-term release of drugs, the stent is a suitable medical device in percutaneous transluminal coronary angioplasty (PTCA) and is called drug eluting stent (DES) [55, 56]. However, fast-release systems are of particular interest in medical interventions where no medical device remains in the body that releases a drug in the long-term. Currently, coated balloon catheters are used for the treatment of atherosclerosis with for instance paclitaxel, which is intended to prevent or ameliorate restenosis [57–59]. This fast-release coatings may be beneficial to deliver the drug during treatment to the site of action. The release experiment over 48 h (Fig 6A) showed on the basis of the fluorescence intensity that almost the entire amount of PEI-$siRNA_f$ particles was released from the PEM within the first hour. After 4 hours the values of all BL approximated to the values of the control glass slide. The glass slide scanning results underlined this finding. At the measuring point 1 h a significant decrease in the fluorescence intensity of all $siRNA_f$ bilayers was observed. The fluorescence intensity of these samples continued to decline at point 4 h, 24 h, and 48 h with an approach to the control values (Fig 6B). In conclusion, an initial burst release followed by minor $siRNA_f$ release could be achieved with the modified drying build-up method. The re-cultivation of the glass slides PEI(HA/PEI)$_2$(HA/PEI-siICAM−1/siSCR)$_{10,24}$ for another 24 h confirmed the burst release because no significant decrease of ICAM−1 expression could be achieved after their deposition on pre-cultured EA.hy926 (Fig 5B).

Next to the transfection efficiency, the cell viability is of great importance for substrate-mediated transfection with PEM systems. Therefore, we used the reverse assay with 24 h cultivation of EA.hy926 and counted the cell number with the CASY$^®$ system. For cells that were cultivated with a monolayer containing 5 µg PEI-siICAM−1 or 5 µg PEI-siSCR, the cell numbers were reduced in comparison to the control cells incubated with an uncoated glass slide. On the other hand the cells that were cultivated with the PEM PEI(HA/PEI)$_2$(HA/PEI-siICAM−1/siSCR)$_{10}$, the cell numbers were higher than the control (Fig 7). The direct comparison between monolayer and the PEM system revealed significant higher cell numbers of EA.hy926 cultivated with PEI(HA/PEI)$_2$(HA/PEI-siICAM−1/siSCR)$_{10}$. We presume that these findings are due to the HA which is incorporated in the PEM system but is not present in the monolayer. Han et al. discovered in their study the positive effect of HA regarding the cytotoxicity of PEI in their HA-PEI delivery system. They detected that the combination of HA-PEI provoked less cytotoxicity than PEI alone [48]. Furthermore, McKee et al. described an anti-inflammatory effect of high molecular weight HA which was used in our and Han's study [45]. We suppose that this effect is able to protect the cells from PEI cytotoxic side effects.

Conclusion

In this study we established a multilayer system consisting of the polyelectrolytes PEI and HA by an LbL technique which successfully transfected cells with siRNA by substrate-mediated transfection. We proofed that the classic LbL dipping method is not capable to provoke a significant reduction of ICAM−1 expression after 24 h. Therefore, we modified the LbL method by a new developed drying method and achieved significant ICAM−1 expression reduction from 3 BL, 5 BL, 7 BL, 10 BL, up to 12 BL. The coating with 10 BL showed the highest knockdown with 44% remaining ICAM−1 expression and transfection efficiency with fluorescent labeled siRNA of 50%. An increase in the number of bilayer up to 24 did not yield any further

reduction of ICAM−1 expression. The release study of the PEMs demonstrated that there is a burst release within the first hour followed by a minor release. The re-cultivation of previously laid out 10 and 24 BL PEMs confirmed this result. We demonstrated by counting the viable cells that the PEM system influences the cell number positively in comparison to the mono-layer system, where cell number was reduced significantly. This new developed modified LbL coating could be easily adapted for medical devices where a fast substrate-mediated transfec-tion of cells is desired, e.g. balloon catheter during PTCA. Therefore, we see great potential for an application in the prevention of restenosis on molecular level after a balloon catheter inter-vention via PTCA The high knockdown results make the construction interesting for further developments in the field of local gene delivery systems.

Author Contributions

Conceptualization: Olivia Koenig, Bernd Neumann, Hans Peter Wendel, Andrea Nolte.

Data curation: Olivia Koenig.

Investigation: Bernd Neumann.

Methodology: Olivia Koenig, Bernd Neumann, Andrea Nolte.

Project administration: Christian Schlensak, Hans Peter Wendel.

Supervision: Hans Peter Wendel, Andrea Nolte.

Visualization: Olivia Koenig.

Writing – original draft: Olivia Koenig.

Writing – review & editing: Hans Peter Wendel, Andrea Nolte.

References

1. Hossfeld S, Nolte A, Hartmann H, Recke M, Schaller M, Walker T, et al. Bioactive coronary stent coating based on layer-by-layer technology for siRNA release. Acta biomaterialia. 2013; 9(5):6741–52. Epub 2013/01/22. https://doi.org/10.1016/j.actbio.2013.01.013 PMID: 23333865.

2. Nolte A, Walker T, Schneider M, Kray O, Avci-Adali M, Ziemer G, et al. Small-interfering RNA-eluting surfaces as a novel concept for intravascular local gene silencing. Molecular medicine (Cambridge, Mass). 2011; 17(11–12):1213–22. Epub 2011/07/28. https://doi.org/10.2119/molmed.2011.00143 PMID: 21792480; PubMed Central PMCID: PMCPmc3321820.

3. Koenig O, Zengerle D, Perle N, Hossfeld S, Neumann B, Behring A, et al. RNA-Eluting Surfaces for the Modulation of Gene Expression as A Novel Stent Concept. Pharmaceuticals (Basel, Switzerland). 2017; 10(1). Epub 2017/02/18. https://doi.org/10.3390/ph10010023 PMID: 28208634; PubMed Central PMCID: PMCPmc5374427.

4. Qu Y, Shi X, Zhang H, Sun W, Han S, Yu C, et al. VCAM-1 siRNA reduces neointimal formation after surgical mechanical injury of the rat carotid artery. Journal of vascular surgery. 2009; 50(6):1452–8. Epub 2009/12/05. https://doi.org/10.1016/j.jvs.2009.08.050 PMID: 19958991.

5. Wang B, Qian H, Yang H, Xu L, Xu W, Yan J. Regression of atherosclerosis plaques in apolipoprotein E-/- mice after lentivirus-mediated RNA interference of CD40. International journal of cardiology. 2013; 163(1):34–9. Epub 2011/06/07. https://doi.org/10.1016/j.ijcard.2011.05.053 PMID: 21640399.

6. Tabernero J, Shapiro GI, LoRusso PM, Cervantes A, Schwartz GK, Weiss GJ, et al. First-in-humans trial of an RNA interference therapeutic targeting VEGF and KSP in cancer patients with liver involve-ment. Cancer discovery. 2013; 3(4):406–17. Epub 2013/01/30. https://doi.org/10.1158/2159-8290.CD-12-0429 PMID: 23358650.

7. Palliser D, Chowdhury D, Wang QY, Lee SJ, Bronson RT, Knipe DM, et al. An siRNA-based microbicide protects mice from lethal herpes simplex virus 2 infection. Nature. 2006; 439(7072):89–94. Epub 2005/11/25. https://doi.org/10.1038/nature04263 PMID: 16306938.

8. Castanotto D, Rossi JJ. The promises and pitfalls of RNA-interference-based therapeutics. Nature. 2009; 457(7228):426–33. https://doi.org/10.1038/nature07758 PMC2702667. PMID: 19158789

9. Fire A, Xu S, Montgomery MK, Kostas SA, Driver SE, Mello CC. Potent and specific genetic interference by double-stranded RNA in Caenorhabditis elegans. Nature. 1998; 391(6669):806–11. Epub 1998/03/05. https://doi.org/10.1038/35888 PMID: 9486653.

10. Elbashir SM, Harborth J, Lendeckel W, Yalcin A, Weber K, Tuschl T. Duplexes of 21-nucleotide RNAs mediate RNA interference in cultured mammalian cells. Nature. 2001; 411(6836):494–8. Epub 2001/05/25. https://doi.org/10.1038/35078107 PMID: 11373684.

11. Nishida H, Matsumoto Y, Kawana K, Christie RJ, Naito M, Kim BS, et al. Systemic delivery of siRNA by actively targeted polyion complex micelles for silencing the E6 and E7 human papillomavirus oncogenes. Journal of controlled release: official journal of the Controlled Release Society. 2016; 231:29–37. Epub 2016/03/17. https://doi.org/10.1016/j.jconrel.2016.03.016 PMID: 26979870.

12. Kenjo E, Asai T, Yonenaga N, Ando H, Ishii T, Hatanaka K, et al. Systemic delivery of small interfering RNA by use of targeted polycation liposomes for cancer therapy. Biological & pharmaceutical bulletin. 2013; 36(2):287–91. Epub 2013/02/02. PMID: 23370357.

13. Navarro G, Sawant RR, Biswas S, Essex S, Tros de Ilarduya C, Torchilin VP. P-glycoprotein silencing with siRNA delivered by DOPE-modified PEI overcomes doxorubicin resistance in breast cancer cells. Nanomedicine (London, England). 2012; 7(1):65–78. Epub 2011/12/24. https://doi.org/10.2217/nnm.11.93 PMID: 22191778; PubMed Central PMCID: PMCPmc3422569.

14. Choi KM, Kim K, Kwon IC, Kim IS, Ahn HJ. Systemic delivery of siRNA by chimeric capsid protein: tumor targeting and RNAi activity in vivo. Molecular pharmaceutics. 2013; 10(1):18–25. Epub 2012/06/06. https://doi.org/10.1021/mp300211a PMID: 22663765.

15. Hoffmann N, Mittnacht U, Hartmann H, Baumer Y, Kjems J, Oberhoffner S, et al. Neuronal and glial responses to siRNA-coated nerve guide implants in vitro. Neuroscience letters. 2011; 494(1):14–8. Epub 2011/03/01. https://doi.org/10.1016/j.neulet.2011.02.043 PMID: 21352894.

16. Katz MG, Fargnoli AS, Pritchette LA, Bridges CR. Gene delivery technologies for cardiac applications. Gene therapy. 2012; 19(6):659–69. Epub 2012/03/16. https://doi.org/10.1038/gt.2012.11 PMID: 22418063; PubMed Central PMCID: PMCPmc3668697.

17. Dykxhoorn DM, Palliser D, Lieberman J. The silent treatment: siRNAs as small molecule drugs. Gene therapy. 2006; 13(6):541–52. Epub 2006/01/07. https://doi.org/10.1038/sj.gt.3302703 PMID: 16397510.

18. Nolte A, Walker T, Schneider M, Kray O, Avci-Adali M, Ziemer G, et al. Small-Interfering RNA–Eluting Surfaces as a Novel Concept for Intravascular Local Gene Silencing. Molecular Medicine. 2011; 17(11–12):1213–22. https://doi.org/10.2119/molmed.2011.00143 PMC3321820. PMID: 21792480

19. Koenig O, Nothdurft D, Perle N, Neumann B, Behring A, Degenkolbe I, et al. An Atelocollagen Coating for Efficient Local Gene Silencing by Using Small Interfering RNA. Molecular therapy Nucleic acids. 2017; 6:290–301. Epub 2017/03/23. https://doi.org/10.1016/j.omtn.2017.01.006 PMID: 28325296; PubMed Central PMCID: PMCPmc5363512.

20. Luc G, Arveiler D, Evans A, Amouyel P, Ferrieres J, Bard J-M, et al. Circulating soluble adhesion molecules ICAM-1 and VCAM-1 and incident coronary heart disease: The PRIME Study. Atherosclerosis. 170(1):169–76. https://doi.org/10.1016/S0021-9150(03)00280-6 PMID: 12957696

21. Castleberry S, Wang M, Hammond PT. Nanolayered siRNA Dressing for Sustained Localized Knockdown. ACS Nano. 2013; 7(6):5251–61. https://doi.org/10.1021/nn401011n PMID: 23672676

22. Holmes CA, Tabrizian M. Substrate-mediated gene delivery from glycol-chitosan/hyaluronic acid polyelectrolyte multilayer films. ACS applied materials & interfaces. 2013; 5(3):524–31. Epub 2013/01/04. https://doi.org/10.1021/am303029k PMID: 23281737.

23. Keeney M, Waters H, Barcay K, Jiang X, Yao Z, Pajarinen J, et al. Mutant MCP-1 protein delivery from layer-by-layer coatings on orthopedic implants to modulate inflammatory response. Biomaterials. 2013; 34(38):10287–95. https://doi.org/10.1016/j.biomaterials.2013.09.028 PMID: 24075408

24. Zhi F, Dong H, Jia X, Guo W, Lu H, Yang Y, et al. Functionalized Graphene Oxide Mediated Adriamycin Delivery and miR-21 Gene Silencing to Overcome Tumor Multidrug Resistance In Vitro. PLOS ONE. 2013; 8(3):e60034. https://doi.org/10.1371/journal.pone.0060034 PMID: 23527297

25. Wood KC, Chuang HF, Batten RD, Lynn DM, Hammond PT. Controlling interlayer diffusion to achieve sustained, multiagent delivery from layer-by-layer thin films. Proceedings of the National Academy of Sciences. 2006; 103(27):10207–12. https://doi.org/10.1073/pnas.0602884103 PMID: 16801543

26. Macdonald ML, Samuel RE, Shah NJ, Padera RF, Beben YM, Hammond PT. Tissue integration of growth factor-eluting layer-by-layer polyelectrolyte multilayer coated implants. Biomaterials. 2011; 32(5):1446–53. Epub 2010/11/19. https://doi.org/10.1016/j.biomaterials.2010.10.052 PMID: 21084117; PubMed Central PMCID: PMCPmc3033887.

27. Hartmann H, Hossfeld S, Schlosshauer B, Mittnacht U, Pêgo AP, Dauner M, et al. Hyaluronic acid / chitosan multilayer coatings on neuronal implants for localized delivery of siRNA nanoplexes. Journal of

Controlled Release. 2013; 168(3):289–97. https://doi.org/10.1016/j.jconrel.2013.03.026 PMID: 23562632

28. Wu L, Wu C, Liu G, Liao N, Zhao F, Yang X, et al. A surface-mediated siRNA delivery system developed with chitosan/hyaluronic acid-siRNA multilayer films through layer-by-layer self-assembly. Applied Surface Science. 2016; 389(Supplement C):395–403. https://doi.org/10.1016/j.apsusc.2016.06.051.

29. Antunes JC, Pereira CL, Molinos M, Ferreira-da-Silva F, Dessì M, Gloria A, et al. Layer-by-Layer Self-Assembly of Chitosan and Poly(γ-glutamic acid) into Polyelectrolyte Complexes. Biomacromolecules. 2011; 12(12):4183–95. https://doi.org/10.1021/bm2008235 PMID: 22032302

30. Haidar ZS, Hamdy RC, Tabrizian M. Protein release kinetics for core–shell hybrid nanoparticles based on the layer-by-layer assembly of alginate and chitosan on liposomes. Biomaterials. 2008; 29(9):1207–15. https://doi.org/10.1016/j.biomaterials.2007.11.012 PMID: 18076987

31. Meng S, Liu Z, Shen L, Guo Z, Chou LL, Zhong W, et al. The effect of a layer-by-layer chitosan–heparin coating on the endothelialization and coagulation properties of a coronary stent system. Biomaterials. 2009; 30(12):2276–83. https://doi.org/10.1016/j.biomaterials.2008.12.075 PMID: 19168214

32. Khademhosseini A, Suh KY, Yang JM, Eng G, Yeh J, Levenberg S, et al. Layer-by-layer deposition of hyaluronic acid and poly-l-lysine for patterned cell co-cultures. Biomaterials. 2004; 25(17):3583–92. https://doi.org/10.1016/j.biomaterials.2003.10.033 PMID: 15020132

33. Picart C, Lavalle P, Hubert P, Cuisinier FJG, Decher G, Schaaf P, et al. Buildup Mechanism for Poly(l-lysine)/Hyaluronic Acid Films onto a Solid Surface. Langmuir. 2001; 17(23):7414–24. https://doi.org/10.1021/la010848g

34. Lutkenhaus JL, McEnnis K, Hammond PT. Nano- and Microporous Layer-by-Layer Assemblies Containing Linear Poly(ethylenimine) and Poly(acrylic acid). Macromolecules. 2008; 41(16):6047–54. https://doi.org/10.1021/ma800003x

35. Boussif O, Lezoualc'h F, Zanta MA, Mergny MD, Scherman D, Demeneix B, et al. A versatile vector for gene and oligonucleotide transfer into cells in culture and in vivo: polyethylenimine. Proceedings of the National Academy of Sciences of the United States of America. 1995; 92(16):7297–301. Epub 1995/08/01. PMID: 7638184; PubMed Central PMCID: PMCPmc41326.

36. Behr J-P. The Proton Sponge: a Trick to Enter Cells the Viruses Did Not Exploit. CHIMIA International Journal for Chemistry. 1997; 51(1–2):34–6.

37. Wood KC, Little SR, Langer R, Hammond PT. A family of hierarchically self-assembling linear-dendritic hybrid polymers for highly efficient targeted gene delivery. Angewandte Chemie (International ed in English). 2005; 44(41):6704–8. Epub 2005/09/21. https://doi.org/10.1002/anie.200502152 PMID: 16173106.

38. Wang XL, Ramusovic S, Nguyen T, Lu ZR. Novel polymerizable surfactants with pH-sensitive amphiphilicity and cell membrane disruption for efficient siRNA delivery. Bioconjugate chemistry. 2007; 18(6):2169–77. Epub 2007/10/18. https://doi.org/10.1021/bc700285q PMID: 17939730.

39. Kim SH, Lee SH, Tian H, Chen X, Park TG. Prostate cancer cell-specific VEGF siRNA delivery system using cell targeting peptide conjugated polyplexes. Journal of drug targeting. 2009; 17(4):311–7. Epub 2009/02/27. https://doi.org/10.1080/10611860902767232 PMID: 19242850.

40. Laurent TC, Laurent UB, Fraser JR. The structure and function of hyaluronan: An overview. Immunology and cell biology. 1996; 74(2):A1–7. Epub 1996/04/01. https://doi.org/10.1038/icb.1996.32 PMID: 8724014.

41. Maharjan AS, Pilling D, Gomer RH. High and Low Molecular Weight Hyaluronic Acid Differentially Regulate Human Fibrocyte Differentiation. PLoS ONE. 2011; 6(10):e26078. https://doi.org/10.1371/journal.pone.0026078 PMC3191166. PMID: 22022512

42. Voigt J, Driver VR. Hyaluronic acid derivatives and their healing effect on burns, epithelial surgical wounds, and chronic wounds: a systematic review and meta-analysis of randomized controlled trials. Wound repair and regeneration: official publication of the Wound Healing Society [and] the European Tissue Repair Society. 2012; 20(3):317–31. Epub 2012/05/09. https://doi.org/10.1111/j.1524-475X.2012.00777.x PMID: 22564227.

43. Hemmrich K, von Heimburg D, Rendchen R, Di Bartolo C, Milella E, Pallua N. Implantation of preadipocyte-loaded hyaluronic acid-based scaffolds into nude mice to evaluate potential for soft tissue engineering. Biomaterials. 2005; 26(34):7025–37. Epub 2005/06/21. https://doi.org/10.1016/j.biomaterials.2005.04.065 PMID: 15964623.

44. Tashiro T, Seino S, Sato T, Matsuoka R, Masuda Y, Fukui N. Oral administration of polymer hyaluronic acid alleviates symptoms of knee osteoarthritis: a double-blind, placebo-controlled study over a 12-month period. TheScientificWorldJournal. 2012; 2012:167928. Epub 2012/12/12. https://doi.org/10.1100/2012/167928 PMID: 23226979; PubMed Central PMCID: PMCPmc3512263.

45. McKee CM, Penno MB, Cowman M, Burdick MD, Strieter RM, Bao C, et al. Hyaluronan (HA) fragments induce chemokine gene expression in alveolar macrophages. The role of HA size and CD44. The

Journal of clinical investigation. 1996; 98(10):2403–13. Epub 1996/11/15. https://doi.org/10.1172/JCI119054 PMID: 8941660; PubMed Central PMCID: PMCPmc507693.

46. Al-Qadi S, Alatorre-Meda M, Zaghloul EM, Taboada P, Remunan-Lopez C. Chitosan-hyaluronic acid nanoparticles for gene silencing: the role of hyaluronic acid on the nanoparticles' formation and activity. Colloids and surfaces B, Biointerfaces. 2013; 103:615–23. Epub 2013/01/01. https://doi.org/10.1016/j.colsurfb.2012.11.009 PMID: 23274155.

47. Kim EJ, Shim G, Kim K, Kwon IC, Oh YK, Shim CK. Hyaluronic acid complexed to biodegradable poly L-arginine for targeted delivery of siRNAs. The journal of gene medicine. 2009; 11(9):791–803. Epub 2009/07/02. https://doi.org/10.1002/jgm.1352 PMID: 19569085.

48. Han SE, Kang H, Shim GY, Kim SJ, Choi HG, Kim J, et al. Cationic derivatives of biocompatible hyaluronic acids for delivery of siRNA and antisense oligonucleotides. Journal of drug targeting. 2009; 17 (2):123–32. Epub 2008/11/18. https://doi.org/10.1080/10611860802472461 PMID: 19012052.

49. Picart C. Polyelectrolyte multilayer films: from physico-chemical properties to the control of cellular processes. Current medicinal chemistry. 2008; 15(7):685–97. Epub 2008/03/14. PMID: 18336282.

50. Schneider A, Richert L, Francius G, Voegel JC, Picart C. Elasticity, biodegradability and cell adhesive properties of chitosan/hyaluronan multilayer films. Biomedical materials (Bristol, England). 2007; 2(1): S45–51. Epub 2008/05/07. https://doi.org/10.1088/1748-6041/2/1/s07 PMID: 18458419.

51. Nolte A, Hossfeld S, Schroeppel B, Mueller A, Stoll D, Walker T, et al. Impact of polyelectrolytes and their corresponding multilayers to human primary endothelial cells. Journal of biomaterials applications. 2013; 28(1):84–99. Epub 2012/03/30. https://doi.org/10.1177/0885328212437610 PMID: 22457040.

52. Nolte A, Hossfeld S, Schroeppel B, Mueller A, Stoll D, Walker T, et al. Impact of polyelectrolytes and their corresponding multilayers to human primary endothelial cells. Journal of Biomaterials Applications. 2013; 28(1):84–99. https://doi.org/10.1177/0885328212437610 PMID: 22457040

53. Long EO. ICAM-1: Getting a Grip on Leukocyte Adhesion. The Journal of Immunology. 2011; 186 (9):5021–3. https://doi.org/10.4049/jimmunol.1100646 PMID: 21505213

54. Minuth WW, Schumacher K, Strehl R, de Vries U. Mikroreaktortechnik für Tissue Engineering. 3 ed. Wintermantel E, Ha S-W, editors. Berlin, Germany: Springer; 2002.

55. Ma X, Oyamada S, Gao F, Wu T, Robich MP, Wu H, et al. Paclitaxel/sirolimus combination coated drug-eluting stent: In vitro and in vivo drug release studies. Journal of pharmaceutical and biomedical analysis. 2011; 54(4):807–11. https://doi.org/10.1016/j.jpba.2010.10.027 PMC3008332. PMID: 21126843

56. Acharya G, Park K. Mechanisms of controlled drug release from drug-eluting stents. Advanced drug delivery reviews. 2006; 58(3):387–401. https://doi.org/10.1016/j.addr.2006.01.016 PMID: 16546289

57. Scheller B, Speck U, Abramjuk C, Bernhardt U, Bohm M, Nickenig G. Paclitaxel balloon coating, a novel method for prevention and therapy of restenosis. Circulation. 2004; 110(7):810–4. Epub 2004/08/11. https://doi.org/10.1161/01.CIR.0000138929.71660.E0 PMID: 15302790.

58. Byrne RA, Neumann F-J, Mehilli J, Pinieck S, Wolff B, Tiroch K, et al. Paclitaxel-eluting balloons, paclitaxel-eluting stents, and balloon angioplasty in patients with restenosis after implantation of a drug-eluting stent (ISAR-DESIRE 3): a randomised, open-label trial. The Lancet. 2013; 381(9865):461–7. https://doi.org/10.1016/S0140-6736(12)61964-3.

59. Alfonso F, García-Guimaraes M, Navarrete G, Cuesta J, Bastante T, Benedicto A, et al. Drug-eluting balloons in coronary interventions: the quiet revolution? Expert Opinion on Drug Delivery. 2017; 14 (7):841–50. https://doi.org/10.1080/17425247.2017.1245291 PMID: 27718756

6.5 List of abbreviations

5'-RLM-RACE-PCR	5´-RNA ligase mediated rapid amplification of cDNA-ends PCR
ACE	angiotensin-converting enzyme
AF	Alexa Fluor
Ago2	Argonaute protein 2
ALS	amyotrophic lateral sclerosis
apoB	apolipoprotein B
ATCOL	Atelocollagen
ATP	adenosine triphosphate
BMS	bare metal stent
bp	base pair
C	degree Celsius
CABG	coronary artery bypass surgery
CAD	coronary artery disease
CAM	cellular adhesion molecule
cDNA	copy deoxyribonucleic acid
CHD	coronary heart disease
CVD	cardiovascular disease
CXCL	chemokine ligand
Da	Dalton
DES	drug-eluting stent
DMEM	Dulbecco's Modified Eagle Medium
DOPE	1,2-dioleoyl-*sn*-glycero-3-phosphoetanolamine
DOSPA	2,3-dioleyloxy-N-[2(sperminecarboxamido)ethyl]-N,N-dimethyl-1-propanaminium trifluoroacetate
dsRNA	double stranded ribonucleic acid
EC	endothelial cell
ECM	extracellular matrix
eGFP	enhanced green fluorescent protein
eNOS	endothelial nitric oxide synthase
ESAM	endothelial cell specific adhesion molecule
ESC/EACTS	European Society of Cardiology/ European Association for Cardio-Thoracic Surgery
FDA	Food and Drug Administration
h	hour
HA	hyaluronic acid
HBV	hepatitis B virus
HIV	human immunodeficiency virus
hVECs	human vascular endothelial cells
ICAM–1	intercellular adhesion molecule–1
IL–1	Interleukin–1
IL–6	Interleukin–6
ISR	in-stent restenosis

JAM	junctional adhesion molecule
K	kilo
KHK	koronare Herzkrankheit
LbL	layer-by-layer
LDL	low-density lipoprotein
LFA1	lymphocyte function-associated antigen 1
LOX–1	lectin-like receptor–1
m	milli
M	molar
MAC1	macrophage–1 antigen
MADCAM1	mucosal vascular addressin cell adhesion molecule 1
MCP–1	monocyte chemoattractant protein–1
M-CSF	macrophage colony-stimulating factor
min	minute
miRNA	micro RNA
MMP	matrix metalloproteinase
mRNA	messenger ribonucleic acid
N/P	nitrogen/phosphate
NF-κB	nuclear factor k-light-chain-enhancer of activated B cells
NO	nitric oxide
NOX2	NADPH oxidase 2
NP	nanoparticle
nt	nucleotide
OAS	2'-5'-oligoadenylate synthetase
oxLDL	oxidized LDL
PBS	phosphate buffered saline
PCI	percutaneous coronary intervention
PCR	polymerase chain reaction
PCSK–9	proprotein convertase subtilisin/kexin type–9 inhibitor
PECAM–1	platelet/endothelial-cell adhesion molecule–1
PEG	poly(ethylene glycol)
PEI	poly(ethylenimine)
PEM	polyelectrolyte multilayer
PGA	poly glycolic acid
PI3K	phosphoinositide 3–kinase
PLA	poly lactic acid
PLGA	poly(lactic-*co*-glycolic acid)
PMN	polymorphonuclear granulocyte
PSGL–1	P-selectin glycoprotein ligand–1
PTCA	percutaneous transluminal coronary angioplasty
qRT-PCR	quantitative Real-Time PCR
RGD	arginine-glycine-aspartate
RISC	ribonucleic acid induced silencing complex
RNA	ribonucleic acid

RNAi	ribonucleic acid interference
SC5b9	serum complement membrane attack complex
scrRNA	scrambled RNA
siRNA	small interfering ribonucleic acid
siSCR	small interfering scrambled RNA
SMC	smooth muscle cell
SOD	superoxide dismutase
STAT1	signal transducers and activators of transcription 1
TAT	thrombin-antithrombin III-complex
TNF-α	tumor necrosis factor-α
VCAM–1	vascular cell adhesion molecule–1
VE-cadherin	vascular endothelial cadherin
VLA4	very late antigen 4
VSMC	vascular smooth muscle cell

7 Acknowledgement

First I would like to thank Prof. Dr. Hans Peter Wendel for the opportunity to work on this project for my thesis to obtain the doctoral degree at the clinical research department of thoracic, cardiac and vascular surgery at the University Hospital Tuebingen. Above all, I am grateful for his friendly and constant encouragement, for his motivation and his patience.

A big thank you goes to PD Dr. Andrea Nolte-Karayel, who has been very supportive throughout the time. With her wealth of ideas, her advices, her motivating nature and constructive discussions, she has contributed greatly to the success of this work.

Special thanks go to Prof. Dr. Stevanović for taking over the second expert opinion of my thesis.

I would also like to thank all past and present members of Prof. Wendel's laboratory for the good and warm working atmosphere. Special thanks to Heidi Steinle, Bernd Neumann, Meltem Aci-Adali, Marcell Post, Silju Kunnakattu, Heidi Stoll, Dr. Sandra Stoppelkamp, Dr. Stefanie Krajewski and Julia Kurz for their support, discussions and motivation. A big thank you goes to Nadja Perle who becomes a very good friend and supported me through the tough but also great times.

Finally, I would like to thank my parents Evelyn and Hartmut, my two sisters Catherine and Sophie, and my grandparents Adelheid and Franz for their support, patience and trust in me. I would like to express a big thank you to my husband Daniel, who motivated me again and again and showed a lot of understanding, patience and trust in me. Thanks also to my two nieces Caroline and Larissa, and my nephew Vincent, who cheered me up with their funny way.